UNIVERSITA' DEGLI STUDI DI SALERNO
FACOLTA' DI SCIENZE MATEMATICHE FISICHE E NATURALI

Dottorato di ricerca in Chimica

Synthesis and properties of linear and cyclic peptoids

-X Cycle- Nuova serie (2008-2011)

Tutor: Prof. Francesco De Riccardis **PhD candidate: Chiara De Cola**
Co-tutor: Prof. Irene Izzo
Coordinatore: Prof. Gaetano Guerra

INDEX

List of abbreviations

Cbz Benzyl chloroformate

DCC *N,N'*-Dicyclohexylcarbodiimide

DCM Dichloromethane

DIPEA Diisopropylethylamine

DMF *N, N'*-dimethylformamide

Fmoc Fluorenylmethyloxycarbonyl chloride

HBTU O-Benzotriazole-N,N,N',N'-tetramethyl-uronium-hexafluorophosphate

HATU O-(7-Azabenzotriazol-1-yl)-N,N,N',N'-tetramethyluronium hexafluorophosphate

PyBOP benzotriazol-1-yl-oxytripyrrolidinophosphonium hexafluorophosphate

PNA Peptide nucleic acid

***t*-Bu** *terz*-Butyl

THF Tetrahydrofuran

Chapter 1

1. Introduction

"Giunto a questo punto della vita, quale chimico, davanti alla tabella del Sistema Periodico, o agli indici monumentali del Beilstein o del Landolt, non vi ravvisa sparsi i tristi brandelli, o i trofei, del proprio passato professionale? Non ha che da sfogliare un qualsiasi trattato, e le memorie sorgono a grappoli: c'è fra noi chi ha legato il suo destino, indelebilmente, al bromo o al propilene o al gruppo –NCO o all'acido glutammico; ed ogni studente in chimica, davanti ad un qualsiasi trattato, dovrebbe essere consapevole che in una di quelle pagine, forse in una sola riga o formula o parola, sta scritto il suo avvenire, in caratteri indecifrabili, ma che diventeranno chiari <<POI>>: dopo il successo o l'errore o la colpa, la vittoria o la disfatta.

Ogni chimico non più giovane, riaprendo alla pagina << verhangnisvoll >> quel medesimo trattato, è percosso da amore o disgusto, si rallegra o si dispera".

Da "Il Sistema Periodico", Primo Levi.

Proteins are vital for essentially every known organism. The development of a deeper understanding of protein–protein interactions and the design of novel peptides, which selectively interact with proteins are fields of active research.

One way how nature controls the protein functions within living cells is by regulating protein–protein interactions. These interactions exist on nearly every level of cellular function which means they are of key importance for virtually every process in a living organism. Regulation of the protein-protein interactions plays a crucial role in unicellular and multicellular organisms, including man, and represents the perfect example of molecular recognition[1].

Synthetic methods like the solid-phase peptide synthesis (SPPS) developed by B. Merrifield[2] made it possible to synthesize polypeptides for pharmacological and clinical testing as well as for use as drugs or in diagnostics.

As a result, different new peptide-based drugs are at present accessible for the treatment of prostate and breast cancer, as HIV protease inhibitors or as ACE inhibitors to treat hypertension and congestive heart failures, to mention only few examples[1].

Unfortunately, these small peptides typically show high conformational flexibility and a low *in-vivo* stability which hampers their application as tools in medicinal diagnostics or molecular biology. A major difficulty in these studies is the conformational flexibility of most peptides and the high dependence of their conformations on the surrounding environment which often leads to a conformational equilibrium. The high flexibility of natural polypeptides is due to the multiple conformations that are energetically possible for each residue of the incorporated amino acids. Every amino acid has two degrees of conformational freedom, N–Cα (Φ) and Cα–CO (Ψ) resulting in approximately 9 stable local conformations[1]. For a small peptide with only 40 amino acids in length the

[1] A. Grauer, B. König *Eur. J. Org. Chem.* **2009**, 5099–5111.
[2] a) R. B. Merrifield, *Federation Proc.* **1962**, *21*, 412; b) R. B. Merrifield, *J. Am. Chem. Soc.* **1964**, *86*, 2149–2154.

number of possible conformations which need to be considered escalates to nearly 1040[3]. This extraordinary high flexibility of natural amino acids leads to the fact that short polypeptides consisting of the 20 proteinogenic amino acids rarely form any stable 3D structures in solution[1]. There are only few examples reported in the literature where short to medium-sized peptides (<30–50 amino acids) were able to form stable structures. In most cases they exist in aqueous solution in numerous dynamically interconverting conformations. Moreover, the number of stable short peptide structures, which are available is very limited, because of the need to use amino acids having a strong structure inducing effect like for example helix-inducing amino acids as leucine, glutamic acid or lysine. In addition, it is dubious whether the solid state conformations determined by X-ray analysis are identical to those occurring in solution or during the interactions of proteins with each other[1]. Despite their wide range of important bioactivities, polypeptides are generally poor drugs. Typically, they are rapidly degraded by proteases *in vivo*, and are frequently immunogenic.

This fact has inspired prevalent efforts to develop peptide mimics for biomedical applications, a task that presents formidable challenges in molecular design.

1.1 Peptidomimetics

One very versatile strategy to overcome such drawbacks is the use of peptidomimetics[4]. These are small molecules, which mimic natural peptides or proteins and thus produce the same biological effects as their natural role models.

They also often show a decreased activity in comparison to the protein from which they are derived. These mimetics should have the ability to bind to their natural targets in the same way as the natural peptide sequences, from which their structure was derived, do and should produce the same biological effects. It is possible to design these molecules in such a way that they show the same biological effects as their peptide role models but with enhanced properties like a higher proteolytic stability, higher bioavailability and also often with improved selectivity or potency. This makes them interesting targets for the discovery of new drug candidates.

For the progress of potent peptidomimetics, it is required to understand the forces that lead to protein–protein interactions with nanomolar or often even higher affinities.

These strong interactions between peptides and their corresponding proteins are mainly based on side chain interactions indicating that the peptide backbone itself is not an absolute requirement for high affinities.

This allows chemists to design peptidomimetics basically from any scaffold known in chemistry by replacing the amide backbone partially or completely by other structures. Peptidomimetics, furthermore, can have some peculiar qualities, such as a good solubility in aqueous solutions, access to facile sequences-specific assembly of monomers containing chemically diverse side chains and the capacity to form stable, biomimetic folded structures[5].

Most important is that the backbone is able to place the amino acid side chains in a defined 3D-position to allow interactions with the target protein, too. Therefore, it is necessary to develop an idea of the required structure of the peptidomimetic to show a high activity against its biological target.

---

[3] J. Venkatraman, S. C. Shankaramma, P. Balaram, *Chem. Rev.* **2001**, *101*, 3131–3152.

[4] J. A. Patch, K. Kirshenbaum, S. L. Seurynck, R. N. Zuckermann and A. E. Barron, in *Pseudo-peptides in Drug Development*, ed. P. E. Nielsen, Wiley-VCH, Weinheim, Germany, **2004**, 1–31.

The most significant parameters for an optimal peptidomimetics are: stereochemistry, charge and hydrophobicity, and these parameters can be examined by systematic exchange of single amino acids with modified amino acid. As a result, the key residues, which are essential for the biological activity, can be identified. As next step the 3D arrangement of these key residues needs to be analyzed by the use of compounds with rigid conformations to identify the most active structure[1]. In general, the development of peptidomimetics is based mainly on the knowledge of the electronic, conformational and topochemical properties of the native peptide to its target.

Two structural factors are particularly important for the synthesis of peptidomimetics with high biological activity: firstly the mimetic has to have a convenient fit to the binding site and secondly the functional groups, polar and hydrophobic regions of the mimetic need to be placed in defined positions to allow the useful interactions to take place[1].

One very successful approach to overcome these drawbacks is the introduction of conformational constraints into the peptide sequence. This can be done for example by the incorporation of amino acids, which can only adopt a very limited number of different conformations, or by cyclisation (main chain to main chain; side chain to main chain or side chain to side chain).[5]

Peptidomimetics, furthermore, can contain two different modifications: amino acid modifications or peptides' backbone modifications.

Figure **1.1** reports the most important ways to modify the backbone of peptides at different positions.

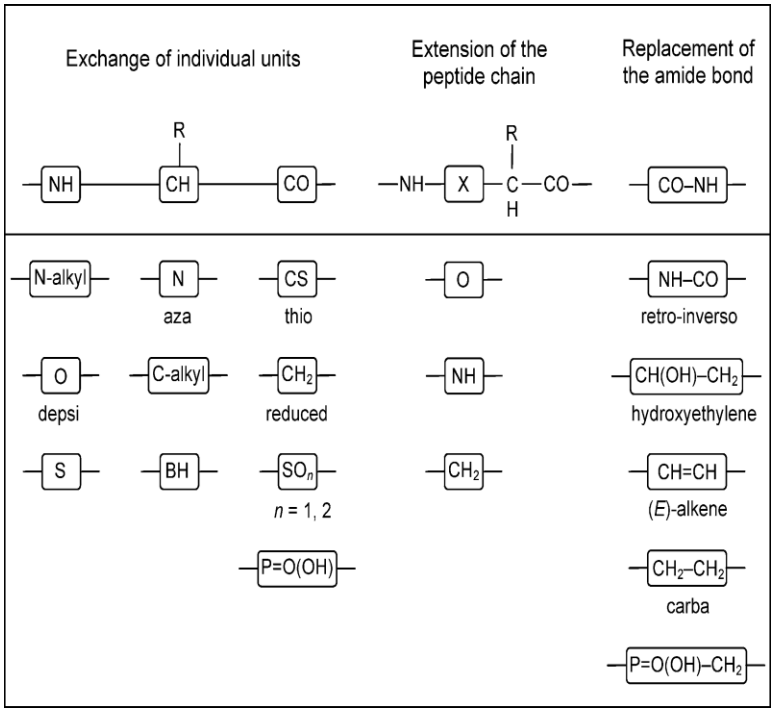

Figure 1.1. Some of the more common modifications to the peptide backbone (adapted from literature).[6]

[5]a) C. Toniolo, M. Goodman, *Introduction to the Synthesis of Peptidomimetics*, in: *Methods of Organic Chemistry: Synthesis of Peptides and Peptidomimetics* (Ed.: M. Goodman), Thieme, Stuttgart, New York, **2003**, vol. E22c, p. 1–2; b) D. J. Hill, M. J. Mio, R. B. Prince, T. S. Hughes, J. S. Moore, *Chem. Rev.* **2001**, *101*, 3893–4012.
[6] J. Gante, *Angew. Chem. Int. Ed. Engl.* **1994**, *33*, 1699–1720.

Backbone peptides modifications are a method for synthesize optimal peptidomimetics, in particular is possible:

- ✓ the replacement of the α-CH group by nitrogen to form azapeptides,
- ✓ the change from amide to ester bond to get depsipeptides,
- ✓ the exchange of the carbonyl function by a CH_2 group,
- ✓ the extension of the backbone (β-amino acids and γ-amino acids),
- ✓ the amide bond inversion (a retro-inverse peptidomimetic),
- ✓ The carba, alkene or hydroxyethylene groups are used in exchange for the amide bond.
- ✓ The shift of the alkyl group from α-CH group to α-N group.

Most of these modifications do not guide to a higher restriction of the global conformations, but they have influence on the secondary structure due to the altered intramolecular interactions like different hydrogen bonding. Additionally, the length of the backbone can be different and a higher proteolytic stability occurs in most cases [1].

1.2 Peptoids: A Promising Class of Peptidomimetics.

If we shift the chain of α-CH group by one position on the peptide backbone, we produced the disappearance of all the intra-chain stereogenic centers and the formation of a sequence of variously substituted *N*-alkylglycines (figure **1.2**).

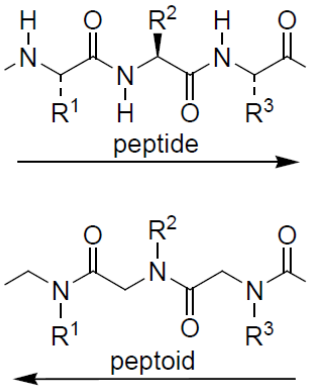

Figure 1.2. Comparison of a portion of a peptide chain with a portion of a peptoid chain.

Oligomers of *N*-substituted glycine, or peptoids, were developed by Zuckermann and co-workers in the early 1990's[7]. They were initially proposed as an accessible class of molecules from which lead compounds could be identified for drug discovery.

Peptoids can be described as mimics of α-peptides in which the side chain is attached to the backbone amide nitrogen instead of the α-carbon (figure **1.2**). These oligomers are an attractive scaffold for biological applications because they can be generated using a straightforward, modular synthesis that allows the incorporation of a wide variety of functionalities[8]. Peptoids have been evaluated as tools to

[7] R. J. Simon, R. S. Kania, R. N. Zuckermann, V. D. Huebner, D. A. Jewell, S. Banville, S. Ng, L.Wang, S. Rosenberg, C. K. Marlowe, D. C. Spellmeyer, R. Tan, A. D. Frankel, D. V. Santi, F. E. Cohen and P. A. Bartlett, *Proc. Natl. Acad. Sci. U. S. A.*, **1992**, *89*, 9367–9371.

study biomolecular interactions,[8] and also hold significant promise for therapeutic applications due to their enhanced proteolytic stabilities[8] and increased cellular permeabilities[9] relative to α-peptides.

Biologically active peptoids have also been discovered by rational design (*i.e.*, using molecular modeling), and were synthesized either individually or in parallel focused libraries[10]. For some applications, a well-defined structure is also necessary for peptoid function to display the functionality in a particular orientation, or to adopt a conformation that promotes interaction with other molecules. However, in other biological applications, peptoids lacking defined structures appear to possess superior activities over structured peptoids.

This introduction will focus primarily on the relationship between peptoid structure and function. A comprehensive review of peptoids in drug discovery, detailing peptoid synthesis, biological applications, and structural studies, was published by Barron, Kirshenbaum, Zuckermann, and co-workers in 2004[4]. Since then, significant advances have been made in these areas, and new applications for peptoids have emerged. In addition, new peptoid secondary structural motifs have been reported, as well as strategies to stabilize those structures. Lastly, the emergence of peptoid with tertiary structures has driven chemists towards new structures with peculiar properties and side chains. Peptoid monomers are linked through polyimide bonds, in contrast to the amide bonds of peptides. Unfortunately, peptoids do not have the hydrogen of the peptide secondary amide, and are consequently incapable of forming the same types of hydrogen bond networks that stabilize peptide helices and *β*-sheets.

The peptoids oligomers backbone is achiral; however stereogenic centers can be included in the side chains to obtain secondary structures with a preferred handedness[4]. In addition, peptoids carrying *N*-substituted versions of the proteinogenic side chains are highly resistant to degradation by proteases, which is an important attribute of a pharmacologically useful peptide mimic[4].

1.3 Conformational studies of peptoids

The fact that peptoids are able to form a variety of secondary structural elements, including helices and hairpin turns, suggests a range of possible conformations that can allow the generation of functional folds.[11]

Some studies of molecular mechanics, have demonstrated that peptoid oligomers bearing bulky chiral (*S*)-*N*-(1-phenylethyl) side chains would adopt a polyproline type I helical conformation, in agreement with subsequent experimental findings[12].

Kirshenbaum *at al.*[12] has shown agreement between theoretical models and the trans amide of *N*-aryl peptoids, and suggested that they may form polyproline type II helices. Combined, these studies suggest that the backbone conformational propensities evident at the local level may be readily translated into the conformations of larger oligomers chains.

N-α-chiral side chains were shown to promote the folding of these structures in both solution and the solid state, despite the lack of main chain chirality and secondary amide hydrogen bond donors crucial to the formation of many α-peptide secondary structures.

---

[8] S. M. Miller, R. J. Simon, S. Ng, R. N. Zuckermann, J. M. Kerr, W. H. Moos, *Bioorg. Med. Chem. Lett.*, **1994,** 4, 2657–2662.
[9] Y. U.Kwon and T. Kodadek, *J. Am. Chem. Soc.*, **2007**, 129, 1508–1509.
[10] T. Hara, S. R. Durell, M. C. Myers and D. H. Appella, *J. Am. Chem. Soc.*, **2006**, 128, 1995–2004.
[11] G. L. Butterfoss, P. D. Renfrew, B. Kuhlman, K. Kirshenbaum, R. Bonneau, *J. Am. Chem. Soc.***, 2009**, *131*, 16798–16807.

While computational studies initially suggested that steric interactions between *N*-α-chiral aromatic side chains and the peptoid backbone primarily dictated helix formation, both intra- and intermolecular aromatic stacking interactions[12] have also been proposed to participate in stabilizing such helices[13].

In addition to this consideration, Gorske *et al.*[14] selected side chain functionalities to look at the effects of four key types of noncovalent interactions on peptoid amide *cis*/*trans* equilibrium: (1) $n\rightarrow\pi^*$ interactions between an amide and an aromatic ring ($n\rightarrow\pi^*$Ar), (2) $n\rightarrow\pi^*$ interactions between two carbonyls ($n\rightarrow\pi^*$ C=O), (3) side chain-backbone steric interactions, and (4) side chain-backbone hydrogen bonding interactions. In figure **1.3** are reported, as example, only $n\rightarrow\pi^*$Ar and $n\rightarrow\pi^*$C=O interactions.

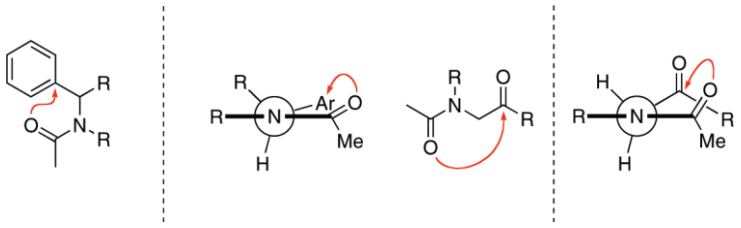

A **B**

Figure 1.3. A: (Left) $n\rightarrow\pi^*$Ar interaction (indicated by the red arrow) proposed to increase of $K_{cis/trans}$ (equilibrium constant between *cis* and *trans* conformation) for peptoid backbone amides. (Right) Newman projection depicting the $n\rightarrow\pi^*$Ar interaction. **B:** (Left) $n\rightarrow\pi^*$C=O interaction (indicated by the red arrow) proposed to reduce $K_{cis/trans}$ for the donating amide in peptoids. (Right) Newman projection depicting the $n\rightarrow\pi^*$C=O interaction.

Other classes of peptoid side chains have been designed to introduce dipole-dipole, hydrogen bonding, and electrostatic interactions stabilizing the peptoid helix.

In addition, such constraints may further rigidify peptoid structure, potentially increasing the ability of peptoid sequences for selective molecular recognition.

In a relatively recent contribution Kirshenbaum[15] reported that peptoids undergo to a very efficient head-to-tail cyclisation using standard coupling agents. The introduction of the covalent constraint enforces conformational ordering, thus facilitating the crystallization of a cyclic peptoid hexamer and a cyclic peptoid octamer.

Peptoids can form well-defined three-dimensional folds in solution, too. In fact, peptoid oligomers with α-chiral side chains were shown to adopt helical structures [16]; a threaded loop structure was formed

[12] C. W. Wu, T. J. Sanborn, R. N. Zuckermann, A. E. Barron, *J. Am. Chem. Soc.* **2001**, *123*, 2958–2963.
[13] T. J. Sanborn, C. W. Wu, R. N. Zuckermann, A. E. Barron, *Biopolymers*, **2002**, *63*, 12–20.
[14] B. C. Gorske, J. R. Stringer, B. L. Bastian, S. A. Fowler, H. E. Blackwell , *J. Am. Chem. Soc*., **2009**, *131*, 16555–16567.
[15] S. B. Y. Shin, B. Yoo, L. J. Todaro, K. Kirshenbaum, *J. Am. Chem. Soc.*, **2007**, 129, 3218-3225.
[16] (a) K. Kirshenbaum, A. E. Barron, R. A. Goldsmith, P. Armand, E. K. Bradley, K. T. V. Truong, K. A. Dill, F. E. Cohen, R. N. Zuckermann, *Proc. Natl. Acad. Sci. U.S.A.* **1998**, *95*, 4303–4308. (b) P. Armand, K. Kirshenbaum, R. A. Goldsmith, S. Farr-Jones, A. E. Barron, K. T. V. Truong, K. A. Dill, D. F. Mierke, F. E. Cohen, R. N. Zuckermann, E. K. Bradley, *Proc. Natl. Acad. Sci. U.S.A.* **1998**, *95*, 4309–4314. (c) C. W. Wu, K. Kirshenbaum, T. J. Sanborn, J. A. Patch, K. Huang, K. A. Dill, R. N. Zuckermann, A. E. Barron, *J. Am. Chem. Soc.* **2003**, *125*, 13525–13530.

by intramolecular hydrogen bonds in peptoid nonamers[20]; head-to-tail macrocyclizations provided conformationally restricted cyclic peptoids.

These studies demonstrate the importance of (1) access to chemically diverse monomer units and (2) precise control of secondary structures to expand applications of peptoid helices.

The degree of helical structure increases as chain length grows, and for these oligomers becomes fully developed at length of approximately 13 residues. Aromatic side chain-containing peptoid helices generally give rise to CD spectra that are strongly reminiscent of that of a peptide α-helix, while peptoid helices based on aliphatic groups give rise to a CD spectrum that resembles the polyproline type-I helical.

1.4 Peptoids' Applications.

The well-defined helical structure associated with appropriately substituted peptoid oligomers can be employed to construct compounds that closely mimic the structures and functions of certain bioactive peptides. In this paragraph, are shown some examples of peptoids that have antibacterial and antimicrobial properties, molecular recognition properties, of metal complexing peptoids, of catalytic peptoids, and of peptoids tagged with nucleobases.

1.4.1 Antibacterial and antimicrobial properties

The antibiotic activities of structurally diverse sets of peptides/peptoids derive from their action on microbial cytoplasmic membranes. The model proposed by Shai–Matsuzaki–Huan[17] (SMH) presumes alteration and permeabilization of the phospholipid bilayer with irreversible damage of the critical membrane functions. Cyclization of linear peptide/peptoid precursors (as a mean to obtain conformational order), has been often neglected[18], despite the fact that nature offers a vast assortment of powerful cyclic antimicrobial peptides[19]. However, macrocyclization of *N*-substituted glycines gives

[17] (a) Matsuzaki, K. Biochim. Biophys. Acta 1999, 1462, 1; (b) Yang, L.; Weiss, T. M.; Lehrer, R. I.; Huang, H. W. Biophys. J. 2000, 79, 2002; (c) Shai, Y. Biochim.Biophys. Acta 1999, 1462, 55.

[18] Chongsiriwatana, N. P.; Patch, J. A.; Czyzewski, A. M.; Dohm, M. T.; Ivankin, A.; Gidalevitz, D.; Zuckermann, R. N.; Barron, A. E. *Proc. Natl. Acad. Sci. U.S.A.* **2008,** 105, 2794.

[19] Interesting examples are: (a) Motiei, L.; Rahimipour, S.; Thayer, D. A.; Wong, C. H.; Ghadiri, M. R. *Chem. Commun*. **2009**, 3693; (b) Fletcher, J. T.; Finlay, J. A.; Callow, J. A.; Ghadiri, M. R. *Chem. Eur. J.* **2007**, 13, 4008; (c) Au, V. S.; Bremner, J. B.; Coates, J.; Keller, P. A.; Pyne, S. G. *Tetrahedron* **2006,** 62, 9373; (d) Fernandez-Lopez, S.; Kim, H.-S.; Choi, E. C.; Delgado, M.; Granja, J. R.; Khasanov, A.; Kraehenbuehl, K.; Long, G.; Weinberger, D. A.; Wilcoxen, K. M.; Ghadiri, M. R. *Nature* **2001**, 412, 452; (e) Casnati, A.; Fabbi, M.; Pellizzi, N.; Pochini, A.; Sansone, F.; Ungaro, R.; Di Modugno, E.; Tarzia, G. *Bioorg. Med. Chem. Lett*. **1996**, 6, 2699; (f) Robinson, J. A.; Shankaramma, C. S.; Jetter, P.; Kienzl, U.; Schwendener, R. A.; Vrijbloed, J. W.; Obrecht, D. *Bioorg. Med. Chem.* **2005**, 13, 2055.

circular peptoids[20], showing reduced conformational freedom[21] and excellent membrane-permeabilizing activity[22].

Antimicrobial peptides (AMPs) are found in myriad organisms and are highly effective against bacterial infections[23]. The mechanism of action for most AMPs is permeabilization of the bacterial cytoplasmic membrane, which is facilitated by their amphipathic structure[24].

The cationic region of AMPs confers a degree of selectivity for the membranes of bacterial cells over mammalian cells, which have negatively charged and neutral membranes, respectively. The hydrophobic portions of AMPs are supposed to mediate insertion into the bacterial cell membrane. Although AMPs possess many positive attributes, they have not been developed as drugs due to the poor pharmacokinetics of α-peptides. This problem creates an opportunity to develop peptoid mimics of AMPs as antibiotics and has sparked considerable research in this area[25].

De Riccardis[26] *et al.* investigated the antimicrobial activities of five new cyclic cationic hexameric α-peptoids comparing their efficacy with the linear cationic and the cyclic neutral counterparts (figure **1.4**).

[20] (a) Craik, D. J.; Cemazar, M.; Daly, N. L. Curr. Opin. Drug Discovery Dev. 2007, 10, 176; (b) Trabi, M.; Craik, D. J. Trend *Biochem. Sci.* **2002**, 27, 132.

[21] (a) Maulucci, N.; Izzo, I.; Bifulco, G.; Aliberti, A.; De Cola, C.; Comegna, D.; Gaeta, C.; Napolitano, A.; Pizza, C.; Tedesco, C.; Flot, D.; De Riccardis, F. *Chem. Commun*. **2008**, 3927; (b) Kwon, Y.-U.; Kodadek, T. *Chem. Commun*. **2008**, 5704; (c) Vercillo, O. E.; Andrade, C. K. Z.; Wessjohann, L. A. *Org. Lett*. **2008**, 10, 205; (d) Vaz, B.; Brunsveld, L. *Org. Biomol. Chem.* **2008**, 6, 2988; (e) Wessjohann, L. A.; Andrade, C. K. Z.; Vercillo, O. E.; Rivera, D. G.. *In Targets in Heterocyclic Systems*; Attanasi, O. A., Spinelli, D., Eds.*; Italian Society of Chemistry*, **2007;** Vol. 10, pp 24–53; (f) Shin, S. B. Y.; Yoo, B.; Todaro, L. J.; Kirshenbaum, K. *J. Am. Chem. Soc*. **2007**, 129, 3218; (g) Hioki, H.; Kinami, H.; Yoshida, A.; Kojima, A.; Kodama, M.; Taraoka, S.; Ueda, K.; Katsu, T. *Tetrahedron Lett*. **2004**, 45, 1091.

[22] (a) Chatterjee, J.; Mierke, D.; Kessler, H. *Chem. Eur. J.* **2008,** 14, 1508; (b) Chatterjee, J.; Mierke, D.; Kessler, H. *J. Am. Chem. Soc*. **2006**, 128, 15164; (c) Nnanabu, E.; Burgess, K. *Org. Lett.* **2006**, 8, 1259; (d) Sutton, P. W.; Bradley, A.; Farràs, J.; Romea, P.; Urpì, F.; Vilarrasa, J. *Tetrahedron* **2000,** 56, 7947; (e) Sutton, P. W.; Bradley, A.; Elsegood, M. R.; Farràs, J.; Jackson, R. F. W.; Romea, P.; Urpì, F.; Vilarrasa, J. *Tetrahedron Lett.* **1999**, 40, 2629.

[23] A. Peschel and H.-G. Sahl, *Nat. Rev. Microbiol.*, **2006**, ***4***, 529–536.

[24] R. E. W. Hancock and H.-G. Sahl, *Nat. Biotechnol.*, **2006**, ***24***, 1551–1557.

[25] For a review of antimicrobial peptoids, see: I. Masip, E. Pèrez Payà, A. Messeguer, *Comb. Chem. High Throughput Screen.*, **2005**, 8, 235–239.

[26] D. Comegna, M. Benincasa, R. Gennaro, I. Izzo, F. De Riccardis, *Bioorg. Med. Chem,*. **2010**, 18, 2010–2018.

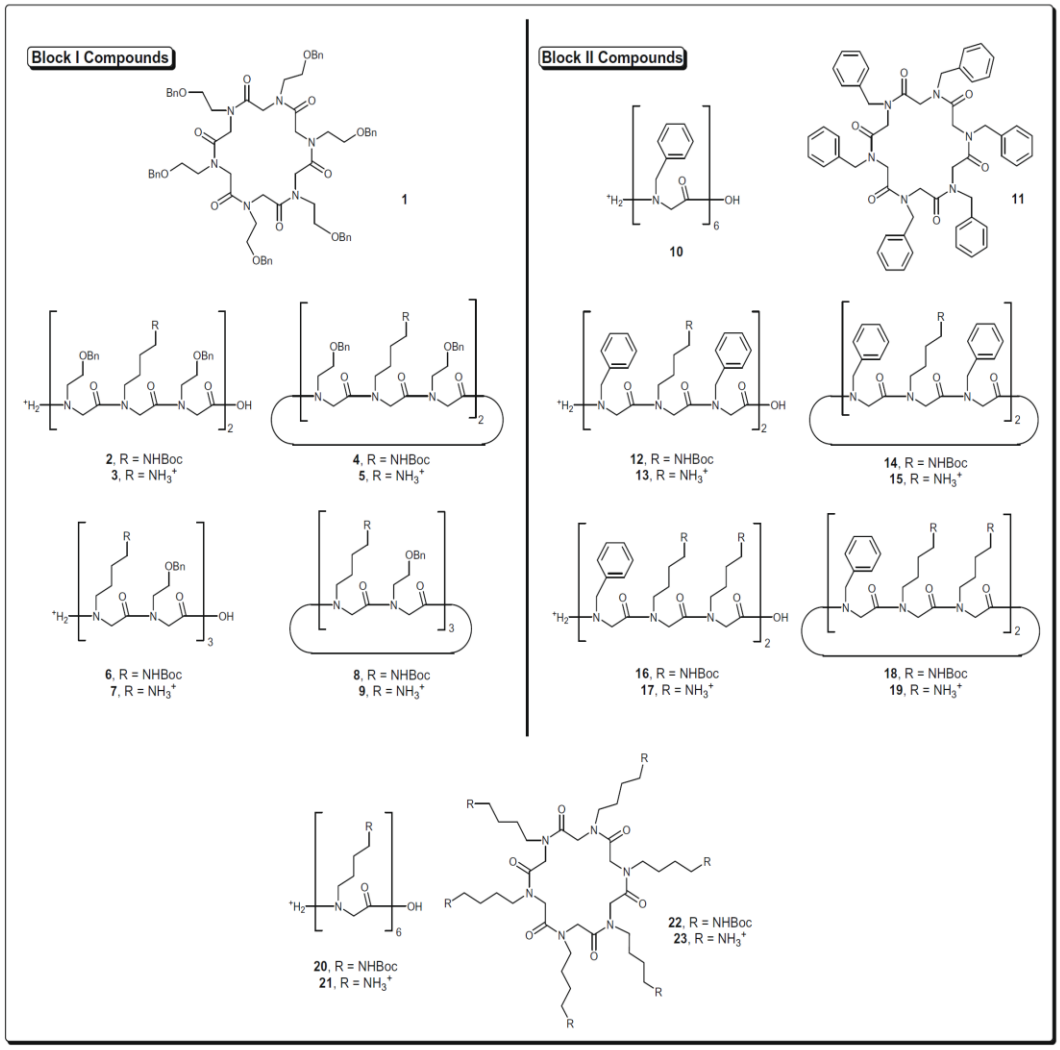

Figure 1.4. Structures of synthesized linear and cyclic peptoids described by De Riccardis *at al*. Bn = benzyl group; Boc= t-butoxycarbonyl group.

The synthesized peptoids have been assayed against clinically relevant bacteria and fungi, including *Escherichia coli*, *Staphylococcus aureus*, *amphotericin* β-resistant *Candida albicans*, and *Cryptococcus neoformans*[27].

The purpose of this study was to explore the biological effects of the cyclisation on positively charged oligomeric *N*-alkylglycines, with the idea to mimic the natural amphiphilic peptide antibiotics. The long-term aim of the effort was to find a key for the rational design of novel antimicrobial compounds using the finely tunable peptoid backbone.

The exploration for possible biological activities of linear and cyclic α-peptoids, was started with the assessment of the antimicrobial activity of the known[21a] *N*-benzyloxyethyl cyclohomohexamer (Figure **1.4**, Block I). This neutral cyclic peptoid was considered a promising candidate in the antimicrobial

[27] M. Benincasa, M. Scocchi, S. Pacor, A. Tossi, D. Nobili, G. Basaglia, M. Busetti, R. J. Gennaro, *Antimicrob. Chemother*. **2006**, 58, 950.

assays for its high affinity to the first group alkali metals (Ka ~ 106 for Na^+, Li^+ and K^+)[21a] and its ability to promote Na^+/H^+ transmembrane exchange through ion-carrier mechanism[28], a behavior similar to that observed for valinomycin, a well known K^+-carrier with powerful antibiotic activity[29]. However, determination of the MIC values showed that neutral chains did not exert any antimicrobial activity against a group of selected pathogenic fungi, and of Gram-negative and Gram-positive bacterial strains even at concentrations up to 1 mM.

Detailed structure–activity relationship (SAR) studies[30] have revealed that the amphiphilicity of the peptides/peptidomimetics and the total number of positively charged residues, impact significantly on the antimicrobial activity. Therefore, cationic versions of the neutral cyclic α-peptoids were planned (Figure **1.4**, block I and block II compounds). In this study were also included the linear cationic precursors to evaluate the effect of macrocyclization on the antimicrobial activity. Cationic peptoids were tested against four pathogenic fungi and three clinically relevant bacterial strains. The tests showed a marked increase of the antibacterial and antifungal activities with cyclization. The presence of charged amino groups also influenced the antimicrobial efficacy, as shown by the activity of the bi- and tricationic compounds, when compared with the ineffective neutral peptoid. These results are the first indication that cyclic peptoids can represent new motifs on which to base artificial antibiotics.

In 2003, Barron and Patch[31] reported peptoid mimics of the helical antimicrobial peptide magainin-2 that had low micromolar activity against *Escherichia coli* (MIC = 5–20 mM) and *Bacillus subtilis* (MIC = 1–5 mM).

The magainins exhibit highly selective and potent antimicrobial activity against a broad spectrum of organisms[5]. As these peptides are facially amphipathic, the magainins have a cationic helical face mostly composed of lysine residues, as well as hydrophobic aromatic (phenylalanine) and hydrophobic aliphatic (valine, leucine and isoleucine) helical faces. This structure is responsible for their activity[4].

Peptoids have been shown to form remarkably stable helices, with physical characteristics similar to those of peptide polyproline type-I helices. In fact, a series of peptoid magainin mimics with this type of three-residue periodic sequences has been synthesized[4] and tested against *E. coli* JM109 and *B. subtulis* BR151. In all cases, peptoids are individually more active against the Gram-positive species. The amount of hemolysis induced by these peptoids correlated well with their hydrophobicity. In summary, these recently obtain results demonstrate that certain amphipathic peptoid sequences are also capable of antibacterial activity.

1.4.2 Molecular Recognition

Peptoids are currently being studied for their potential to serve as pharmaceutical agents and as chemical tools to study complex biomolecular interactions. Peptoid–protein interactions were first demonstrated in a 1994 report by Zuckermann and co-workers,[8] where the authors examined the high-affinity binding of peptoid dimers and trimers to G-protein-coupled receptors. These groundbreaking studies have led to the identification of several peptoids with moderate to good affinity and, more

[28] C. De Cola, S. Licen, D. Comegna, E. Cafaro, G. Bifulco, I. Izzo, P. Tecilla, F. De Riccardis, *Org. Biomol. Chem.* **2009**, 7, 2851.
[29] N. R. Clement, J. M. Gould, *Biochemistry,* **1981**, 20, 1539.
[30] J. I. Kourie, A. A. Shorthouse, *Am. J. Physiol. Cell. Physiol.* **2000**, 278, C1063.
[31] J. A. Patch and A. E. Barron, *J. Am. Chem. Soc.*, **2003**, 125, 12092– 12093.

importantly, excellent selectivity for protein targets that implicated in a range of human diseases. There are many different interactions between peptoid and protein, and these interactions can induce a certain inhibition, cellular uptake and delivery. Synthetic molecules capable of activating the expression of specific genes would be valuable for the study of biological phenomena and could be therapeutically useful. From a library of ~100000 peptoid hexamers, Kodadek and co-workers recently identified three peptoids (**24-26**) with low micromolar binding affinities for the coactivator CREB-binding protein (CBP) *in vitro* (Figure **1.5**)[9]. This coactivator protein is involved in the transcription of a large number of mammalian genes, and served as a target for the isolation of peptoid activation domain mimics. Of the three peptoids, only **24** was selective for CBP, while peptoids **25** and **26** showed higher affinities for bovine serum albumin. The authors concluded that the promiscuous binding of **25** and **26** could be attributed to their relatively "sticky" natures (*i.e.*, aromatic, hydrophobic amide side chains).

Inhibitors of proteasome function that can intercept proteins targeted for degradation would be valuable as both research tools and therapeutic agents. In 2007, Kodadek and co-workers[32] identified the first chemical modulator of the proteasome 19S regulatory particle (which is part of the 26S proteasome, an approximately 2.5 MDa multi-catalytic protease complex responsible for most non-lysosomal protein degradation in eukaryotic cells). A "one bead one compound" peptoid library was constructed by split and pool synthesis.

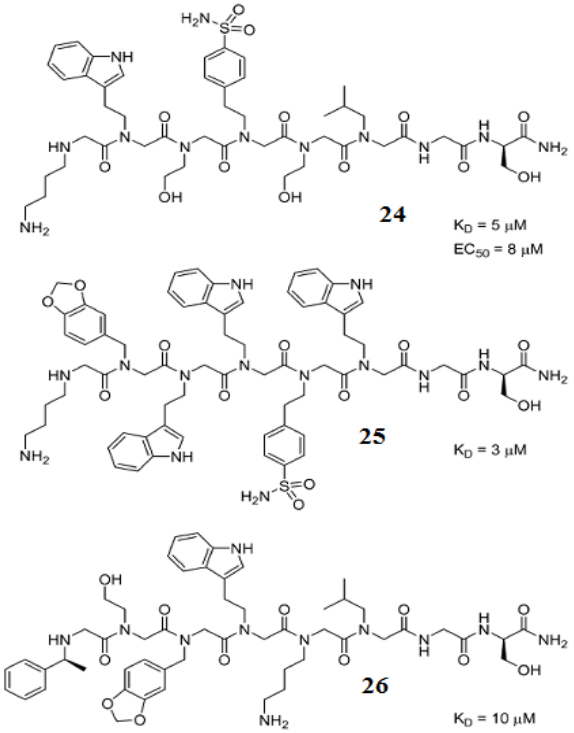

Figure 1.5. Peptoid hexamers **24**, **25**, and **26** reported by Kodadek and co-workers and their dissociation constants (KD) for coactivator CBP[33]. Peptoid **24** was able to function as a transcriptional activation domain mimic (EC_{50} = 8 mM).

[32] H. S. Lim, C. T. Archer, T. Kodadek *J. Am. Chem. Soc*., **2007,** 129, 7750.

Each peptoid molecule was capped with a purine analogue in hope of biasing the library toward targeting one of the ATPases, which are part of the 19S regulatory particle. Approximately 100 000 beads were used in the screen and a purine-capped peptoid heptamer (**27**, Figure **1.6**) was identified as the first chemical modulator of the 19S regulatory particle. In an effort to evidence the pharmacophore of **27**[33] (by performing a "glycine scan", similar to the "alanine scan" in peptides) it was shown that just the core tetrapeptoid was necessary for the activity.

Interestingly, the synthesis of the shorter peptoid **27** gave, in the experiments made on cells, a 3- to 5-fold increase in activity relative to **28**. The higher activity in the cell-based essay was likely due to increased cellular uptake, as **27** does not contain charged residues.

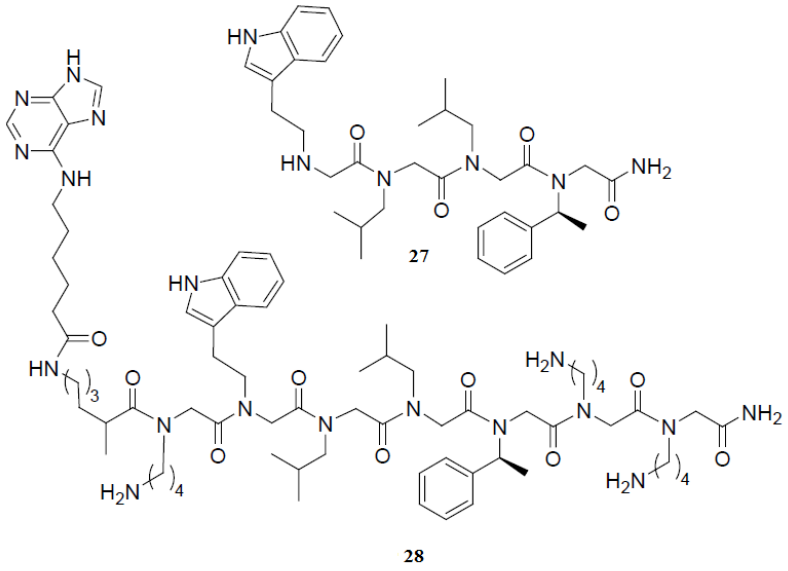

Figure 1.6. Purine capped peptoid heptamer (**28**) and tetramer (**27**) reported by Kodadek preventing protein degradation

1.4.3 Metal Complexing Peptoids

A desirable attribute for biomimetic peptoids is the ability to show binding towards receptor sites. This property can be evoked by proper backbone folding due to:

1) local side-chain stereoelectronic influences,

2) coordination with metallic species,

3) presence of hydrogen-bond donor/acceptor patterns.

Those three factors can strongly influence the peptoids' secondary structure, which is difficult to observe due to the lack of the intra-chain C=O···H–N bonds, present in the parent peptides.

Most peptoids' activities derive by relatively unstructured oligomers. If we want to mimic the sophisticated functions of proteins, we need to be able to form defined peptoid tertiary structure folds and introduce functional side chains at defined locations. Peptoid oligomers can be already folded into helical secondary structures. They can be readily generated by incorporating bulky chiral side chains

[33] H.S. Lim, C. T. Archer, Y. C. Kim, T. Hutchens, T. Kodadek *Chem. Commun.*, **2008**, 1064.

into the oligomer[22,34-35]. Such helical secondary structures are extremely stable to chemical denaturants and temperature[13]. The unusual stability of the helical structure may be a consequence of the steric hindrance of backbone φ angle by the bulky chiral side chains[36].

Zuckermann and co-workers synthesized biomimetic peptoids with zinc-binding sites[8], since zinc-binding motifs in protein are well known. Zinc typically stabilizes native protein structures or acts as a cofactor for enzyme catalysis[37-38]. Zinc also binds to cellular cysteine-rich metallothioneins solely for storage and distribution[39]. The binding of zinc is typically mediated by cysteines and histidines[50-51]. In order to create a zinc-binding site, they incorporated thiol and imidazole side chains into a peptoid two-helix bundle.

Classic zinc-binding motifs, present in proteins and including thiol and imidazole moieties, were aligned in two helical peptoid sequences, in a way that they could form a binding site. Fluorescence resonance energy transfer (FRET) reporter groups were located at the edge of this biomimetic structure in order to measure the distance between the two helical segments and probe and, at the same time, the zinc binding propensity (**29**, Figure **1.7**).

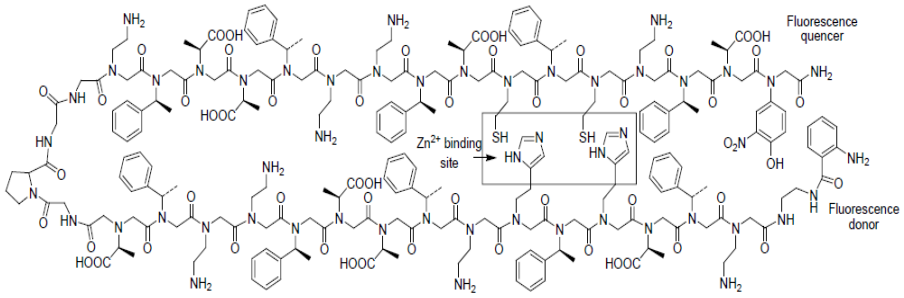

29

Figure 1.7. Chemical structure of **29**, one of the twelve folded peptoids synthesized by Zuckermann, able to form a Zn^{2+} complex.

Folding of the two helix bundles was allowed by a Gly-Gly-Pro-Gly middle region. The study demonstrated that certain peptoids were selective zinc binders at nanomolar concentration.

The formation of the tertiary structure in these peptoids is governed by the docking of preorganized peptoid helices as shown in these studies[40].

A survey of the structurally diverse ionophores demonstrated that the cyclic arrangement represents a common archetype equally promoted by chemical design[22f] and evolutionary pressure**.** Stereoelectronic effects caused by N- (and C-) substitution[22f] and/or by cyclisation, dictate the conformational ordering of peptoids' achiral polyimide backbone. In particular, the prediction and the assessment of the covalent

[34] Wu, C. W.; Kirshenbaum, K.; Sanborn, T. J.; Patch, J. A.; Huang, K.; Dill, K. A.; Zuckermann, R. N.; Barron, A. E. *J. Am. Chem. Soc.* **2003**, *125*, 13525–13530.
[35] Armand, P.; Kirshenbaum, K.; Falicov, A.; Dunbrack, R. L., Jr.; Dill,K. A.; Zuckermann, R. N.; Cohen, F. E. *Folding Des.* **1997**, *2*, 369–375.
[36] K. Kirshenbaum, R. N. Zuckermann, K. A. Dill, *Curr. Opin. Struct. Biol.* **1999**, *9*, 530–535.
[37] Coleman, J. E. *Annu. Re*V. *Biochem.* **1992**, *61*, 897–946.
[38] Berg, J. M.; Godwin, H. A. *Annu. Re*V. *Biophys. Biomol. Struct.* **1997**, *26*, 357–371.
[39] Cousins, R. J.; Liuzzi, J. P.; Lichten, L. A. *J. Biol. Chem.* **2006**, *281*, 24085–24089.
[40] B. C. Lee, R. N. Zuckermann, K. A. Dill, *J. Am. Chem. Soc.* **2005**, *127*, 10999–11009.

constraints induced by macrolactamization appears crucial for the design of conformationally restricted peptoid templates as preorganized synthetic scaffolds or receptors. In 2008 were reported the synthesis and the conformational features of cyclic tri-, tetra-, hexa-, octa and deca- *N*-benzyloxyethyl glycines (**30**-**34**, figure **1.8**)[21a].

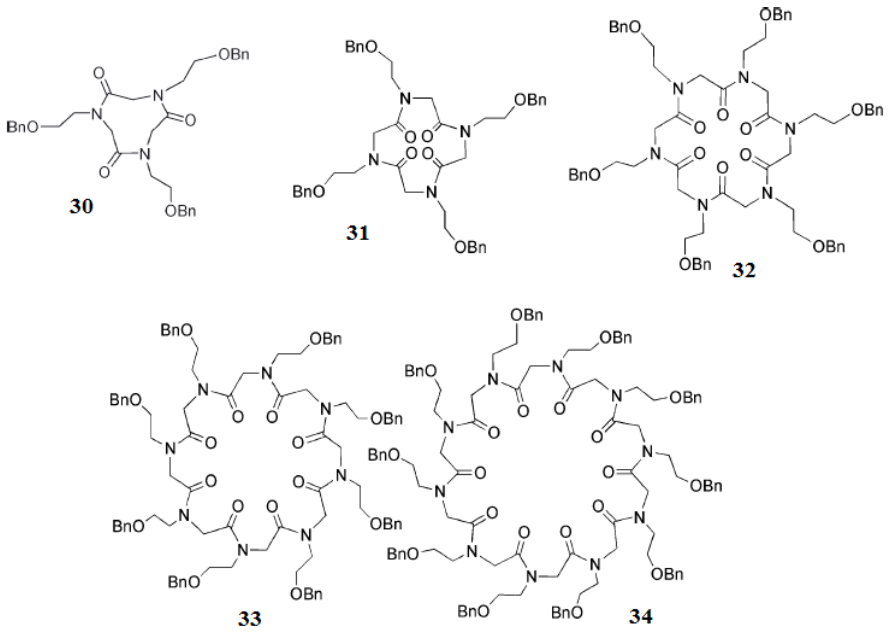

Figure 1.8. Structure of cyclic tri-, tetra-, hexa-, octa and deca- *N*-benzyloxyethyl glycines.

It was found, for the flexible eighteen-membered *N*-benzyloxyethyl cyclic peptoid **32**, high binding constants with the first group alkali metals (*K*a ~ 106 for Na^+, Li^+ and K^+), while, for the rigid *cis–trans–cis–trans* cyclic tetrapeptoid **31**, there was no evidence of alkali metals complexation. The conformational disorder in solution was seen as a propitious auspice for the complexation studies. In fact, the stepwise addition of sodium picrate to **32**, induced the formation of a new chemical species, whose concentration increased with the gradual addition of the guest. The conformational equilibrium between the free host and the sodium complex, resulted in being slower than the NMR-time scale, giving, with an excess of guest, a remarkably simplified ^{1}H NMR spectrum, reflecting the formation of a 6-fold symmetric species (Figure **1.9**).

Figure 1.9. Picture of the predicted lowest energy conformation for the complex **32** with sodium.

A conformational search on **32** as a sodium complex suggested the presence of an S_6-symmetry axis passing through the intracavity sodium cation (Figure **1.9**). The electrostatic (ion–dipole) forces stabilize

this conformation, hampering the ring inversion up to 425 K. The complexity of the r.t. ^{1}H NMR spectrum recorded for the cyclic **33**, demonstrated the slow exchange of multiple conformations on the NMR time scale. Stepwise addition of sodium picrate to **33**, induced the formation of a complex with a remarkably simplified ^{1}H NMR spectrum. With an excess of guest, we observed the formation of an 8-fold symmetric species (Figure **1.10**) was observed.

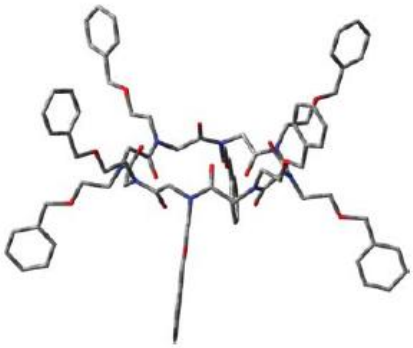

Figure 1.10. Picture of the predicted lowest energy conformations for **33** without sodium cations.

Differently from the twenty-four-membered **33**, the *N*-benzyloxyethyl cyclic homologue **34** did not yield any ordered conformation in the presence of cationic guests. The association constants (Ka) for the complexation of **32, 33** and **34** to the first group alkali metals and ammonium, were evaluated in H_2O–$CHCl_3$ following Cram's method (Table **1.1**) [41]. The results presented in Table **1.1** show a good degree of selectivity for the smaller cations.

host 32			
Picrate salt	R[a]	K_a [M^{-1}]	$-\Delta G^\circ$ [kcal/mol]
Li^+	0.17	0.95×10^6	8.1
Na^+	0.35	3.3×10^6	8.9
K^+	0.24	0.94×10^6	8.1
Rb^+	0.126	0.41×10^6	7.7
Cs^+	0.085	0.21×10^6	7.2
NH_4^+	0.18	0.38×10^6	7.6
host 33			
Picrate salt	R[a]	K_a [M^{-1}]	$-\Delta G^\circ$ [kcal/mol]
Li^+	0.14	0.66×10^6	7.9
Na^+	0.17	0.73×10^6	8.0
K^+	0.26	1.1×10^6	8.2
Rb^+	0.25	1.3×10^6	8.3
Cs^+	0.29	15×10^6	8.4
NH_4^+	0.25	0.65×10^6	7.9
host 34			
Picrate salt	R[a]	K_a [M^{-1}]	$-\Delta G^\circ$ [kcal/mol]
Li^+	0.13	0.58×10^6	7.9
Na^+	0.14	0.55×10^6	7.8
K^+	0.23	1.2×10^6	8.3
Rb^+	0.19	0.73×10^6	8.0
Cs^+	0.21	0.77×10^6	8.0
NH_4^+	0.18	0.39×10^6	7.6

[a] [Guest]/[host] in $CHCl_3$ layer at equilibrium.

Table 1.1 R, K_a, and ΔG° for cyclic peptoid hosts **32, 33** and **34** complexing picrate salt guests in $CHCl_3$ at 25 °C; figures within ±10% in multiple experiments, guest/host stoichiometry for extractions was assumed as 1:1.

[41] K. E. Koenig, G. M. Lein, P. Stuckler, T. Kaneda and D. J. Cram, *J. Am. Chem. Soc.*, **1979**, 101, 3553.

The ability of cyclic peptoids to extract cations from bulk water to an organic phase prompted us to verify their transport properties across a phospholipid membrane.

The two processes were clearly correlated although the latter is more complex implying, after complexation and diffusion across the membrane, a decomplexation step.[42-43] In the presence of NaCl as added salt, only compound **32** showed ionophoric activity while the other cyclopeptoids are almost inactive. Cyclic peptoids have different cation binding preferences and, consequently, they may exert selective cation transport. These results are the first indication that cyclic peptoids can represent new motifs on which to base artificial ionophoric antibiotics.

1.4.5 Catalytic Peptoids

An interesting example of the imaginative use of reactive heterocycles in the peptoid field, can be found in the "foldamers" mimics. "Foldamers" mimics are synthetic oligomers displaying conformational ordering. Peptoids have never been explored as platform for asymmetric catalysis. Kirshenbaum reported the synthesis of a library of helical "peptoid" oligomers enabling the oxidative kinetic resolution (OKR) of 1-phenylethanol induced by the catalyst TEMPO (2,2,6,6-tetramethylpiperidine-1-oxyl) (figure **1.14**)[44].

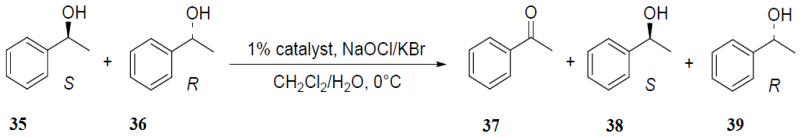

Figure 1.14. Oxidative kinetic resolution of enantiomeric phenylethanols **35** and **36.**

The TEMPO residue was covalently integrated in properly designed chiral peptoid backbones, which were used as asymmetric components in the oxidative resolution.

The study demonstrated that the enantioselectivity of the catalytic peptoids (built using the chiral (*S*)- and (*R*)-phenylethyl amines) depended on three factors: 1) the handedness of the asymmetric environment derived from the helical scaffold, 2) the position of the catalytic centre along the peptoid backbone, and 3) the degree of conformational ordering of the peptoid scaffold. The highest activity in the OKR (e.e. > 99%) was observed for the catalytic peptoids with the TEMPO group linked at the N-terminus, as evidenced in the peptoid backbones **39** (39 is also mentioned in figure **1.14**) and **40** (reported in figure **1.15**). These results revealed that the selectivity of the OKR was governed by the global structure of the catalyst and not solely from the local chirality at sites neighboring the catalytic centre.

[42] R. Ditchfield, *J. Chem. Phys.*, **1972**, 56, 5688.
[43] K. Wolinski, J. F. Hinton and P. Pulay, *J. Am. Chem. Soc*., **1990**, 112, 8251.
[44] G. Maayan, M. D. Ward, and K. Kirshenbaum, *Proc. Natl. Acad. Sci. USA*, **2009**, 106, 13679.

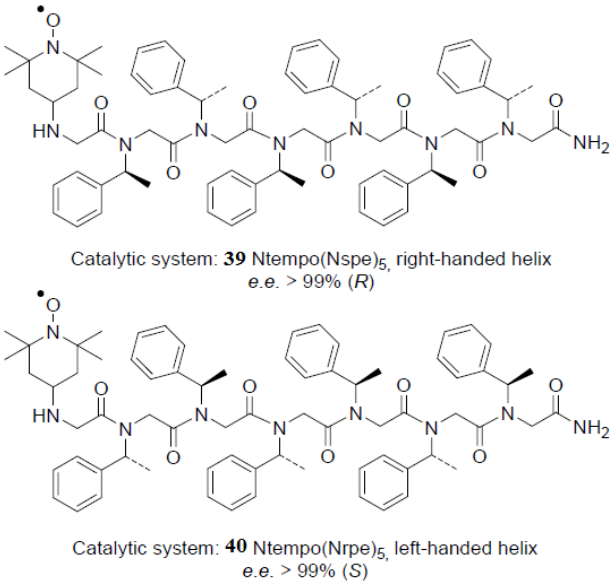

Figure 1.15. Catalytic biomimetic oligomers **39** and **40**

1.4.6 PNA and Peptoids Tagged With Nucleobases.

Nature has selected nucleic acids for storage (DNA primarily) and transfer of genetic information (RNA) in living cells, whereas proteins fulfill the role of carrying out the instructions stored in the genes in the form of enzymes in metabolism and structural scaffolds of the cells. However, no examples of protein as carriers of genetic information have yet been identified.

Self-recognition by nucleic acids is a fundamental process of life. Although, in nature, proteins are not carriers of genetic information, pseudo peptides bearing nucleobases, denominate "peptide nucleic acids" (PNA, **41**, figure **1.16**),[4] can mimic the biological functions of DNA and RNA (**42** and **43**, figure **1.16**).

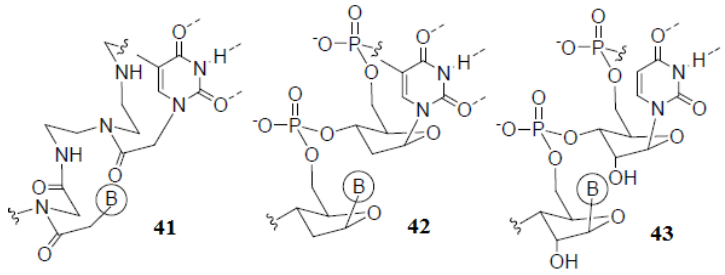

Figure 1.16. Chemical structure of PNA (**19**), DNA (**20**), RNA (**21**). B = nucleobase

The development of the aminoethylglycine polyamide (peptide) backbone oligomer with pendant nucleobases linked to the glycine nitrogen *via* an acetyl bridge now often referred to PNA, was inspired by triple helix targeting of duplex DNA in an effort to combine the recognition power of nucleobases with the versatility and chemical flexibility of peptide chemistry[4]. PNAs were extremely good structural mimics of nucleic acids with a range of interesting properties:

- ✓ DNA recognition,
- ✓ Drug discovery:

1. RNA targeting
2. DNA targeting
3. Protein targeting
4. Cellular delivery
5. Pharmacology

✓ Nucleic acid detection and analysis,
✓ Nanotechnology,
✓ Pre-RNA world.

The very simple PNA platform has inspired many chemists to explore analogs and derivatives in order to understand and/or improve the properties of this class DNA mimics. As the PNA backbone is more flexible (has more degrees of freedom) than the phosphodiester ribose backbone, one could hope that adequate restriction of flexibility would yield higher affinity PNA derivates.

The success of PNAs made it clear that oligonucleotide analogues could be obtained with drastic changes from the natural model, provided that some important structural features were preserved.

The PNA scaffold has served as a model for the design of new compounds able to perform DNA recognition. One important aspect of this type of research is that the design of new molecules and the study of their performances are strictly interconnected, inducing organic chemists to collaborate with biologists, physicians and biophysicists.

An interesting property of PNAs, which is useful in biological applications, is their stability to both nucleases and peptidases, since the "unnatural" skeleton prevents recognition by natural enzymes, making them more persistent in biological fluids.[45] The PNA backbone, which is composed by repeating *N*-(2 aminoethyl)glycine units, is constituted by six atoms for each repeating unit and by a two atom spacer between the backbone and the nucleobase, similarly to the natural DNA. However, the PNA skeleton is neutral, allowing the binding to complementary polyanionic DNA to occur without repulsive electrostatic interactions, which are present in the DNA:DNA duplex. As a result, the thermal stability of the PNA:DNA duplexes (measured by their melting temperature) is higher than that of the natural DNA:DNA double helix of the same length.

In DNA:DNA duplexes the two strands are always in an antiparallel orientation (with the 5'-end of one strand opposed to the 3'- end of the other), while PNA:DNA adducts can be formed in two different orientations, arbitrarily termed parallel and antiparallel (figure **1.17**), both adducts being formed at room temperature, with the antiparallel orientation showing higher stability.

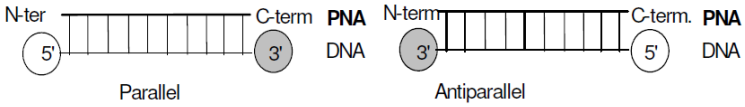

Figure 1.17. Parallel and antiparallel orientation of the PNA:DNA duplexes

PNA can generate triplexes PAN-DNA-PNA, the base pairing in triplexes occurs *via* Watson-Crick and Hoogsteen hydrogen bonds (figure **1.18**).

[45] Demidov V.A., Potaman V.N., Frank-Kamenetskii M. D., Egholm M., Buchardt O., Sonnichsen S. H., Nielsen P.E., *Biochem. Pharmscol.* **1994**, *48*, 1310.

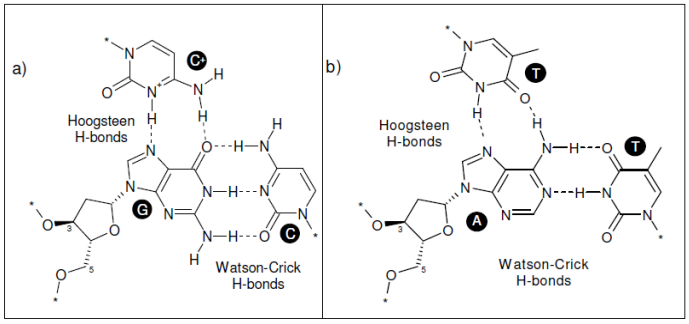

Figure 1.18. Hydrogen bonding in triplex PNA2/DNA: C+GC (a) and TAT (b)

In the case of triplex formation, the stability of these type of structures is very high: if the target sequence is present in a long dsDNA tract, the PNA can displace the opposite strand by opening the double helix in order to form a triplex with the other, thus inducing the formation of a structure defined as "P-loop", in a process which has been defined as "strand invasion" (figure **1.19**).[46]

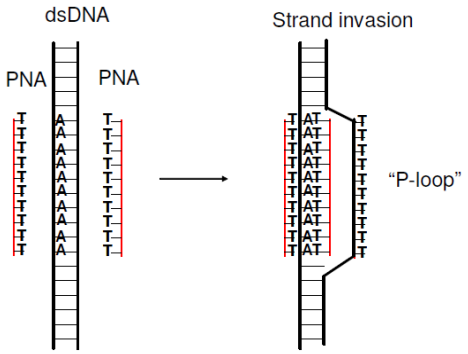

Figure 1.19. Mechanism of strand invasion of double stranded DNA by triplex formation

However, despite the excellent attributes, PNA has two serious limitations: low water solubility[47] and poor cellular uptake[48].

Many modifications of the basic PNA structure have been proposed in order to improve their performances in term of affinity and specificity towards complementary oligonucleotide sequences. A modification introduced in the PNA structure can improve its properties generally in three different ways:

i) Improving DNA binding affinity;

ii) Improving sequence specificity, in particular for directional preference (antiparallel vs parallel) and mismatch recognition;

[46] Egholm M., Buchardt O., Nielsen P.E., Berg R.H., *J. Am. Chem. Soc.*, **1992**, *114*,1895.

[47] (a) U. Koppelhus and P. E. Nielsen, *Adv. Drug. Delivery Rev*., **2003**, *55*, 267; (b) P. Wittung, J. Kajanus, K. Edwards, P. E. Nielsen, B. Nordén, and B. G. Malmstrom, FEBS Lett., **1995**, 365, 27.

[48] (a) E. A. Englund, D. H. Appella, Angew. Chem. Int. Ed., **2007**, *46*, 1414; (b) A. Dragulescu-Andrasi, S. Rapireddy, G. He, B. Bhattacharya, J. J. Hyldig-Nielsen, G. Zon, and D. H. Ly, *J. Am. Chem. Soc.*, **2006**, *128*, 16104; (c) P. E. Nielsen, Q. Rev. Biophys., **2006**, 39, 1; (d) A. Abibi, E. Protozanova, V. V. Demidov, and M. D. Frank-Kamenetskii, Biophys. J., **2004**, *86*, 3070.

iii) Improving bioavailability, (cell internalization, pharmacokinetics, etc.).

Structure activity relationships showed that the original design containing a 6-atom repeating unit and a 2-atom spacer between backbone and the nucleobase was optimal for DNA recognition. Introduction of different functional groups with different charges/polarity/flexibility have been described and are extensively reviewed in several papers[49,50,51]. These studies showed that a "constrained flexibility" was necessary to have good DNA binding (figure **1.20**).

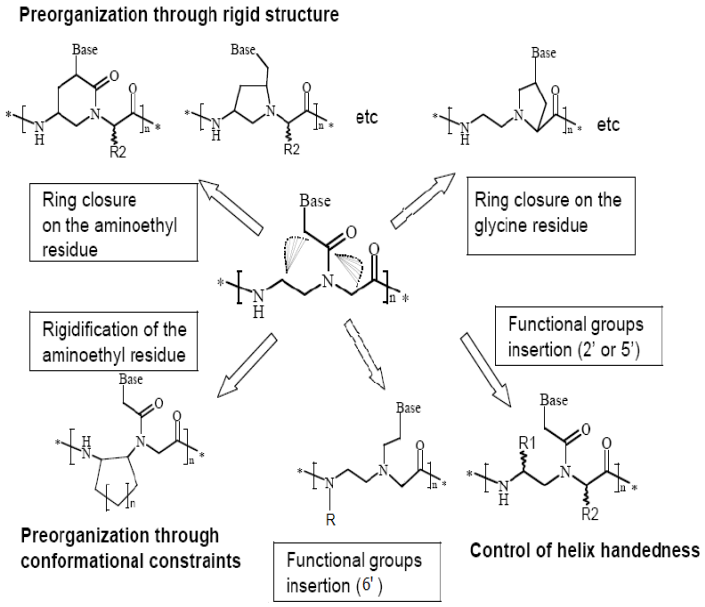

Figure 1.20. Strategies for inducing preorganization in the PNA monomers[59].

The first example of "*peptoid* nucleic acid" was reported by Almarsson and Zuckermann[52]. The shift of the amide carbonyl groups away from the nucleobase (towards thebackbone) and their replacement with methylenes, resulted in a nucleosidated peptoid skeleton (**44**, figure **1.21**). Theoretical calculations showed that the modification of the backbone had the effect of abolishing the "strong hydrogen bond between the side chain carbonyl oxygen (α to the methylene carrying the base) and the backbone amide of the next residue", which was supposed to be present on the PNA and considered essential for the DNA hybridization.

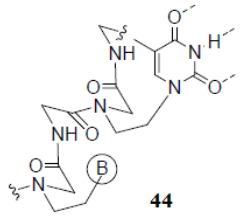

Figure 1.21. *Peptoid* nucleic acid

[49] a) Kumar, V. A., *Eur. J. Org. Chem.*, **2002**, 2021-2032. b) Corradini R.; Sforza S.; Tedeschi T.; Marchelli R.; *Seminar in Organic Synthesis*, Società Chimica Italiana, **2003**, 41-70.
[50] Sforza, S.; Haaima, G.; Marchelli, R.; Nielsen, P.E.. *Eur. J. Org. Chem*. **1999**, 197-204.
[51] Sforza, S.; Galaverna, G.; Dossena, A.; Corradini, R.; Marchelli, R. *Chirality*, **2002**, *14*, 591-598.
[52] O. Almarsson, T. C. Bruice, J. Kerr, and R. N. Zuckermann, *Proc. Natl. Acad. Sci. USA*, **1993**, *90*, 7518.

Another interesting report, demonstrating that the peptoid backbone is compatible with hybridization, came from the Eschenmoser laboratory in 2007[53]. This finding was part of an exploratory work on the pairing properties of triazine heterocycles (as recognition elements) linked to peptide and peptoid oligomeric systems. In particular, when the backbone of the oligomers was constituted by condensation of iminodiacetic acid (**45** and **46**, Figure **1.22**), the hybridization experiments, conducted with oligomer **45** and $d(T)_{12}$, showed a T_m = 22.7 °C.

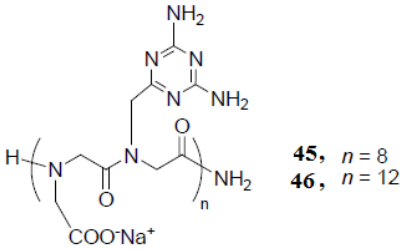

Figure 1.22. Triazine-tagged oligomeric sequences derived from an iminodiacetic acid peptoid backbone.

This interesting result, apart from the implications in the field of prebiotic chemistry, suggested the preparation of a similar peptoid oligomers (made by iminodiacetic acid) incorporating the classic nucleobase thymine (**47** and **48**, figure **1.23**)[54].

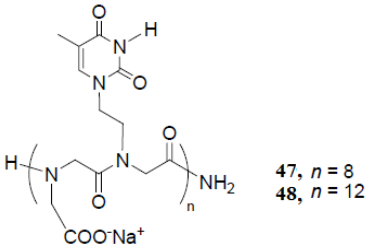

Figure 1.23. Thymine-tagged oligomeric sequences derived from an iminodiacetic acid backbone

The peptoid oligomers **47** and **48** showed thymine residues separated by the backbone by the same number of bonds found in nucleic acids (figure **1.24**, bolded black bonds). In addition, the spacing between the recognition units on the peptoid framework was similar to that present in the DNA (bolded grey bonds).

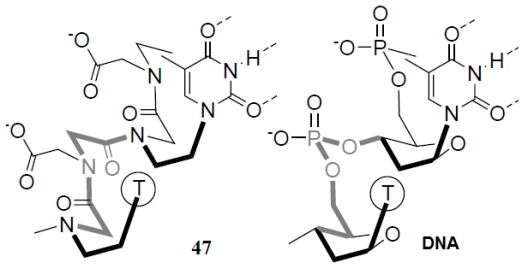

Figure 1.24. Backbone thymines positioning in the peptoid oligomer (**47**) and in the A-type DNA.

[53] G. K. Mittapalli, R. R. Kondireddi, H. Xiong, O. Munoz, B. Han, F. De Riccardis, R. Krishnamurthy, and A. Eschenmoser, *Angew. Chem. Int. Ed*., **2007**, 46, 2470.
[54] R. Zarra, D. Montesarchio, C. Coppola, G. Bifulco, S. Di Micco, I. Izzo, and F. De Riccardis, *Eur. J. Org. Chem*., **2009**, 6113.

However, annealing experiments demonstrated that peptoid oligomers **47** and **48** do not hybridize complementary strands of $d(A)_{16}$ or poly-r(A). It was claimed that possible explanations for those results resided in the conformational restrictions imposed by the charged oligoglycine backbone and in the high conformational freedom of the nucleobases (separated by two methylenes from the backbone).

Small backbone variations may also have large and unpredictable effects on the nucleosidated peptoid conformation and on the binding to nucleic acids as recently evidenced by Liu and co-workers[55], with their synthesis and incorporation (in a PNA backbone) of *N*γ-ε-aminoalkyl residues (**49**, Figure **1.25**).

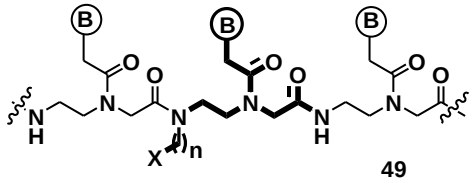

X= NH_2 (or other functional group)

Figure 1.25. Modification on the N^{γ}- in an unaltered PNA backbone

Modification on the γ-nitrogen preserves the achiral nature of PNA and therefore causes no stereochemistry complications synthetically.

Introducing such a side chain may also bring about some of the beneficial effects observed of a similar side chain extended from the R- or γ-C. In addition, the functional headgroup could also serve as a suitable anchor point to attach various structural moieties of biophysical and biochemical interest.

Furthermore, given the ease in choosing the length of the peptoid side chain and the nature of the functional headgroup, the electrosteric effects of such a side chain can be examined systematically. Interestingly, they found that the length of the peptoid-like side chain plays a critical role in determining the hybridization affinity of the modified PNA. In the Liu systematic study, it was found that short polar side chains (protruding from the γ-nitrogen of *peptoid-based* PNAs) negatively influence the hybridization properties of modified PNAs, while longer polar side chains positively modulate the nucleic acids binding. The reported data did not clarify the reason of this effect, but it was speculated that factors different from electrostatic interaction are at play in the hybridization.

1.5 Peptoid synthesis

The relative ease of peptoid synthesis has enabled their study for a broad range of applications. Peptoids are routinely synthesized on linker-derivatized solid supports using the monomeric or submonomer synthesis method. Monomeric method was developed by Merrifield[2] and its synthetic procedures commonly used for peptides, mainly are based on solid phase methodologies (*e.g.* scheme **1.1**).

The most common strategies used in peptide synthesis involve the Boc and the Fmoc protecting groups.

[55] X.-W. Lu, Y. Zeng, and C.-F. Liu, Org. Lett., **2009**, 11, 2329.

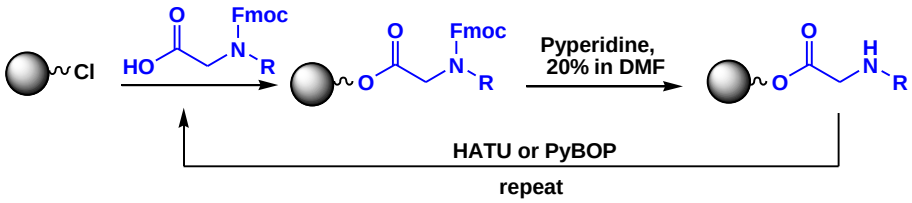

Scheme 1.1. monomer synthesis of peptoids

Peptoids can be constructed by coupling *N*-substituted glycines using standard α-peptide synthesis methods, but this requires the synthesis of individual monomers[4], this is based by a two-step monomer addition cycle. First, a protected monomer unit is coupled to a terminus of the resin-bound growing chain, and then the protecting group is removed to regenerate the active terminus. Each side chain requires a separate N^{α}-protected monomer.

Peptoid oligomers can be thought of as condensation homopolymers of *N*-substituted glycine. There are several advantages to this method, but the extensive synthetic effort required to prepare a suitable set of chemically diverse monomers is a significant disadvantage of this approach. Additionally, the secondary *N*-terminal amine in peptoid oligomers is more sterically hindered than primary amine of an amino acid, for this reason coupling reactions are slower.

Sub-monomeric method, instead, was developed by Zuckermann *et al.* (Scheme **1.2**)[56].

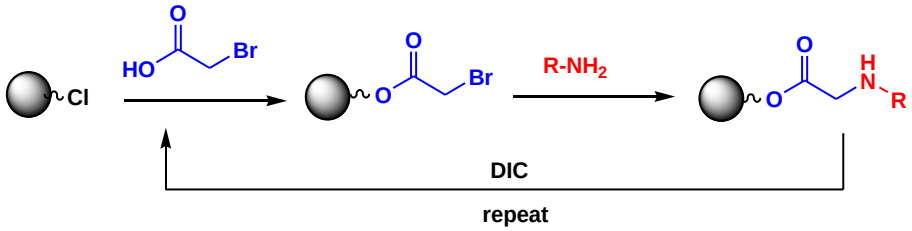

Scheme 1.2. Sub-monomeric synthesis of peptoids

Sub-monomeric method consists in the construction of peptoid monomer from *C*- to *N*-terminus using *N*,*N*-diisopropylcarbodiimide (DIC)-mediated acylation with bromoacetic acid, followed by amination with a primary amine. This two-step sequence is repeated iteratively to obtain the desired oligomer. Thereafter, the oligomer is cleaved using trifluoroacetic acid (TFA) or by hexafluorisopropanol, scheme **1.2**. Interestingly no protecting groups are necessary for this procedure.

The availability of a wide variety of primary amines facilitates the preparation of chemically and structurally divergent peptoids.

1.6 Synthesis of PNA monomers and oligomers

The first step for the synthesis of PNA, is the building of PNA's monomer. The monomeric unit is constituted by an *N*-(2-aminoethyl)glycine protected at the terminal amino group, which is essentially a pseudopeptide with a reduced amide bond. The monomeric unit can be synthesized following several methods and synthetic routes, but the key steps is the coupling of a modified nucleobase with the secondary amino group of the backbone by using standard peptide coupling reagents (*N*,*N'*-dicyclohexylcarbodiimide, DCC, in the presence of 1-hydroxybenzotriazole, HOBt). Temporary masking the carboxylic group as alkyl or allyl ester is also necessary during the coupling reactions. The

[56] R. N. Zuckermann, J. M. Kerr, B. H. Kent, and W. H. Moos, *J. Am. Chem. Soc.*, **1992**, 114, 10646.

protected monomer is then selectively deprotected at the carboxyl group to produce the monomer ready for oligomerization. The choice of the protecting groups on the amino group and on the nucleobases depends on the strategy used for the oligomers synthesis. The similarity of the PNA monomers with the amino acids allows the synthesis of the PNA oligomer with the same synthetic procedures commonly used for peptides, mainly based on solid phase methodologies. The most common strategies used in peptide synthesis involve the Boc and the Fmoc protecting groups. Some "tactics", on the other hand, are necessary in order to circumvent particularly difficult steps during the synthesis (i.e. difficult sequences, side reactions, epimerization, etc.). In scheme **1.3**, a general scheme for the synthesis of PNA oligomers on solid-phase is described.

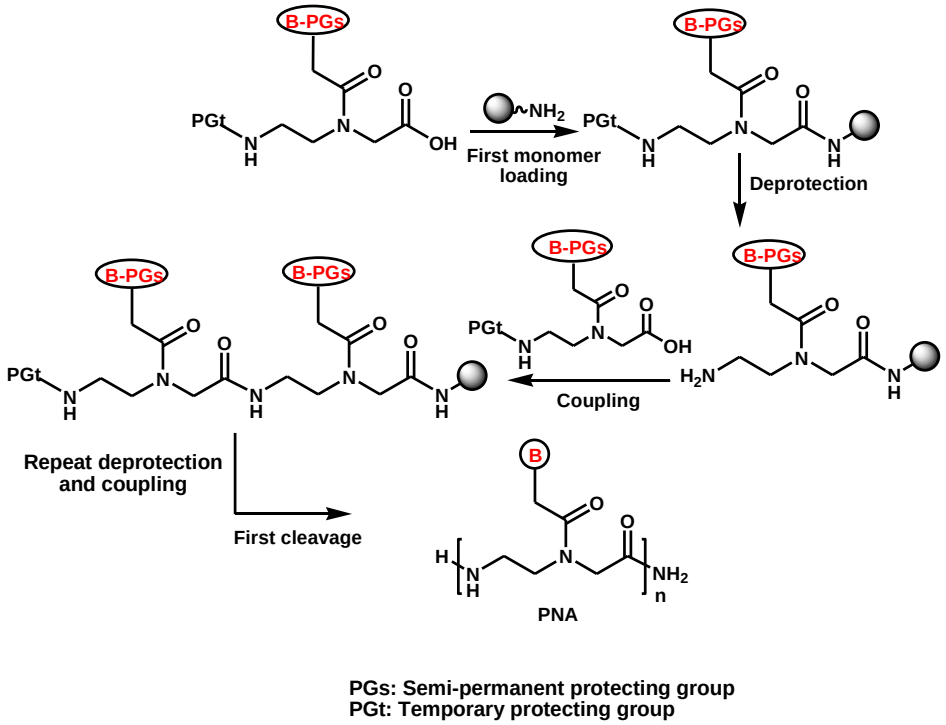

Scheme 1.3. Typical scheme for solid phase PNA synthesis.

The elongation takes place by deprotecting the *N*-terminus of the anchored monomer and by coupling the following N-protected monomer. Coupling reactions are carried out with HBTU or, better, its 7-aza analogue HATU[57] which gives rise to yields above 99%. Exocyclic amino groups present on cytosine, adenine and guanine may interfere with the synthesis and therefore need to be protected with semi-permanent groups orthogonal to the main *N*-terminal protecting group.

In the Boc strategy the amino groups on nucleobases are protected as benzyloxycarbonyl derivatives (Cbz) and actually this protecting group combination is often referred to as the Boc/Cbz strategy. The Boc group is deprotected with trifluoroacetic acid (TFA) and the final cleavage of PNA from the resin, with simultaneous deprotection of exocyclic amino groups in the nucleobases, is carried out with HF or with a mixture of trifluoroacetic and trifluoromethanesulphonic acids (TFA/TFMSA). In the Fmoc strategy, the Fmoc protecting group is cleaved under mild basic conditions with piperidine, and is

[57] Nielsen P. E., Egholm M., Berg R. H., Buchardt O., *Anti-Cancer Drug Des.* **1993**, 8, 53.

therefore compatible with resin linkers, such as MBHA-Rink amide or chlorotrityl groups, which can be cleaved under less acidic conditions (TFA) or hexafluoisopropanol. Commercial available Fmoc monomers are currently protected on nucleobases with the benzhydryloxycarbonyl (Bhoc) groups, also easily removed by TFA. Both strategies, with the right set of protecting group and the proper cleavage condition, allow an optimal synthesis of different type of classic PNA or modified PNA.

1.7 Aims of the work

The objective of this research, is to gain new insights in the use of peptoids as tools for structural studies and biological applications. Five are the themes developed in the present thesis:

1. **Carboxyalkyl Peptoid PNAs**. N^{γ}-carboxyalkyl modified peptide nucleic acids (PNAs), containing the four canonical nucleobases, were prepared *via* solid-phase oligomerization. The inserted modified peptoid monomers (figures **1.26**: **50** and **51**) were constructed through simple synthetic procedures, utilizing proper glycidol and iodoalkyl electrophiles.

GTAGAT*$_{50}$CACT–Gly–NH$_2$,	**52**
G T*$_{50}$AGAT*$_{50}$CAC T*$_{50}$–Gly–NH$_2$,	**53**
GTAGAT*$_{51}$CACT–Gly–NH$_2$,	**54**
G T*$_{51}$AGAT*$_{51}$CAC T*$_{51}$–Gly–NH$_2$,	**55**

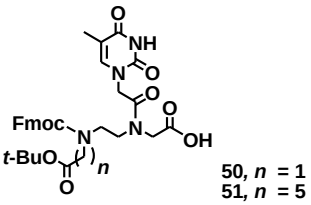

Figure 1.26. Modified peptoid monomers

Synthesis of PNA oligomers was realized by inserting modified peptoid monomers into a canonical PNA, by this way four different modified PNA oligomers were obtained (figure **1.27**).

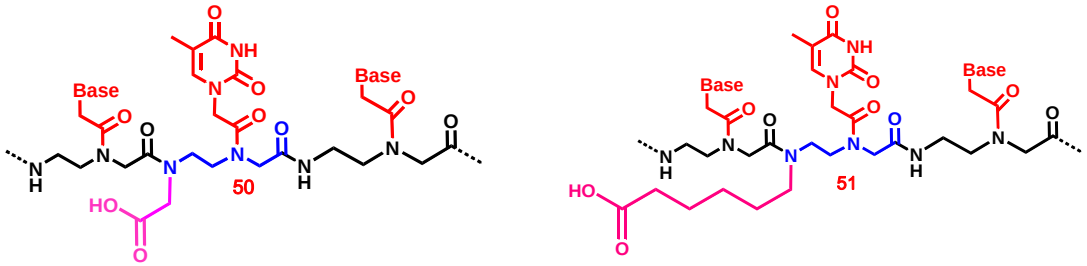

Figure 1.27. Modified PNA.

Thermal denaturation studies performed, in collaboration with Prof. R. Corradini from the University of Parma, with complementary antiparallel DNA strands, demonstrated that the length of the N^{γ}-side chain strongly influences the modified PNAs hybridization properties. Moreover, multiple negative

charges on the oligoamide backbone, when present on γ-nitrogen C_6 side chains, proved to be beneficial for the oligomers water solubility and DNA hybridization specificity.

2. **Structural analysis of cyclopeptoids and their complexes**. The aim of this work was the studies of structural properties of cyclopeptoids in their free and complexed form (figure **1.27**: **56, 57** and **58**).

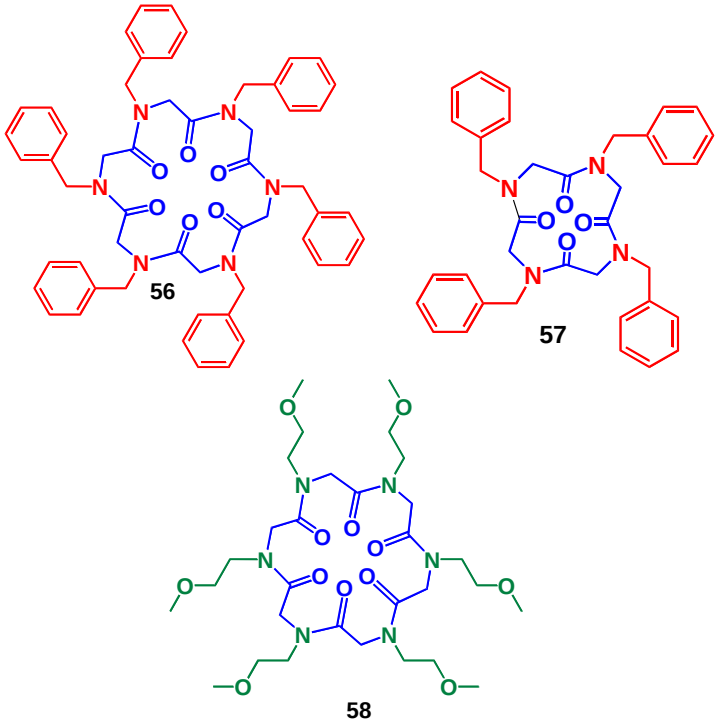

Figure 1.27. *N*-Benzyl-cyclohexapeptoid **56**, *N*-benzyl-cyclotetrapeptoid **57** and *N*-metoxyethyl-cyclohexapeptoid **58**.

The synthesis of hexa- and tetra- *N*-benzyl glycine linear oligomers and of hexa- *N*-metoxyethyl glycine linear oligomer (**59, 60** and **61**, figure **1.28**), was accomplished on solid-phase (2-chlorotrityl resin) using the "sub-monomer" approach.[58]

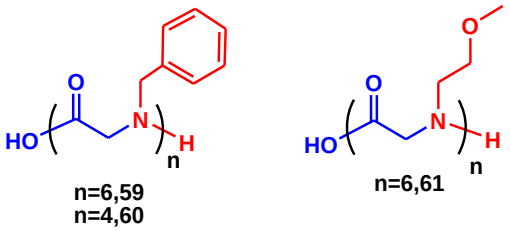

Figure 1.28. linear *N*-Benzyl-hexapeptoid **59**, linear *N*-benzyl tetrapeptoid **60** and linear *N*-metoxyethyl-hexapeptoid **61**.

[58] R. N. Zuckermann, J. M. Kerr, B. H. Kent, and W. H. Moos, *J. Am. Chem. Soc.*, **1992**, *114*, 10646.

All cycles obtained were crystallized and caractherizated by X-ray analysis in collaboration with Dott. Consiglia Tedesco from the University of Salerno and Dott. Loredana Erra from European Synchrotron Radiation Facility (ESRF), Grenoble, France.

3. **Cationic cyclopeptoids as potential macrocyclic nonviral vectors.**

The aim of this work was the synthesis of three different cationic cyclopeptoids (figure **1.28**: **62, 63** and **64**) to assess their efficiency in DNA cell transfection, in collaboration with Prof. G. Donofrio of the University of Parma.

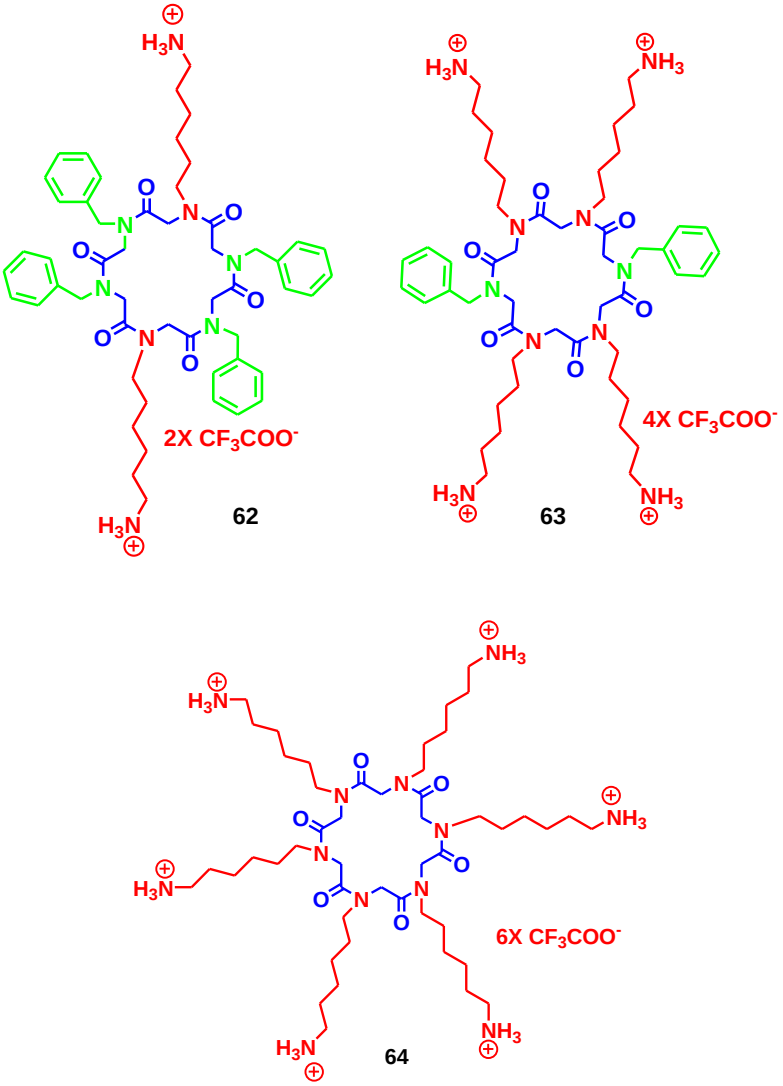

Figure 1.29. Di-cationic cyclohexapeptoid **62,** Tetra-cationic cyclohexapeptoid **63**, Hexa-cationic cyclohexapeptoid **64.**

4. **Complexation with Gd^{3+} of carboxyethyl cyclopeptoids as possible contrast agents in MRI.** Three cyclopeptoids **65**, **66** and **67** (figure **1.30**) containing polar side chains, were synthesized and, in collaboration with Prof. S. Aime, of the University of Torino, the complexation properties with Gd^{3+} were evaluated.

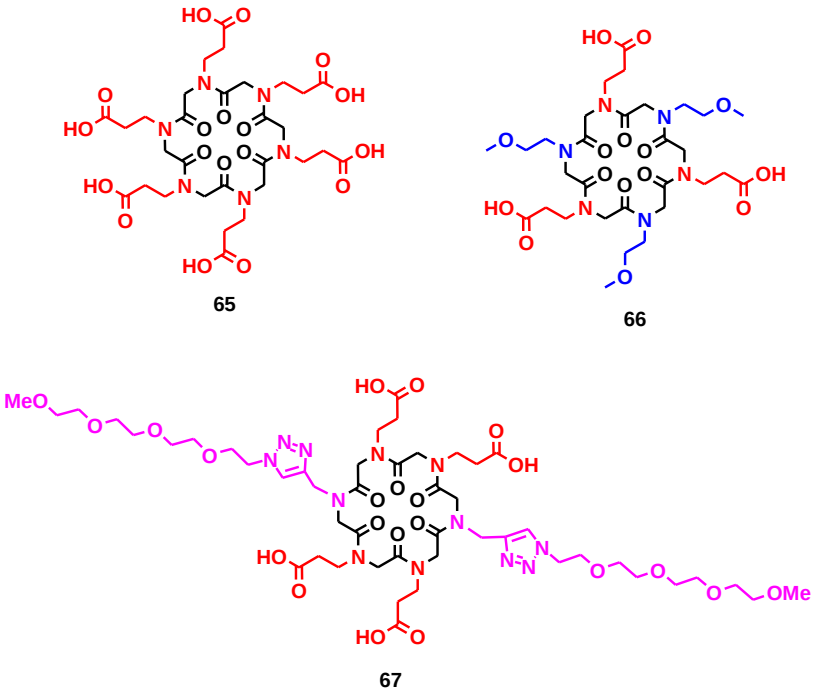

Figure 1.29. Hexacarboxyethyl cyclohexapeptiod **65**, Tricarboxyethyl ciclohexapeprtoid **66** and tetracarboxyethyl cyclopeptoids **67**.

5. **Cyclopeptoids as mimetic of natural defensins[59].** In this work some linear and cyclopeptoids with specific side chains (-SH groups) were synthetized. The aim was to introduce, by means of sulfur bridges, peptoid backbone constrictions and to mimic natural defensins (figure **1.30,** block **I: 68** hexa-linear and related cycles **69** and **70**; block **II: 71** octa-linear and related cycles **72** and **73**; block **III: 74** dodeca-linear and related cycles **75**, **76** and **77**; block **IV:** 7**8** dodeca-linear diprolinate and related cycles **79**, **80** and **81**).

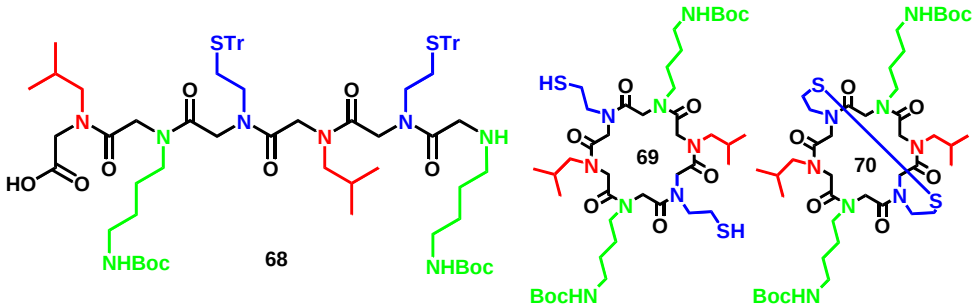

Figure 1.30, block I. Structures of the hexameric linear (**68**) and corresponding cyclic **69** and **70.**

[59] a) W. Wang, S.M. Owen, D. L. Rudolph, A. M. Cole, T. Hong, A. J. Waring, R. B. Lal, and R. I. Lehrer *The Journal of Immunology*, **2010**, 515-520; b) D. Yang, A. Biragyn, D. M. Hoover, J. Lubkowski, J. J. Oppenheim *Annu. Rev. Immunol*. **2004**, 181-215.

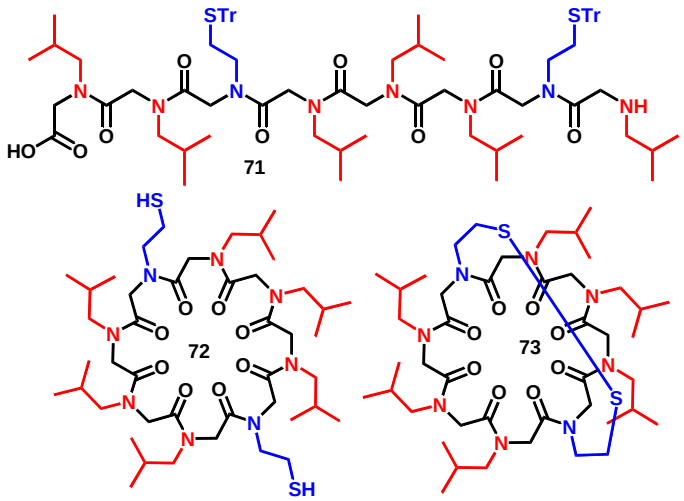

Figure 1.30, block II. Structures of octameric linear (**71**) and corresponding cyclic **72** and **73**

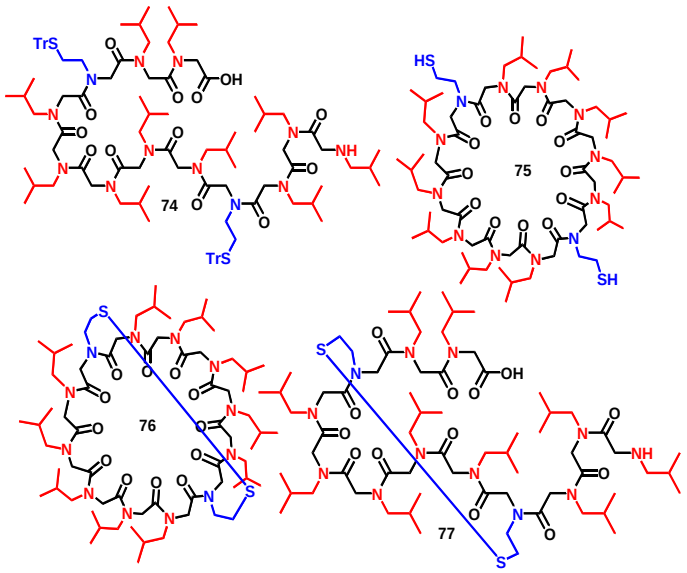

Figure 1.30, block III. Structures of linear (**74**) and corresponding cyclic **75, 76** and **77.**

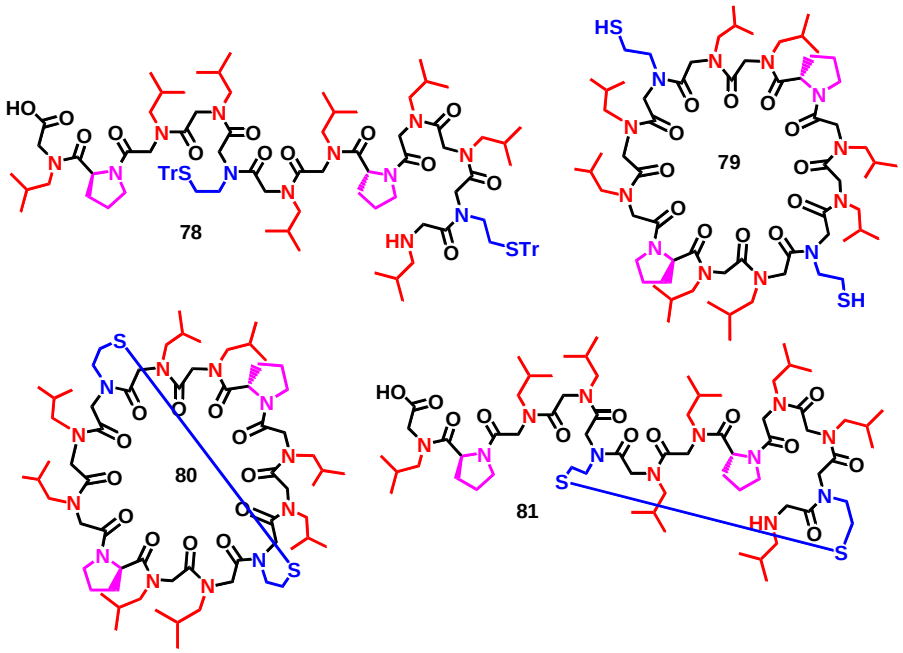

Figure 1.30, block IV. Structures of dodecameric linear diprolinate (**78**) and corresponding cyclic **79, 80** and **81.**

Chapter 2

2. Carboxyalkyl Peptoid PNAs: Synthesis and Hybridization Properties.

2.1 Introduction

The considerable biological stability, the excellent nucleic acids binding properties, and the appreciable chemical simplicity, make PNA an invaluable tool in molecular biology.[60] Unfortunately, despite the remarkable properties, PNA has two serious limitations: low water solubility[61] and poor cellular uptake[62].

Considerable efforts have been made to circumvent these drawbacks, and a conspicuous number of new analogs have been proposed[63], including those with the γ-nitrogen modified *N*-(2-aminoethyl)-glycine (aeg) units[64]. In a contribution by the Nielsen group,[65] an accurate investigation on the N^{γ}-methylated PNA hybridization properties was reported. In this study it was found that the formation of PNA-DNA (or RNA) duplexes was not altered in case of a 30% N^{γ}-methyl nucleobase substitution. However, the hybridization efficiency per *N*-methyl unit in a PNA, decreased with the increasing of the *N*-methyl content.

The negative impact of the γ-*N* alteration reported by Nielsen, did not discouraged further investigations. The potentially informational triazine-tagged oligoglycines systems,[66] the oligomeric thymine-functionalized peptoids,[5d] the achiral N^{γ}-ω-aminoalkyl nucleic acids,[5a] constitute convincing example of γ-nitrogen beneficial modification. In particular, the Liu group contribution,[5a] revealed an unexpected electrosteric effect played by the N^{γ}-side chain length. In their stringent analysis it was demonstrated that while short ω-amino N^{γ}-side chains negatively influenced the modified PNAs hybridisation properties, longer ω-amino N^{γ}-side chains positively modulated nucleic acids binding. It was also found that suppression of the positive ω-aminoalkyl charge (*i.e.* through acetylation) caused no reduction in the hybridization affinity, suggesting that factors different from mere electrostatic stabilizing interactions were at play in the hybrid aminopeptoid-PNA/DNA (RNA) duplexes[67].

Considering the interesting results achieved in the case of *N*-(2-alkylaminoethyl)-glycine units[5,6], and on the basis of poor hybridization properties showed by two fully peptoidic homopyrimidine oligomers synthesized by our group,[5b] it was decided to explore the effects of anionic residues at the γ-nitrogen in a PNA framework on the *in vitro* hybridization properties.

---

[60] (a) Nielsen, P. E. *Mol. Biotechnol.* **2004**, *26*, 233-248; (b) Brandt, O.; Hoheisel, J. D. *Trends Biotechnol.* **2004**, *22*, 617-622; (c) Ray, A.; Nordén, B. *FASEB J.* **2000**, *14*, 1041-1060.

[61] Vernille, J. P.; Kovell, L. C.; Schneider, J. W. *Bioconjugate Chem.* **2004**, *15*, 1314-1321.

[62] (a) Koppelhus, U.; Nielsen, P. E. *Adv. Drug. Delivery Rev.* **2003**, *55*, 267-280; (b) Wittung, P.; Kajanus, J.; Edwards, K.; Nielsen, P. E.; Nordén, B.; Malmstrom, B. G. *FEBS Lett.* **1995**, *365*, 27-29.

[63] (a) De Koning, M. C.; Petersen, L.; Weterings, J. J.; Overhand, M.; van der Marel, G. A.; Filippov, D. V. *Tetrahedron* **2006**, *62*, 3248–3258; (b) Murata, A.; Wada, T. *Bioorg. Med. Chem. Lett.* **2006**, *16*, 2933–2936; (c) Ma, L.-J.; Zhang, G.-L.; Chen, S.-Y.; Wu, B.; You J.-S.; Xia, C.-Q. *J. Pept. Sci.* **2005**, *11*, 812–817.

[64] (a) Lu, X.-W.; Zeng, Y.; Liu, C.-F. *Org. Lett.* **2009**, *11*, 2329-2332; (b) Zarra, R. ; Montesarchio, D.; Coppola, C.; Bifulco, G.; Di Micco, S.; Izzo, I.; De Riccardis, F. *Eur. J. Org. Chem.* **2009**, 6113-6120; (c) Wu, Y.; Xu, J.-C.; Liu, J.; Jin, Y.-X. *Tetrahedron* **2001**, *57*, 3373-3381; (d) Y. Wu, J.-C. Xu. *Chin. Chem. Lett.* **2000**, *11*, 771-774.

[65] Haaima, G.; Rasmussen, H.; Schmidt, G.; Jensen, D. K.; Sandholm Kastrup, J.; Wittung Stafshede, P.; Nordén, B.; Buchardt, O.; Nielsen, P. E. *New. J. Chem.* **1999**, *23*, 833-840.

[66] Mittapalli, G. K.; Kondireddi, R. R.; Xiong, H.; Munoz, O.; Han, B.; De Riccardis, F.; Krishnamurthy, R.; Eschenmoser, A. *Angew. Chem. Int. Ed.* **2007**, *46*, 2470-2477.

[67] The authors suggested that longer side chains could stabilize amide *Z* configuration, which is known to have a stabilizing effect on the PNA/DNA duplex. See: Eriksson, M.; Nielsen, P. E. *Nat. Struct. Biol.*, **1996**, *3*, 410-413.

The *N*-(carboxymethyl) and the *N*-(carboxypentamethylene) N^{γ}-residues, present in the monomers **50** and **51** (figure **2.1**) were chosen in order to evaluate possible side chains length-dependent thermal denaturations effects, and with the aim to respond to the pressing water-solubility issue, which is crucial for the specific subcellular distribution[68].

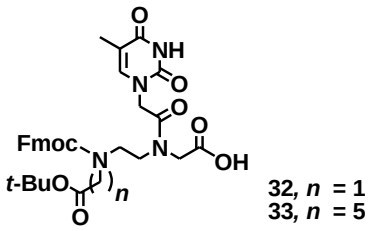

Figure 2.1. Modified peptoid PNA monomers

The synthesis of a negative charged *N*-(2-carboxyalkylaminoethyl)-glycine backbone (negative charged PNA are rarely found in literature)[69] was based on the idea to take advantage of the availability of a multitude of efficient methods for the gene cellular delivery based on the interaction of carriers with negatively charged groups. Most of the nonviral gene delivery systems are, in fact, based on cationic lipids[70] or cationic polymers[71] interacting with negative charged genetic vectors. Furthermore, the neutral backbone of PNA prevents them to be recognized by proteins which interact with DNA, and PNA-DNA chimeras should be synthesized for applications such as transcription factors scavenging (decoy)[72] or activation of RNA degradation by RNase-H (as in antisense drugs).

This lack of recognition is partly due to the lack of negatively charged groups and of the corresponding electrostatic interactions with the protein counterpart[73].

In the present work we report the synthesis of the *bis*-protected thyminylated N^{γ}-ω-carboxyalkyl monomers **50** and **51** (figure **2.1**), the solid-phase oligomerization and the base-pairing behaviour of four oligomeric peptoid sequences **52-55** (figure **2.2**) incorporating, in various extent and in different positions, the monomers **50** and **51.**

[68] Koppelius, U.; Nielsen, P. E. *Adv. Drug Deliv. Rev.* **2003**, *55*, 267-280.
[69] (a) Efimov, V. A.; Choob, M. V.; Buryakova, A. A.; Phelan, D.; Chakhmakhcheva, O. G. *Nucleosides, Nucleotides Nucleic Acids* **2001**, *20*, 419-428; (b) Efimov, V. A.; Choob, M. V.; Buryakova, A. A.; Kalinkina, A. L.; Chakhmakhcheva, O. G. *Nucleic Acids Res.* **1998**, *26*, 566-575; (c) Efimov, V. A.; Choob, M. V.; Buryakova, A. A.; Chakhmakhcheva, O. G. *Nucleosides Nucleotides* **1998**, *17*, 1671-1679; (d) Uhlmann, E.; Will, D. W.; Breipohl, G.; Peyman, A.; Langner, D.; Knolle, J.; O'Malley, G. *Nucleosides Nucleotides* **1997**, *16*, 603-608; (e) Peyman, A.; Uhlmann, E.; Wagner, K.; Augustin, S.; Breipohl, G.; Will, D. W.; Schäfer, A.; Wallmeier, H. *Angew. Chem. Int. Ed.* **1996**, *35*, 2636–2638.
[70] Ledley, F. D. *Hum. Gene Ther.* **1995**, *6*, 1129–1144.
[71] Wu, G. Y.; Wu, C. H. *J. Biol. Chem.* **1987**, *262***,** 4429–4432.
[72]Gambari, R.; Borgatti, M.; Bezzerri, V.; Nicolis, E.; Lampronti, I.; Dechecchi, M. C.; Mancini, I.; Tamanini, A.; Cabrini, G. *Biochem. Pharmacol.*, **2010**, *80*, 1887-1894.
[73] Romanelli, A.; Pedone, C.; Saviano, M.; Bianchi, N.; Borgatti, M.; Mischiati, C.; Gambari R. *Eur. J. Biochem.*, **2001**, *268*, 6066–6075.

GTAGAT*$_{50}$CACT–Gly–NH$_2$,	**52**
G T*$_{50}$AGAT*$_{50}$CAC T*$_{50}$–Gly–NH$_2$,	**53**
GTAGAT*$_{51}$CACT–Gly–NH$_2$,	**54**
G T*$_{51}$AGAT*$_{51}$CAC T*$_{51}$–Gly–NH$_2$,	**55**

Figure 2.2. Structures of target oligomers **52-55**. T* represents the modified thyminylated *N*$^{\gamma}$-ω-carboxyalkyl monomers. T*$_{50}$ incorporates monomer **50**, T*$_{51}$ incorporates monomer **51**.

The carboxy termini of the modified mixed purine/pyrimidine decamer PNA sequences were linked to a glycinamide unit. T*$_1$ and T*$_2$ represent the insertion of the modified **50** and **51** *N*$^{\gamma}$-ω-carboxyalkyl monomer units, respectively.

The mixed-base sequence has been chosen since it has been proposed by Nielsen and coworkers and subsequently used by several groups as a benchmark for the evaluation of the effect of modification of the PNA structure on PNA:DNA thermal stability[74].

2.2. Results and discussion

2.2.1 Chemistry

The elaboration of monomers **50** and **51** (figure **2.1**), suitable for the Fmoc-based oligomerization, took advantage of the chemistry utilized to construct the regular PNA monomers. In particular, the synthesis of the *N*-protected monomer **50** started with the *t*-Bu-glycine (**82**) glycidol amination[5], as shown in scheme **2.1**. *N*-fluorenylmethoxycarbonyl protection of the adduct **85**, and subsequent diol oxidative cleavage, gave the labile aldehyde **86**. Compound **86** was subjected to reductive amination in the presence of methylglycine to obtain the triply protected *bis*-carboxyalkyl ethylenediamine key intermediate **87**.

The 2-(7-aza-1H-benzotriazole-1-yl)-1,1,3,3-tetramethyluronium hexafluorophosphate (HATU), promoted condensation of **87** with thymine-1-acetic acid gave the expected tertiary amide **88**.

Careful LiOH-mediated hydrolysis allowed to preserve the base-labile Fmoc group, affording the target monomer unit **50**.

[74] (a) Sforza, S.; Tedeschi, T.; Corradini, R.; Marchelli, R. *Eur. J. Org. Chem.*, **2007**, 5879–5885; (b) Englund, E. A.; Appella, D. H. *Org. Lett.*, **2005**, *7*, 3465-3467; (c) Sforza, S.; Corradini, R.; Ghirardi, S.; Dossena, A.; Marchelli, R. *Eur. J. Org. Chem.*, **2000**, 2905-2913.

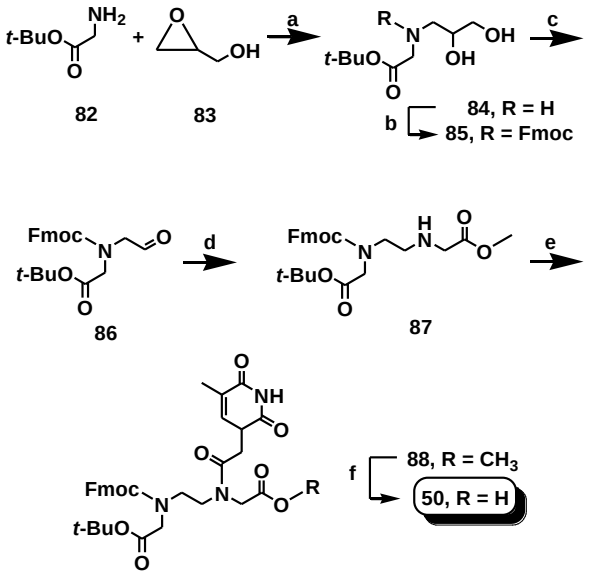

Scheme 2.1. Synthesis of the PNA monomer **50**. Reagents and conditions: a) glycidol, DMF, DIPEA, 70°C, 3 days, 41%; b) fluorenylmethoxycarbonyl chloride (Fmoc-Cl), $NaHCO_3$, 1,4-dioxane/H_2O, overnight, 63%; c) $NaIO_4$, THF/H_2O, 2h, 97%; d) $H_2NCH_2COOCH_3$, $NaHB(AcO)_3$, triethylamine in CH_2Cl_2, overnight, 70%; e) thymine-1-acetic acid, Et_3N, HATU in DMF, overnight, 49%; f) $LiOH \cdot H_2O$, 1,4-dioxane /H_2O, 0°C, 30 min., 69%.

The synthesis of compound **51** required a different strategy, due to the low yields obtained in the glycidol opening induced by the *t*-butyl ester of the 6-aminocaproic acid (**89**, see the experimental section). A better electrophile was devised in the benzyl 2-iodoethylcarbamate (**65**,[75] Scheme **2.2**). The nucleophilic displacement gave the secondary amine **95**, containing the Cbz-protected ethylendiamine core. Compound **95**, after a straightforward protective group adjustment and a subsequent reductive amination, produced the fully protected *bis*-carboxyalkyl ethylenediamine key intermediate **98**. This last was reacted with thymine-1-acetic acid and benzotriazole-1-yl-oxy-tris-pyrrolidino-phosphonium hexafluorophosphate (PyBOP), as condensing agent, and gave the amide **99**. Finally, after careful chemoselective hydrolysis of the methyl ester, the required monomer **51** was obtained in acceptable yields.

[75] Bolognese, A.; Fierro O.; Guarino, D.; Longobardo, L.; Caputo, R. *Eur. J. Org. Chem.* **2006**, 169-173.

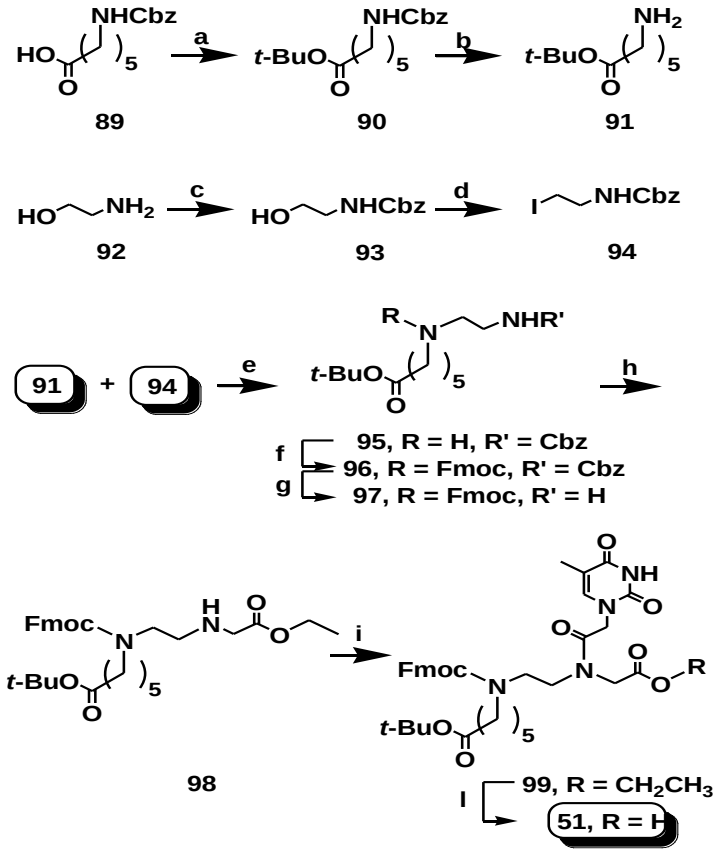

Scheme 2.2. Synthesis of the PNA monomer **51**. Reagents and conditions: a) *t*-Butanol, DMAP, DCC, CH_2Cl_2, overnight, 58%; b) H_2, Pd/C (10 % w/w), acetic acid, methanol, 1h and 30 min., quant.; c) Cbz-Cl, CH_2Cl_2, 0°C, overnight, quant.; d) I_2, imidazole, PPh_3, CH_2Cl_2, 3h, 77%; e) K_2CO_3, CH_3CN, reflux, overnight, 67%, f) fluorenylmethoxycarbonyl chloride (Fmoc-Cl), $NaHCO_3$, 1,4-dioxane/H_2O, overnight, 97%; g) H_2, Pd/C (10 % w/w), acetic acid, methanol; 1h, quant.; h) ethyl glyoxalate, $NaHB(AcO)_3$, triethylamine in CH_2Cl_2, overnight, 25%; i) thymine-1-acetic acid, Et_3N, PyBOP in DMF; overnight, 70% l) LiOH, 1,4-dioxane/H_2O, 30 min., 30%.

The oligomers **52-55** were manually assembled in a stepwise fashion on a Rink-amide NOVA-PEG resin solid support. The unmodified PNA monomers were coupled using 2-(1H-benzotriazole-1-yl)-1,1,3,3-tetramethyluronium hexafluoro-phosphate (HBTU). HATU was used for the coupling reactions involving the less reactive secondary amino groups of the modified monomers **50** and **51**. The decamers were detached from the solid support and quantitatively deprotected from the *t*-butyl protecting groups, using a 9:1 mixture of trifluoroacetic acid and *m*-cresol. The water-soluble oligomers were purified by RP-HPLC, yielding the desired **52-55** as pure compounds. Their identity was confirmed by MALDI-TOF mass spectrometry.

2.2.2 Hybridization studies

In order to verify the ability of decamers **49-52** to bind complementary DNA, UV-monitored melting experiments were performed mixing the water-soluble oligomers with the complementary antiparallel

deoxyribonucleic strands (5 μM concentration, ε= 260 nm). Table **2.1** presents the thermal stability studies of the duplexes formed between the modified PNAs and the DNA anti-parallel strand, in comparison with the unmodified PNA.

The data obtained clearly demonstrated that the distance of the negative charged carboxy group from the oligoamide backbone strongly affects the PNA:DNA duplex stability. In particular, when the γ-nitrogen brings an acetic acid substituent (with a single methylene distancing the oligoamide backbone and the charged group, entry 2), a drop of 5.4 °C in T_m of the carboxypeptoid-PNA/DNA(ap) duplex is observed, when compared with unmodified PNA (entry 1). Triple insertion of monomer **50** (entry 3), results in a decrease of 2.6 °C per *N*-acetyl unit, showing no N^{γ}-substitution detrimental additive effects on the annealing properties. In both cases the ability to discriminate closely related sequences is magnified, respect to the unmodified PNA.

Table 2.1. Thermal stabilities (T_m, °C) of modified PNA/DNA duplexes

Entry	PNA	Anti-parallel D duplex[a]	DNA mis-matcl
1	Ac-GTAGATCACT–Gly–NH_2 (PNA sequence)[8a]	**48.6**	**36.4**
2	GTAGAT*$_{50}$CACT–Gly–NH_2, (**52**)	**43.2**	**33.5**
3	GT*$_{50}$AGAT*$_{50}$CACT*$_{50}$–Gly–NH_2, (**53**)	**40.7**	**34.4**
4	GTAGAT*$_{51}$CACT–Gly–NH_2, (**54**)	**44.8**	**30.8**
5	G T*$_{51}$AGAT*$_{51}$CAC T*$_{51}$–Gly–NH_2, (**55**)	**44.1**	**35.6**
6	5'–GTAGATCACT–3' (DNA sequence)[9]	**33.5**	**26.5**

[a]5'–AGTGATCTAC–3'
[b]5'–AGTGGTCTAC–3'

For the binding of the N^{γ}-caproic acid derivatives with the full-matched antiparallel DNA, the table shows an evident increase of the affinity (entry 4 and 5), when compared with the modified sequences with shorter side chains (entry 2 and 3). Comparison with the corresponding aegPNA showed, for the single insertion, a 3.8 °C T_m drop, while, for triple substitution, a T_m decrease of 1.5 °C per N^{γ}-alkylated monomer. It is also worth noting, in both **54** and **55**, the slight increase of the binding specificity (ΔT_m = 5.6 °C and 0.8 °C, entry 4 and 5) respect to unmodified PNA.

In previous studies, reporting the performances of backbone modified PNA containing negatively charged monomers derived from amino acids, the drop in melting temperature was found to be 3.3 °C in the case of L-Asp monomer and 2.3° C in the case of D-Glu. The present results are in line with these data, with a decrease in melting temperatures which still allows stronger binding than natural DNA (entry 6). Thus it is possible to introduce negatively charged groups via alkylation of the amide nitrogen in the PNA backbone without significant loss of stability of the PNA-DNA duplex, provided that a five methylene spacer is used.

2.3. Conclusions

In this work, we have constructed two orthogonally protected N^{γ}-ω-carboxy alkylated units. The successful insertion in PNA-based decamers, through standard solid-phase synthesis protocols, and the following hybridization studies, in the presence of DNA antiparallel strand, demonstrate that the N^{γ}-substitution with negative charged groups is compatible with the formation of a stable PNA:DNA duplex. The present study also extends the observation that correlates the efficacy of the nucleic acids hybridization with the length of the N^{γ} alkyl substitution,[5a] expanding the validity also to N^{γ}-ω-negative charged side chains. The newly produced structures can create new possibilities for PNA with functional groups enabling further improvement in their ability to perform gene-regulation.

2.4 Experimental section

2.4.1 General Methods.

All reactions involving air or moisture sensitive reagents were carried out under a dry argon or nitrogen atmosphere using freshly distilled solvents. Tetrahydrofuran (THF) was distilled from $LiAlH_4$ under argon. Toluene and CH_2Cl_2 were distilled from CaH_2. Glassware was flame-dried (0.05 Torr) prior to use. When necessary, compounds were dried in vacuo over P_2O_5 or by azeotropic removal of water with toluene under reduced pressure. Starting materials and reagents purchased from commercial suppliers were generally used without purification unless otherwise mentioned. Reaction temperatures were measured externally; reactions were monitored by TLC on Merck silica gel plates (0.25 mm) and visualized by UV light, I_2, or by spraying with H_2SO_4-$Ce(SO_4)_2$, phosphomolybdic acid or ninhydrin solutions and drying. Flash chromatography was performed on Merck silica gel 60 (particle size: 0.040-0.063 mm) and the solvents employed were of analytical grade. Yields refer to chromatographically and spectroscopically (^{1}H- and ^{13}C-NMR) pure materials. The NMR spectra were recorded on Bruker DRX 400, (^{1}H at 400.13 MHz, ^{13}C at 100.03 MHz), Bruker DRX 250 (^{1}H at 250.13 MHz, ^{13}C at 62.89 MHz), and Bruker DRX 300 (^{1}H at 300.10 MHz, ^{13}C at 75.50 MHz) spectrometers. Chemical shifts (δ) are reported in ppm relatively to the residual solvent peak ($CHCl_3$, δ = 7.26, $^{13}CDCl_3$, δ: = 77.0; CD_2HOD, δ = 3.34, $^{13}CD_3OD$, δ = 49.0) and the multiplicity of each signal is designated by the following abbreviations: s, singlet; d, doublet; t, triplet; q, quartet; quint, quintuplet; m, multiplet; br, broad. Coupling costants (*J*) are quoted in Hz. Homonuclear decoupling, COSY-45 and DEPT experiments completed the full assignment of each signal. Elemental analyses were performed on a CHNS-O FlashEA apparatus (Thermo Electron Corporation) and are reported in percent abundance. High resolution ESI-MS spectra were performed on a Q-Star Applied Biosystem mass spectrometer. ESI-MS analysis in positive ion mode was performed using a Finnigan LCQ Deca ion trap mass spectrometer (ThermoFinnigan, San Josè, CA, USA) and the mass spectra were acquired and processed using the Xcalibur software provided by Thermo Finnigan. Samples were dissolved in 1:1 CH_3OH/H_2O, 0.1 % formic acid, and infused in the ESI source by using a syringe pump; the flow rate was 5 μl/min. The capillary voltage was set at 4.0 V, the spray voltage at 5 kV, and the tube lens offset at -40 V. The capillary temperature was 220 °C. MALDI TOF mass spectrometric analyses were performed on a PerSeptive Biosystems Voyager-De Pro MALDI mass spectrometer in the Linear mode using α-cyano-4-hydroxycinnamic acid as the matrix. HPLC analyses were performed on a Jasco BS 997-01 series, equipped with a quaternary pumps Jasco PU-2089 Plus, and an UV detector Jasco MD-2010 Plus. The

resulting residues were purified by semipreparative reverse-phase C18 (Waters, Bondapak, 10 μm, 125Å, 7.8 × 300 mm).

2.4.2 Chemistry

✓ *Tert-butyl 2-(2,3-dihydroxypropylamino)acetate (**55**).*

To a solution of glycidol (**83**, 436 μL, 6.56 mmol) in DMF (5 mL), glycine *t*-butyl ester (**82**, 1.00 g, 5.96 mmol) in DMF (10 mL), and DIPEA (1600 μL, 8.94 mmol) were added. The reaction mixture was refluxed for three days. $NaHCO_3$ (0.50 g, 5.96 mmol) was added and the solvent was concentrated *in vacuo* to give the crude product, which was purified by flash chromatography ($CH_2Cl_2/CH_3OH/NH_3$ 2.0 M solution in ethyl alcohol, from: 100/0/0.1 to 88/12/0.1) to give **84** (0.50 g, 41%) as a yellow pale oil; [Found: C, 52.7; H, 9.4. $C_9H_{19}NO_4$ requires C, 52.67; H, 9.33%]; R_f (97/3/0.1, $CH_2Cl_2/CH_3OH/NH_3$ 2.0M solution in ethyl alcohol) 0.36; δ_H (400.13 MHz $CDC1_3$) 1.42 (9H, s, $(C\underline{H}_3)_3C$), 2.62 (1H, dd, *J* 12.0, 7.7 Hz, $CH\underline{H}CH(OH)CH_2OH$), 2.71 (1H, dd, *J* 12.0, 2.9 Hz, $C\underline{H}HCH(OH)CH_2OH$), 3.28 (2H, br s, $C\underline{H}_2COO$*t*-Bu), 3.51 (1H, dd, *J* 11.0, 5.4 Hz, $CH_2CH(OH)CH\underline{H}OH$), 3.62 (1H, dd, *J* 11.0, 1.2 Hz, $CH_2CH(OH)C\underline{H}HOH$), 3.72 (1H, m, $CH_2C\underline{H}(OH)CH_2OH$); δ_C (100.03 MHz, $CDCl_3$) 29.2, 52.6, 53.1, 66.4, 71.6, 82.7, 172.8; *m/z* (ES) 206 (MH^+); (HRES) MH^+, found 206.1390. $C_9H_{20}NO_4^+$ requires 206.1392.

✓ *(9H-fluoren-9-yl) methyl (tert-butoxycarbonyl) methyl 2,3dihydroxypropylcarbamate (**85**):*

To a solution of **84** (0.681 g, 3.33 mmol) in a 1:1 mixture of 1,4-dioxane/water (46 mL), $NaHCO_3$ (0.559 g, 6.66 mmol) was added. The mixture was sonicated until complete dissolution and, Fmoc-Cl (1.03 g, 3.99 mmol) was added. The reaction mixture was stirred overnight, then, through addition of a saturated solution of $NaHSO_4$, the pH was adjusted to 3 and the solvent was concentrated *in vacuo* to remove the excess of 1,4-dioxane. The water layer was extracted with CH_2Cl_2 (three times), the organic phase was dried over $MgSO_4$, filtered and the solvent evaporated *in vacuo* to give the crude product, which was purified by flash chromatography (CH_2Cl_2/CH_3OH, from: 100/0 to 90/10) to give **85** (0.90 g, 63%) as a yellow pale oil; [Found: C, 67.4; H, 6.9. $C_{24}H_{29}NO_6$ requires C, 67.43; H, 6.84%]; R_f (95/5/0.1, $CH_2Cl_2/CH_3OH/NH_3$ 2.0M solution in ethyl alcohol) 0.44; δ_H (300.10 MHz $CDC1_3$, mixture of rotamers) 1.45 (9H, s, $(C\underline{H}_3)_3C$), 3.04-3.25 (1.7 H, m, $C\underline{H}_2CH(OH)CH_2OH$), 3.40 (0.3 H, m, $C\underline{H}_2CH(OH)CH_2OH$), 3.43-3.92 (3H, m, $CH_2C\underline{H}(OH)CH_2OH$, $CH_2CH(OH)C\underline{H}_2OH$), 3.93 (2H, br s, $C\underline{H}_2$COOt-Bu), 4.22 (0.9H, m, C<u>H</u>-Fmoc and $C\underline{H}_2$-Fmoc), 4.42 (1.4H, br d. *J* 9.0 Hz, $C\underline{H}_2$-Fmoc), 4.61 (0.7H, m, *J* 9.0 Hz, C<u>H</u>-Fmoc), 7.29 (2H, br t, *J* 7.0 Hz, Ar. (Fmoc)), 7.38 (2H, br t, *J* 7.0 Hz, Ar. (Fmoc)), 7.57 (2H, br d, *J* 9.0 Hz, Ar. (Fmoc)), 7.76 (2H, br d, *J* 9.0 Hz, Ar. (Fmoc); δ_C (75.50 MHz, $CDCl_3$, mixture of rotamers) 28.2, 47.4, 52.1, 52.3, 52.9, 53.2, 63.5, 64.0, 67.3, 68.1, 68.5, 70.1, 70.5, 83.1, 120.1, 120.2, 124.9, 125.2, 127.3, 127.9, 128.0, 141.5, 143.8, 156.4, 157.3, 170.4, 171.3; *m/z* (ES) 428 (MH^+); (HRES) MH^+, found 428.2070. $C_{24}H_{30}NO_6^+$ requires 428.2073.

✓ *(9H-fluoren-9-yl) methyl (tert-butoxycarbonyl) methylformylmethylcarbamate (**86**):*

To a solution of **85** (0.80 g, 1.87 mmol) in a 5:1 mixture of THF and water (5 mL), sodium periodate (0.44 g, 2.06 mmol) was added in one portion. The mixture was sonicated for 15 min and stirred for another 2 hours at room temperature. The reaction mixture was filtered, the filtrate was washed with CH_2Cl_2 and the solvent evaporated *in vacuo*. The crude product was dissolved in CH_2Cl_2/H_2O, and the organic phase was dried over $MgSO_4$, filtered and the solvent evaporated *in vacuo* to give the labile

aldehyde **86** (0.72 g, 97%), as white solid; R_f (92/8 CH_2Cl_2/CH_3OH) 0.56; crude **86** was used immediately in the subsequent reductive amination reaction; δ_H (300.10 MHz $CDC1_3$, mixture of rotamers) 1.43 (4.05H, s, $(C\underline{H}_3)_3C$), 1.45 (4.95H, s, $(C\underline{H}_3)_3C$), 3.81 (0.9H, br s, $C\underline{H}_2COO$-*t*Bu), 3.99 (2H, br s, $C\underline{H}_2CHO$), and $C\underline{H}_2COO$-*t*Bu, overlapped), 4.08 (1.1H, s, $C\underline{H}_2CHO$), 4.22-4.19 (1H, m, C<u>H</u>-Fmoc), 4.42 (1.1H, d, *J* 6.0 Hz, $C\underline{H}_2$-Fmoc), 4.50 (0.9H, d, *J* 6.0 Hz, $C\underline{H}_2$-Fmoc), 7.29 (0.9H, br t, *J* 7.0 Hz, Ar. (Fmoc)), 7.38 (1.1H, t, *J* 7.0 Hz, Ar. (Fmoc)), 7.49 (0.9H, d, *J* 9.0 Hz, Ar. (Fmoc)), 7.56 (1.1H, d, *J* 9.0 Hz, Ar. (Fmoc)), 7.73 (2H, m, Ar. (Fmoc)), 9.35 (0.45H, br s, C<u>H</u>O), 9.64 (0.55H, br s, C<u>H</u>O); δ_C (75.50 MHz, $CDCl_3$) 28.2, 47.3, 50.6, 50.8, 57.8, 58.4, 68.1, 68.6, 82.6, 82.7, 120.2, 124.9, 125.2, 127.3, 128.0, 141.5, 143.8, 143.9, 156.0, 156.4, 168.6, 168.7, 198.7; *m/z* (ES) 396 (MH^+); (HRES) MH^+, found 396.1809. $C_{23}H_{26}NO_5^+$ requires 396.1811.

✓ *(9H-fluoren-9-yl) methyl (tert-butoxycarbonyl) methyl 2-((methoxycarbonyl)methylamino)ethylcarbamate (**87**):*

To a solution of crude aldehyde **86** (0.72 g, 1.83 mmol) in dry CH_2Cl_2 (12 mL), a solution of glycine methyl ester hydrochloride (0.30 g, 2.39 mmol) and Et_3N (0.41 mL, 2.93 mmol) was added. The reaction mixture was stirred for 1 h. Sodium triacetoxyborohydride (0.78 g, 3.66 mmol) was then added and the reaction mixture was stirred overnight at room temperature. The resulting mixture was washed with an aqueous saturated solution of $NaHCO_3$ and the aqueous phase extracted with CH_2Cl_2 (three times). The organic phase was dried over $MgSO_4$, filtered and the solvent evaporated *in vacuo* to give the crude product, which was purified by flash chromatography (AcOEt/petroleum ether/NH_3 2.0M solution in ethyl alcohol, from: 40/60/0.1 to 90/10/0.1) to give **87** (0.60 g, 70%) as a colorless oil; [Found: C, 66.7; H, 6.9. $C_{26}H_{32}N_2O_6$ requires C, 66.65; H, 6.88%]; R_f (98/2/0.1, $CH_2Cl_2/CH_3OH/NH_3$ 2.0M solution in ethyl alcohol) 0.63; δ_H (400.13 MHz $CDC1_3$, mixture of rotamers) 1.45 (9H, s, $(C\underline{H}_3)_3C$), 2.56 (0.9H, t, *J* 6.0 Hz, N(Fmoc)$CH_2C\underline{H}_2NH$), 2.83 (1.1H, t, *J* 6.0, N(Fmoc)$CH_2C\underline{H}_2NH$), 3.27 (0.9H, t, *J* 6.0 Hz, N(Fmoc)$C\underline{H}_2CH_2NH$), 3.29 (0.9H, s, $C\underline{H}_2COOMe$), 3.44 (1.1H, s, $C\underline{H}_2COOMe$), 3.49 (1.1H, t, *J* 6.0 Hz, N(Fmoc)$C\underline{H}_2CH_2NH$), 3.72 (3H, s, $C\underline{H}_3$), 3.91 (0.9H, s, $C\underline{H}_2COOtBu$), 3.96 (1.1H, s, $C\underline{H}_2COOtBu$), 4.21 (0.45H, t, *J* 6.0 Hz, $CH_2C\underline{H}$Fmoc), 4.26 (0.55H, t, *J* 6.0 Hz, $CH_2C\underline{H}$Fmoc), 4.37 (1.1H, d, *J* 6.0 Hz, $C\underline{H}_2CH$Fmoc), 4.51 (0.9H, d, *J* 6.0 Hz, $C\underline{H}_2CH$Fmoc), 7.29 (2 H, t, *J* 7.0 Hz, Ar. (Fmoc)), 7.39 (2 H, t, *J* 7.0 Hz, Ar. (Fmoc)), 7.58 (2 H, m, Ar. (Fmoc)), 7.75 (2 H, d, *J* 7.0 Hz, Ar. (Fmoc)); δ_C (100.03 MHz, $CDCl_3$) 27.8, 47.0, 47.2, 47.4, 48.2, 48.6, 50.1, 50.3, 50.5, 53.3, 67.2, 67.6, 81.5, 81.7, 119.7, 124.7, 124.9, 126.8, 127.5, 141.0, 143.7, 156.0, 156.2, 168.7, 169.4, 171.9, 172.1; *m/z* (ES) 469 (MH^+); (HRES) MH^+, found 469.2341. $C_{26}H_{33}N_2O_6^+$ requires 469.2339.

✓ *Compound **88**:*

To a solution of **87** (0.60 g, 1.28 mmol) in DMF (30 mL), thymine-1-acetic acid (0.35 g, 1.90 mmol), HATU (0.73 g, 1.90 mmol) and triethylamine (0.54 mL, 3.84 mmol) were added. The reaction mixture was stirred overnight, concentrated *in vacuo*, dissolved in CH_2Cl_2 (20 mL) and washed 1M HCl solution. The aqueous layer was extracted with CH_2Cl_2 (three times). The combined organic phases were dried over $MgSO_4$, filtered and the solvent evaporated *in vacuo* to give a crude material, which was purified by flash chromatography (AcOEt/petroleum ether, from: 30/70 to 100/0) to give **88** (0.40 g, 49%) as yellow oil; [Found: C, 64.4; H, 6.2. $C_{34}H_{39}N_3O_9$ requires C, 64.44; H, 6.20%]; R_f (8/2,

AcOEt/petroleum ether) 0.38; δ_H (300.10 MHz $CDC1_3$, mixture of rotamers) 1.39-1.44 (9H, m, $(C\underline{H}_3)_3C$), 1.88 (3H, br s, $C\underline{H}_3$-thymine), 2.99 (0.3H, m, $C\underline{H}_2CH_2N$(Fmoc)), 3.08 (0.3H, m, $C\underline{H}_2CH_2N$(Fmoc)), 3.52 (2.8H, m, $C\underline{H}_2CH_2N$(Fmoc) and $CH_2C\underline{H}_2N$(Fmoc)), 3.77-3.89 (3.6H, m, $CH_2C\underline{H}_2N$(Fmoc) and $C\underline{H}_3OOC$), 3.96-4.38 (6H m, $C\underline{H}_2$-thymine, $C\underline{H}_2COOCH_3$, $C\underline{H}_2COO$-*t*Bu), 4.45-4.80 (3H, m, C<u>H</u>(Fmoc) and $C\underline{H}_2CH$(Fmoc)), 6.90-7.06 (1H, complex signal, C<u>H</u>-thymine), 7.28 (2H, m, Ar. (Fmoc)), 7.41 (2H, t, *J* 7.0 Hz, Ar (Fmoc)), 7.55 (2 H, d, *J* 7.0 Hz, Ar. (Fmoc)), 7.75 (2H, t, *J* 7.0 Hz, Ar. (Fmoc)), 8.86 (1H, br s, N<u>H</u>-thymine); δ_C (75.5 MHz, $CDCl_3$) 12.5, 28.2, 31.6, 36.6, 47.2, 47.4, 47.5, 47.8, 48.2, 49.1, 50.6, 51.8, 52.1, 52.5, 53.0, 66.5, 68.2, 82.3, 82.5, 110.5, 120.2, 124.5, 124.8, 125.14, 125.3, 127.3, 127.4, 127.5, 128.0, 128.1, 141.3, 141.4, 143.8, 144.0, 151.1, 156.4, 162.7, 164.4, 169.1, 169.2; *m/z* (ES) 634 (MH^+); (HRES) MH^+, found 634.2767. $C_{34}H_{40}N_4O_9^+$ requires 634.2765.

✓ *Compound **50**:*

To a solution of **88** (0.40 g, 0.63 mmol) in a 1:1 mixture of 1,4-dioxane/water (8 mL) at 0 °C, $LiOH{\cdot}H_2O$ (58 mg, 1.39 mmol) was added. The reaction mixture was stirred for 30 minutes and a saturated solution of $NaHSO_4$ was added until pH~3. The aqueous layer was extracted with CH_2Cl_2 (three times) and once with AcOEt. The combined organic phases were dried over $MgSO_4$, filtered and the solvent evaporated *in vacuo* to give a crude material, which was purified by flash chromatography (CH_2Cl_2/CH_3OH/ AcOH, from: 95/5/0.1 to 80/20/0.1) to give **50** (0.27 g, 69%) as a white solid; [Found: C, 63.0; H, 6.0. $C_{33}H_{37}N_3O_9$ requires C, 63.96; H, 6.02%]; R_f (9/1/0.1, CH_2Cl_2/CH_3OH/NH_3 2.0M solution in ethyl alcohol) 0.12; δ_H (250.13 MHz $CDC1_3$, mixture of rotamers) 1.39-1.43 (9H, m, $(C\underline{H}_3)_3C$), 1.83 (3H, br s, $C\underline{H}_3$ (thymine)), 3.03 (0.3H, m, $C\underline{H}_2CH_2N$(Fmoc)), 3.17 (0.3H, m, $C\underline{H}_2CH_2N$(Fmoc)), 3.55-3.72 (2.8H, m, $C\underline{H}_2CH_2N$(Fmoc) and $CH_2C\underline{H}_2N$(Fmoc)), 3.95-4.06 (6.6H m, $CH_2C\underline{H}_2N$(Fmoc), $C\underline{H}_2$-thymine, $C\underline{H}_2COOH$, $C\underline{H}_2COO$-*t*Bu), 4.14-4.77 (3H, m, C<u>H</u>(Fmoc) and $C\underline{H}_2CH$(Fmoc)), 6.97-7.11 (1H, complex signal, C<u>H</u>-thymine), 7.23-7.40 (4H, m, Ar. (Fmoc)), 7.55 (2 H, d, *J* 7.0 Hz, Ar. (Fmoc)), 7.75 (2H, m, Ar. (Fmoc)), 10.00 (1H, br s, N<u>H</u>-thymine); δ_C (75.50 MHz, $CDCl_3$) 12.3, 28.2, 29.9, 46.4, 47.3, 48.7, 50.2, 50.9, 53.6, 68.3, 82.3, 82.6, 110.8, 120.2, 124.9, 125.2, 125.3, 127.3, 127.5, 128.0, 141.4, 142.1, 143.8, 144.0, 151.7, 156.6, 165.0, 165.2, 168.2, 169.0, 169.2, 172.3; *m/z* (ES) 620 (MH^+); (HRES) MH^+, found 620.2611. $C_{33}H_{38}N_3O_9^+$ requires 620.2608.

✓ *Benzyl 5-(tert-butoxycarbonyl)pentylcarbamate (**90**):*

To a solution of **89**, (3.00 g, 11.3 mmol), DMAP (0.14 g, 1.13 mmol) and *t*-BuOH (1.30 mL, 13.9 mmol), in dry CH_2Cl_2 (5.0 mL), a solution of DCC (13.6 mL, 13.6 mmol, 1.0 M in CH_2Cl_2) was added. The reaction mixture was filtered, the filtrate washed with CH_2Cl_2 and the solvent evaporated *in vacuo* to give the crude product, which was purified by flash chromatography (AcOEt/petroleum ether, from: 10/90 to 100/0) to give **90** (2.10 g, 58%) as white solid; [Found: C, 67.2; H, 8.4. $C_{14}H_{19}NO_4$ requires C, 67.26; H, 8.47%]; R_f (97/3 CH_2Cl_2/CH_3OH) 0.84; δ_H (400.13 MHz $CDC1_3$) 1.31 (2H, q, *J* 6.5 Hz, $C\underline{H}_2CH_2CH_2COO$*t*-Bu), 1.41 (9H, s, $COOC(C\underline{H}_3)_3$), 1.48 (2H, q, *J* 6.5 Hz, $CH_2C\underline{H}_2CH_2NH$), 1.56 (2H, q, *J* 6.5 Hz, $CH_2C\underline{H}_2CH_2COO$*t*-Bu), 2.18 (2H, t, *J* 6.5 Hz, $CH_2CH_2C\underline{H}_2COO$*t*-Bu), 3.15 (2H, q, *J* 6.5 Hz, $CH_2CH_2C\underline{H}_2NH$), 4.91 (1H, br s, N<u>H</u>), 5.07 (2H, br s, $C\underline{H}_2Bn$), 7.32 (5H, m, Ar.); δ_C (75.50 MHz, $CDCl_3$) 24.5, 26.0, 28.0, 29.5, 35.3, 40.8, 66.4, 79.9, 127.9, 128.0, 128.3, 136.6, 156.3, 172.8; *m/z* (ES) 322 (MH^+); (HRES) MH^+, found 322.2015. $C_{18}H_{28}NO_4^+$ requires 322.2018.

✓ *Tert-butyl 6-aminohexanoate (**91**):*

To a solution of **90** (1.95 g, 6.07 mmol) in dry MeOH (150 mL), acetic acid (1.39 mL, 24.0 mmol) and palladium on charcoal (10% w/w, 0.19 g) were added. The reaction mixture was stirred under a hydrogen atmosphere at room temperature for 1 h and filtered through celite. The solvent was evaporated *in vacuo* to give crude **91** (1.13 g, 100%, colorless oil) which was used in the next step without purification; R_f (95/5, CH_2Cl_2/CH_3OH) 0.46; δ_H (400.13 MHz $CDC1_3$) 1.33 (2H, q, *J* 6.5 Hz, $C\underline{H}_2CH_2CH_2COO$*t*-Bu), 1.39 (9H, s, $COOC(C\underline{H}_3)_3$), 1.55 (2H, q, *J* 6.5 Hz, $CH_2CH_2CH_2C\underline{H}_2CH_2NH$), 1.62 (2H, q, *J* 6.5 Hz, $CH_2C\underline{H}_2CH_2COO$*t*-Bu), 2.17 (2H, t, *J* 6.5 Hz, $CH_2CH_2C\underline{H}_2COO$*t*-Bu), 2.84 (2H, t, *J* 6.5 Hz, $CH_2CH_2C\underline{H}_2NH$); δ_C (75.50 MHz, $CDCl_3$) 24.3, 25.8, 27.2, 28.0, 35.1, 39.4, 80.2, 177.2; *m/z* (ES) 188 (MH^+); (HRES) MH^+, found 188.1647. $C_{10}H_{22}NO_2^+$ requires 188.1651.

✓ *Benzyl 2-hydroxyethylcarbamate (**93**):*

To a solution of ethanolamine (**92**, 2.00 g, 32.8 mmol) in dry CH_2Cl_2 (30 mL) at 0°C, a solution Cbz-Cl (3.73 mL, 26.2 mmol) in dry CH_2Cl_2 (20 mL) was slowly added. The reaction mixture was stirred for 2 hours at 0°C and at room temperature overnight. The resulting mixture was washed with an aqueous saturated solution of $NaHCO_3$ and the aqueous phase extracted with CH_2Cl_2. (three times). The organic phase was dried over $MgSO_4$, filtered and the solvent evaporated *in vacuo* to give crude **93** (5.11 g, 100%, yellow pale oil) which was used in the next step without purification; R_f (92/8, CH_2Cl_2/CH_3OH) 0.47; δ_H (250.13 MHz $CDC1_3$) 3.36 (2H, br t, *J* 6.5 Hz, $C\underline{H}_2OH$), 3.71 (2H, q, *J* 6.5 Hz, $C\underline{H}_2NH$), 5.11 (2H, s, $C\underline{H}_2Bn$), 7.35 (5H, m, Ar.); δ_C (62.89 MHz, $CDCl_3$) 43.3, 61.7, 66.7, 127.9, 128.0, 128.4, 136.2, 157.0; *m/z* (ES) 196 (MH^+); (HRES) MH^+, found 196.0970. $C_{10}H_{14}NO_3^+$ requires 196.0974.

✓ *Benzyl 2-iodoethylcarbamate (**94**):*

To a solution of PPh_3 (2.66 g, 10.2 mmol) in CH_2Cl_2 (10 mL), I_2 (2.59 g, 10.2 mmol) in CH_2Cl_2 (10 mL) was slowly added. The reaction mixture was stirred for 30 min. Imidazole (1.39 g, 20.4 mmol) in CH_2Cl_2 (10 mL) was then added and the reaction mixture was stirred for further 30 min. Finally, **93** (1.00 g, 5.13 mmol) was added and the reaction mixture stirred for 3 hours. The resulting mixture was washed with an aqueous saturated solution of $NaHCO_3$ and 10 %w/w of $Na_2S_2O_3$ and the aqueous phase extracted with CH_2Cl_2 (three times). The organic phase was dried over $MgSO_4$, filtered and the solvent evaporated *in vacuo* to give a crude material, which was purified by flash chromatography (AcOEt/petroleum ether, from: 0/100 to 100/0) to give **94** (1.20 g, 77%) as white amorphous solid; [Found: C, 39.4; H, 4.0. $C_{10}H_{12}INO_2$ requires C, 39.36; H, 3.96%]; R_f (6/4, AcOEt/petroleum ether) 0.88; δ_H (250.13 MHz $CDC1_3$) 3.25 (2H, t, *J* 6.5 Hz, $C\underline{H}_2I$), 3.55 (2H, q, *J* 6.5 Hz, $C\underline{H}_2NH$), 5.11 (2H, s, $C\underline{H}_2Bn$), 7.36 (5H, m, Ar.); δ_C (62.89 MHz, $CDCl_3$) 5.1, 43.0, 66.5, 127.8, 128.1, 128.2, 136.0, 155.8; *m/z* (ES) 306 (MH^+); (HRES) MH^+, found 305.9989. $C_{10}H_{13}INO_2^+$ requires 305.9991.

✓ *Benzyl 2-(5-(tert-butoxycarbonyl)pentylamino) ethylcarbamate (**95**):*

To a solution of **91** (0.35 g, 1.87 mmol) in dry acetonitrile (10 mL), at reflux, K_2CO_3 (0.88 g, 6.38 mmol) was added. The reaction mixture was stirred for 10 min. After that, a solution of **94** (0.40 g, 1.31 mmol) in dry acetonitrile (5 mL), was added and the reaction mixture was stirred at reflux overnight. The product was filtered and the crude was purified by flash column chromatograph, (CH_2Cl_2/CH_3OH, from: 100/0 to 90/10) to give **95** (0.32 g, 67%) as yellow light oil; [Found: C, 65.9; H, 8.6. $C_{20}H_{32}N_2O_4$ requires C, 65.91; H, 8.62%]; R_f (93/7, CH_2Cl_2/CH_3OH) 0.71; δ_H (300.10 MHz $CDC1_3$) 1.35 (2H, q, *J* 6.5 Hz, $CH_2CH_2C\underline{H}_2CH_2CH_2NH$), 1.43 (9H, s, $COOC(C\underline{H}_3)_3$), 1.57 (2H, q, *J* 6.0 Hz, $CH_2CH_2CH_2C\underline{H}_2CH_2NH$), 1.67 (2H, q, *J* 6.0 Hz, $CH_2C\underline{H}_2CH_2CH_2CH_2NH$), 2.21 (2H, t, *J* 6.0 Hz,

OOCC$\underline{H}_2$CH$_2$), 2.82 (2H, t, *J* 6.0 Hz, CH$_2$CH$_2$CH$_2$CH$_2$C$\underline{H}_2$NH), 2.99 (2H, t, *J* 6.0 Hz, CONHCH$_2$C$\underline{H}_2$NH), 3.46 (2H, q, *J* 6.0 Hz, CONHC$\underline{H}_2$CH$_2$NH), 5.09 (2H, s, C$\underline{H}_2$Ar), 5.73 (1H, br s, N$\underline{H}$COO), 7.34 (5H, m, Ar.); δ_C (75.50 MHz, $CDCl_3$) 24.4, 26.2, 27.9, 35.0, 39.3, 48.4, 48.6, 66.6, 79.9, 127.9, 128.0, 128.3, 136.1, 156.6, 172.8; *m/z* (ES) 365 (MH^+); (HRES) MH^+, found 365.2437. $C_{20}H_{33}N_2O_4^+$ requires 365.2440.

✓ *Compound (**96**):*

To a solution of **95** (0.32 g, 0.88 mmol) in a 1:1 mixture of 1,4-dioxane/water (20 mL), $NaHCO_3$ (148 mg, 1.76 mmol) was added. The mixture was sonicated until complete dissolution and, Fmoc-Cl (0.29 g, 1.12 mmol) was added. The reaction mixture was stirred overnight, then, through addition of a saturated of $NaHSO_4$, the pH was adjusted to 3 and the solvent was concentrated *in vacuo* to remove the excess of dioxane. The water layer was extracted with CH_2Cl_2 (three times), the organic phase was dried over $MgSO_4$, filtered and the solvent evaporated *in vacuo* to give the crude product, which was purified by flash chromatography (CH_2Cl_2/CH_3OH, from: 100/0 to 98/2) to give **96** (0.50 g, 97%) as a yellow light oil; [Found: C, 71.7; H, 7.3. $C_{35}H_{42}N_2O_6$ requires C, 71.65; H, 7.22%]; R_f (95/5, CH_2Cl_2/CH_3OH) 0.61; δ_H (400.13 MHz $CDC1_3$, mixture of rotamers) 1.08-1.60 (15H, m, CH$_2$C$\underline{H}_2$C$\underline{H}_2$C$\underline{H}_2$CH$_2$N, COOC(C$\underline{H}_3$)$_3$), 2.16 (2H, t, *J* 6.0 Hz, C$\underline{H}_2$COO), 2.85 (0.8H, br s, CH$_2$CH$_2$CH$_2$CH$_2$C$\underline{H}_2$N), 2.96 (2.4H, CONHCH$_2$C$\underline{H}_2$N and CH$_2$CH$_2$CH$_2$CH$_2$C$\underline{H}_2$N), 3.13 (0.8H, br s, CONHCH$_2$C$\underline{H}_2$N), 3.30 (2H, br s, CONHC$\underline{H}_2$CH$_2$N), 4.19 (1H, br s, CH$_2$C$\underline{H}$Fmoc), 4.53-4.57 (2H, br s, C$\underline{H}_2$CHFmoc), 5.05 (2H, br s, C$\underline{H}_2$Ar), 7.29 (7H, m, Ar. (Cbz) and Ar. (Fmoc)), 7.38 (2H, t, *J* 7.0 Hz, Ar. (Fmoc)), 7.55 (2 H, d, *J* 7.0 Hz, Ar. (Fmoc)), 7.76 (2H, t, *J* 7.0 Hz, Ar. (Fmoc)); δ_C (62.89 MHz, $CDCl_3$) 24.5, 25.9, 27.8, 27.9, 35.2, 39.2, 39.6, 46.2, 46.8, 47.1, 47.6, 66.3, 79.7, 119.6, 124.4, 126.8, 127.4, 127.8, 128.2, 136.4, 141.1, 143.7, 155.6, 156.3, 172.7; *m/z* (ES) 587 (MH^+); (HRES) MH^+, found 587.3120. $C_{35}H_{43}N_2O_6^+$ requires 587.3121.

✓ *Compound (**97**):*

To a solution of **96** (150 mg, 0.26 mmol) in dry MeOH (9 mL), acetic acid (29 μL, 0.512 mmol) and palladium on charcoal (10%w/w, 15 mg) were added. The reaction mixture was stirred under a hydrogen atmosphere at room temperature for 1 h and filtered through celite. The solvent was evaporated *in vacuo* to give crude **97** (118 mg, 100%, colorless oil) which was used in the next step without purification; R_f (95/5, CH_2Cl_2/CH_3OH) 0.13; δ_H (300.10 MHz $CDC1_3$, mixture of rotamers) 1.05-1.60 (15H, m, CH$_2$C$\underline{H}_2$C$\underline{H}_2$C$\underline{H}_2$CH$_2$N, COOC(C$\underline{H}_3$)$_3$), 2.15 (2H, t, *J* 6.0 Hz, C$\underline{H}_2$COO), 2.60 (0.6H, br s, CH$_2$CH$_2$CH$_2$CH$_2$C$\underline{H}_2$N), 2.90-3.20 (4H, CONHCH$_2$C$\underline{H}_2$N, CH$_2$CH$_2$CH$_2$CH$_2$C$\underline{H}_2$N, CONHCH$_2$C$\underline{H}_2$N and CONHC$\underline{H}_2$CH$_2$N), 3.38 (1.4H, br s, CONHC$\underline{H}_2$CH$_2$N), 4.19 (1H, br s, CH$_2$C$\underline{H}$Fmoc), 4.52 (2H, m, C$\underline{H}_2$CHFmoc), 7.38 (4H, m, Ar. (Fmoc)), 7.54 (2 H, d, *J* 7.0 Hz, Ar. (Fmoc)), 7.74 (2H, t, *J* 7.0 Hz, Ar. (Fmoc)); δ_C (100.03 MHz, $CDCl_3$) 22.6, 24.4, 24.7, 25.9, 26.1, 28.1, 35.1, 25.4, 38.8, 42.4, 46.5, 47.3, 47.9, 53.4, 67.0, 80.1, 119.8, 119.9, 124.0, 124.6, 126.9, 127.1, 127.7, 140.5, 141.3, 143.8, 149.0, 155.8, 157.1, 172.7, 172.9; *m/z* (ES) 453 (MH^+); (HRES) MH^+, found 453.2740. $C_{27}H_{37}N_2O_4^+$ requires 453.2748.

✓ *Compound (**98**):*

To a solution of **97** (115 mg, 0.26 mmol) in CH_2Cl_2 (5 mL), ethyl glyoxalate (33 μL, 0.33 mmol), Et_3N (54 μL, 0.38 mmol) and $NaHB(OAc)_3$ (109 mg, 0.52 mmol) were added. The reaction mixture was

stirred overnight. The resulting mixture was washed with an aqueous saturated solution of $NaHCO_3$ and the aqueous phase extracted with CH_2Cl_2 (three times). The organic phase was dried over $MgSO_4$, filtered and the solvent evaporated *in vacuo* to give the crude product, which was purified by flash chromatography (AcOEt/petroleum ether, from: 60/40 to 100/0) to give **98** (35 mg, 25%) as white light oil; [Found: C, 69.2; H, 7.9. $C_{31}H_{42}N_2O_6$ requires C, 69.12; H, 7.86%]; R_f (95/5/0.1, $CH_2Cl_2/CH_3OH/NH_3$ 2.0M solution in ethyl alcohol) 0.46; δ_H (300.10 MHz $CDC1_3$, mixture of rotamers) 1.00-1.80 (18H, m, $CH_2C\underline{H}_2C\underline{H}_2C\underline{H}_2CH_2N$, $COOC(C\underline{H}_3)_3$ and $COOCH_2C\underline{H}_3$), 2.18 (2H, t, *J* 6.0 Hz, $C\underline{H}_2COOC(CH_3)_3$), 2.46 (0.8H, br s, $CH_2CH_2CH_2CH_2C\underline{H}_2N$), 2.74 (1.2H, br s, $CH_2CH_2CH_2CH_2C\underline{H}_2N$), 2.90-3.45 (6H, m, $COC\underline{H}_2NHC\underline{H}_2C\underline{H}_2N$,), 4.18-4.23 (3H, m, $COOC\underline{H}_2CH_3$, $CH_2C\underline{H}$Fmoc), 4.52 (2H, m, $C\underline{H}_2$CHFmoc), 7.31 (2 H, t, *J* 7 Hz, Ar. (Fmoc)), 7.39 (2 H, t, *J* 7 Hz, Ar. (Fmoc)), 7.57 (2 H, d, *J* 7 Hz, Ar. (Fmoc)), 7.75 (2H, t, *J* 7 Hz, Ar. (Fmoc)); δ_C (100.03 MHz, $CDCl_3$, mixture of rotamers) 14.1, 24.7, 26.1, 28.0, 35.3, 46.8, 47.3, 47.8, 50.6, 60.7, 66.5, 79.9, 119.8, 124.6, 126.9, 127.5, 141.3, 144.0, 155.9, 156.2, 172.2, 172.9; *m/z* (ES) 539 (MH^+); (HRES) MH^+, found 539.3117. $C_{31}H_{43}N_2O_6^+$ requires 539.3121.

✓ *Compound (**99**):*

To a solution of **98** (100 mg, 0.186 mmol) in DMF (6 mL), thymine-1-acetic acid (55 mg, 0.30 mmol), PyBOP (154 mg, 0.30 mmol) and triethylamine (83 μL, 0.60 mmol) were added. The reaction mixture was stirred overnight, concentrated *in vacuo*, dissolved in CH_2Cl_2 (20 mL) and washed 1M HCl solution. The aqueous layer was extracted with CH_2Cl_2 (three times). The combined organic phases were dried over $MgSO_4$, filtered and the solvent evaporated *in vacuo* to give a crude material, which was purified by flash chromatography (AcOEt/petroleum ether, from: 30/70 to 100/0) to give **99** (92 mg, 70%) as amorphous white solid; [Found: C, 64.7; H, 6.9. $C_{38}H_{48}N_4O_9$ requires C, 64.76; H, 6.86%]; R_f (6/40, AcOEt/petroleum ether) 0.11; δ_H (250.13 MHz $CDC1_3$, mixture of rotamers) 1.00-1.60 (18H, m, $CH_2C\underline{H}_2C\underline{H}_2C\underline{H}_2CH_2N$, $COOC(C\underline{H}_3)_3$ and $COOCH_2C\underline{H}_3$), 1.89 (3H, s, $C\underline{H}_3$-thymine), 2.18 (2H, m, $C\underline{H}_2COOC(CH_3)_3$), 2.95-3.65 (6H, m, $NHC\underline{H}_2C\underline{H}_2NC\underline{H}_2$), 4.00-4.80 (9H, m, $C\underline{H}_2OOCC\underline{H}_2NHCH_2$, $C\underline{H}_2C\underline{H}$Fmoc and $C\underline{H}_2$-thymine), 6.94-7.00 (1H, complex signal, C<u>H</u>-thymine), 7.39 (2 H, t, *J* 7.0 Hz, Ar. (Fmoc)), 7.42 (2 H, t, *J* 7.0 Hz, Ar. (Fmoc)), 7.56 (2 H, d, *J* 7.0 Hz, Ar. (Fmoc)), 7.76 (2H, t, *J* 7.0 Hz, Ar. (Fmoc)), 8.43 (1H, br s, N<u>H</u>-thymine); δ_C (75.50 MHz, $CDCl_3$, mixture of rotamers) 12.1, 13.9, 24.6, 26.0, 28.0, 35.3, 46.4, 46.7, 47.2, 47.8, 48.1, 50.7, 61.7, 66.9, 80.1, 110.6, 111.0, 119.9, 124.6, 127.0, 127.6, 141.3, 143.8, 143.9, 151.2, 156.4, 164.3, 167.7, 168.9, 173.0; *m/z* (ES) 705 (MH^+); (HRES) MH^+, found 705.3498. $C_{38}H_{49}N_4O_9^+$ requires 705.3500.

✓ *Compound (**51**):*

To a solution of **99** (175 mg, 0.25 mmol) in a 1:1 mixture of 1,4-dioxane/water (6 mL) at 0 °C, $LiOH{\cdot}H_2O$ (23 mg, 0.55 mmol) was added. The reaction mixture was stirred for 30 minutes and saturated solution of $NaHSO_4$ added until pH~3. The aqueous layer was extracted with CH_2Cl_2 (three times) and once with AcOEt. The combined organic phases were dried over $MgSO_4$, filtered and the solvent evaporated *in vacuo* to give a crude material, which was purified by flash chromatography (CH_2Cl_2/CH_3OH, from: 95/5 to 80/20) to give **51** (50 mg, 30%) as amorphous white solid; [Found: C, 64.0; H, 6.6. $C_{36}H_{44}N_4O_9$ requires C, 63.89; H, 6.55%]; R_f (9/1/0.1, $CH_2Cl_2/CH_3OH/NH_3$ 2.0M solution in ethyl alcohol) 0.22; δ_H (400.13 MHz $CDC1_3$, mixture of rotamers) 1.00-1.50 (15H, m, $CH_2C\underline{H}_2C\underline{H}_2C\underline{H}_2CH_2N$ and $COOC(C\underline{H}_3)_3$), 1.86 (3H, s, $C\underline{H}_3$-thymine), 2.17 (2H, m, *J* 6.0 Hz, $C\underline{H}_2COOC(CH_3)_3$), 2.90-3.70 (6H, m, $NHC\underline{H}_2C\underline{H}_2NC\underline{H}_2$), 3.90-4.85 (7H, m, $OCC\underline{H}_2NHCH_2$,

C$\underline{H}_2$C$\underline{H}$Fmoc and C$\underline{H}_2$-thymine), 7.02 (1H, br s, C$\underline{H}$-thymine), 7.10-7.45 (4H, m, Ar. (Fmoc)), 7.57 (2 H, d, *J* 7.0 Hz, Ar. (Fmoc)), 7.77 (2H, t, *J* 7.0 Hz, Ar. (Fmoc)); 10.00 (1H, br s, N$\underline{H}$-thymine); δ_C (100.03 MHz, $CDCl_3$, mixture of rotamers) 13.5, 22.7, 25.9, 26.0, 27.3, 28.8, 29.4, 29.7, 36.6, 36.7, 45.8, 47.8, 48.5, 48.8, 49.6, 54.7, 68.3, 81.4, 81.6, 111.8, 111.9, 121.2, 125.9, 126.5, 128.3, 129.0, 129.5, 130.3, 139.1, 142.6, 142.9, 145.0, 145.1, 152.6, 157.7, 166.2, 169.0, 172.7, 174.4; *m/z* (ES) 677 (MH^+); (HRES) MH^+, found 677.3185. $C_{36}H_{45}N_4O_9^+$ requires 677.3187.

✓ *Low yield synthesis of tert-butyl 6-(2,3-dihydroxypropylamino) hexanoate and unwanted tert-butyl 6-(bis(2,3-dihydroxypropyl) amino) hexanoate:*

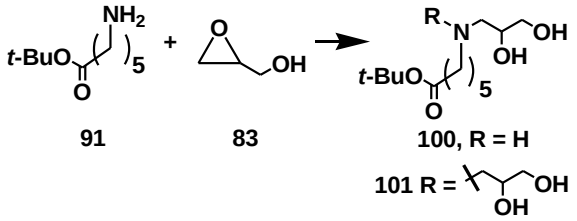

To a solution of glycidol (**83**, 134 µL, 2.02 mmol) in DMF (3 mL), *t*-butyl 6-aminohexanoate (**91**, 456 mg, 2.44 mmol) in DMF (3 mL), and DIPEA (0.55 mL, 3.17 mmol) were added. The reaction mixture was refluxed for three days. $NaHCO_3$ (320 mg, 1.79 mmol) was added and the solvent was concentrated *in vacuo* to give the crude product, which was purified by flash chromatography (CH_2Cl_2/CH_3OH/NH_3 2.0M solution in ethyl alcohol, from: 100/0/0.1 to 88/12/0.1) to give **100** (60 mg, 11%) and **101** (320 mg, 47%). **100**: yellow pale oil; [Found: C, 59.8; H, 10.5. $C_{13}H_{27}NO_4$ requires C, 59.74; H, 10.41%]; R_f (90/10/0.1, CH_2Cl_2/CH_3OH/NH_3 2.0M solution in ethyl alcohol) 0.31; δ_H (300.10 MHz $CDC1_3$) 1.31 (2H, q, *J* 6.5 Hz, C$\underline{H}_2$CH_2CH_2COO*t*-Bu), 1.43 (9H, s, COOC(C$\underline{H}_3$)$_3$), 1.52 (2H, quint., *J* 6.5 Hz, CH_2C$\underline{H}_2$$CH_2$NH), 1.57 (2H, q, *J* 6.5 Hz, CH_2C$\underline{H}_2$$CH_2$COO*t*-Bu), 2.20 (2H, t, *J* 6.5 Hz, CH_2CH_2C$\underline{H}_2$COO*t*-Bu), 2.58 (2H, m, C$\underline{H}_2$NHCH_2CH(OH)CH_2(OH)), 2.69 (1H, dd, *J* 15.0, 6.0 Hz, NHC$\underline{H}$HCH(OH)CH_2(OH)), 2.80 (1H, dd, *J* 15.0, 3.0 Hz, CH$\underline{H}$CH(OH)CH_2(OH)), 3.59 (1H, dd, *J* 9.0, 3.0 Hz, CH_2CH(OH)C$\underline{H}$H(OH)), 3.70 (1H, dd, *J* 9.0, 3.0 Hz, CH_2CH(OH)CH$\underline{H}$(OH)), 3.77 (1H, m, CH_2C$\underline{H}$(OH)CH_2(OH)); δ_C (62.89 MHz, $CDCl_3$) 24.6, 26.4, 27.9, 28.7, 35.2, 49.2, 51.8, 65.1, 69.7, 80.0, 173.0; *m/z* (ES) 262 (MH^+); (HRES) MH^+, found 262.2017. $C_{13}H_{28}NO_4^+$ requires 262.2018. **101**: yellow oil; [Found: C, 57.3; H, 9.8. $C_{16}H_{33}NO_6$ requires C, 57.29; H, 9.92%]; R_f (90/10/0.1, CH_2Cl_2/CH_3OH/NH_3 2.0M solution in ethyl alcohol) 0.44; δ_H (400.13 MHz, $CDC1_3$, mixture of diastereoisomers) 1.27 (2H, q, *J* 6.5 Hz, C$\underline{H}_2$CH_2CH_2COO*t*-Bu), 1.43 (11H, m, COOC(C$\underline{H}_3$)$_3$ and CH_2C$\underline{H}_2$$CH_2$NH), 1.57 (2H, q, *J* 6.5 Hz, CH_2C$\underline{H}_2$$CH_2$COO*t*-Bu), 2.19 (2H, t, *J* 6.5 Hz, CH_2CH_2C$\underline{H}_2$COO*t*-Bu), 2.40-2.60 (6H, m, C$\underline{H}_2$NH[(C$\underline{H}_2$CH(OH)CH_2(OH)]$_2$), 3.50 (2H, m, NH[CH_2CH(OH)C$\underline{H}$H(OH)]$_2$), 3.63 (2H, m, NH[CH_2CH(OH)CH$\underline{H}$(OH)]$_2$), 3.77 (2H, m, NH[CH_2C$\underline{H}$(OH)CH_2(OH)]$_2$); δ_C (62.89 MHz, $CDCl_3$, mixture of diastereoisomers) 26.1, 27.5, 28.0, 29.3, 29.4, 36.7, 56.8, 56.9, 58.3, 59.1, 66.0, 66.2, 70.5, 71.0, 81.5, 174.6; *m/z* (ES) 336 (MH^+); (HRES) MH^+, found 336.2383. $C_{16}H_{34}NO_6^+$ requires 336.2386.

2.4.3 General procedure for manual solid-phase oligomerization.

PNA oligomers were assembled on a Rink amide PEGA resin using the above obtained Fmoc-protected PNA modified monomers as well as normal PNA monomers.

Rink amide PEGA resin (50 – 100 mg) was first swelled in CH_2Cl_2 for 30 minutes. Normal PNA monomers (from Link Technologies) was provided by Advance Biosystem Italia srl. The Fmoc group was then deprotected by 20% piperidine in DMF (8 min x 2). The resin was washed with DMF and CH_2Cl_2 and was indicated to be positive by the Kaiser test. The resin was preloaded with a Fmoc-Glycine and subsequently, the coupling of the monomers (PNA or PNA modified) was conducted with either one of the following two methods (A and B). Method A: monomer (5 eq), HBTU (4.9 eq) and DIPEA (10 eq); method B: modified monomer (2 eq), HATU (2 eq) and DIPEA (10 eq). When the monomer was coupled to a primary amine, i.e., to a classic PNA monomer, method A was used; when the coupling was to a secondary amine, i.e., to a modified PNA monomer, method B was used. The coupling mixture was added directly to the Fmoc-deprotected resin. The coupling reaction required 30 minutes at room temperature for the introduction of both normal and modified monomers, in case of method B the coupling time was raised to 6 h, and the resin was then washed by DMF/ CH_2Cl_2. The Fmoc deprotection and monomer coupling cycles were continued until the coupling of the last residue. After every coupling the oligomer was capped by adding 5% acetic anhydride and 6% DIPEA in DMF and the reaction vessel was shaken for 1 min (twice), and subsequently washed with a solution of 5% of DIPEA in DMF. The resin was always washed thoroughly with DMF/ CH_2Cl_2. The cleavage from the resin was achieved by addition of a solution of 90% TFA and 10% m-cresol. The PNA was then precipitated adding 10 volumes of diethyl ether, cooled at -18°C for at least 2 h and finally collected through centrifugation (5 minutes @ 5000 rpm). The resulting residue was redisolved in H_2O and purified by semipreparative reverse-phase C18 (Waters, Bondapak, 10 μm, 125Å, 7.8 × 300 mm) gradient elution from 100% H_2O (0.1% TFA, eluent A) to 60% CH_3CN (0.1%TFA, eluent B) in 30 min. The product was then lyophilized to get a white solid. MALDI-TOF MS analysis confirmed the expected structures for the four oligomers (**49**-**52**), with peaks at the following *m*/*z* values: compound **49** *m*/*z* **(**MALDI-TOF MS – negative mode) 2839 $(M–H)^-$, calcd. for $C_{112}H_{140}N_{59}O_{33}^-$ 2839.11, 60%; compound **50** *m*/*z* **(**MALDI-TOF MS – negative mode) 2955 $(M–H)^-$, calcd. For $C_{116}H_{144}N_{59}O_{37}^-$ 2955.12, 57%; compound **51** *m*/*z* **(**MALDI-TOF MS – negative mode) 2895 $(M–H)^-$, calcd. for $C_{116}H_{148}N_{59}O_{33}^-$ 2895.17, 62%; compound **52** *m*/*z* **(**MALDI-TOF MS – negative mode) 3123 $(M–H)^-$, calcd. for $C_{128}H_{168}N_{59}O_{37}^-$ 3123.31, 65%.

2.4.4 Thermal denaturation studies

DNA oligonucleotides were purchased from CEINGE Biotecnologie avanzate s.c. a r.l.

The PNA oligomers and DNA were hybridized in a buffer 100 mM NaCl, 10 mM sodium phosphate and 0.1 mM EDTA, pH 7.0. The concentrations of PNAs were quantified by measuring the absorbance (A_{260}) of the PNA solution at 260 nm. The values for the molar extinction coefficients (ε_{260}) of the individual bases are: ε_{260} (A) = 13.7 mL/(μmole x cm), ε_{260} (C)= 6.6 mL/(μmole x cm), ε_{260} (G) = 11.7 mL/(μmole x cm), ε_{260} (T) = 8.6 mL/(μmole x cm) and molar extinction coefficient of PNA was calculated as the sum of these values according to sequence.

The concentrations of DNA and modified PNA oligomers were 5 μM each for duplex formation. The samples were first heated to 90 °C for 5 min, followed by gradually cooling to room temperature. Thermal denaturation profiles (Abs vs. T) of the hybrids were measured at 260 nm with an UV/Vis Lambda Bio 20 Spectrophotometer equipped with a Peltier Temperature Programmer PTP6 interfaced to a personal computer. UV-absorption was monitored at 260 nm from in a 18-90°C range at the rate of 1 °C per minute. A melting curve was recorded for each duplex. The melting temperature (T_m) was determined from the maximum of the first derivative of the melting curves

Chapter 3

3. Structural analysis of cyclopeptoids and their complexes

3.1. Introduction

Many small proteins include intramolecular side-chain constraints, typically present as disulfide bonds within cystine residues.

The installation of these disulfide bridges can stabilize three-dimensional structures in otherwise flexible systems. Cyclization of oligopeptides has also been used to enhance protease resistance and cell permeability. Thus, a number of chemical strategies have been employed to develop novel covalent constraints, including lactam and lactone bridges, ring-closing olefin metathesis,[76] click chemistry,[77-78] as well as many other approaches.[2] Because peptoids are resistant to proteolytic degradation[79], the objectives for cyclization are aimed primarily at rigidifying peptoid conformations. Macrocyclization requires the incorporation of reactive species at both termini of linear oligomers that can be synthesized on suitable solid support. Despite extensive structural analysis of various peptoid sequences, only one X-ray crystal structure has been reported of a linear peptoid oligomer.[80] In contrast, several crystals of cyclic peptoid hetero-oligomers have been readily obtained, indicating that macrocyclization is an effective strategy to increase the conformational order of cyclic peptoids, relative to linear oligomers. For example, the crystals obtained from hexamer **102** and octamer **103** (figure **3.1**) provided the first high-resolution structures of peptoid hetero-oligomers determined by X-ray diffraction.

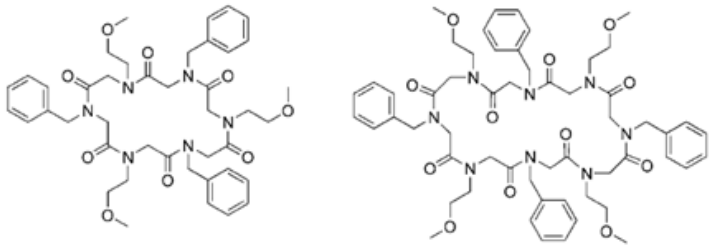

102 **103**

Figure 3.1. Cyclic peptoid hexamer **102** and octamer **103.** The sequence of cis/trans amide bonds depicted is consistent with X-ray crystallographic studies.

Cyclic hexamer **102** reveals a combination of four *cis* and two *trans* amide bonds, with the cis bonds at the corners of a roughly rectangular structure, while the backbone of cyclic octamer **103** exhibits four *cis* and four *trans* amide bonds. Perhaps the most striking observation is the orientation of the side chains in cyclic hexamer **102,** (figure **3.2**) as the pendant groups of the macrocycle alternate in opposing directions relative to the plane defined by the backbone.

[76] H. E. Blackwell, J. D. Sadowsky, R. J. Howard, J. N. Sampson, J. A. Chao, W. E. Steinmetz, D. J. O_Leary, R. H. Grubbs, *J. Org. Chem*. **2001**, 66, 5291 –5302.

[77] S. Punna, J. Kuzelka, Q. Wang, M. G. Finn, *Angew. Chem. Int. Ed.* **2005**, 44, 2215 –2220.

[78] Y. L. Angell, K. Burgess, *Chem. Soc. Rev.* 2007, 36, 1674 –1689.

[79] S. B. Y. Shin, B. Yoo, L. J. Todaro, K. Kirshenbaum, *J. Am. Chem. Soc*. **2007**, 129, 3218 –3225.

[80] B. Yoo, K. Kirshenbaum, *Curr. Opin. Chem. Biol.* **2008,** 12, 714 –721.

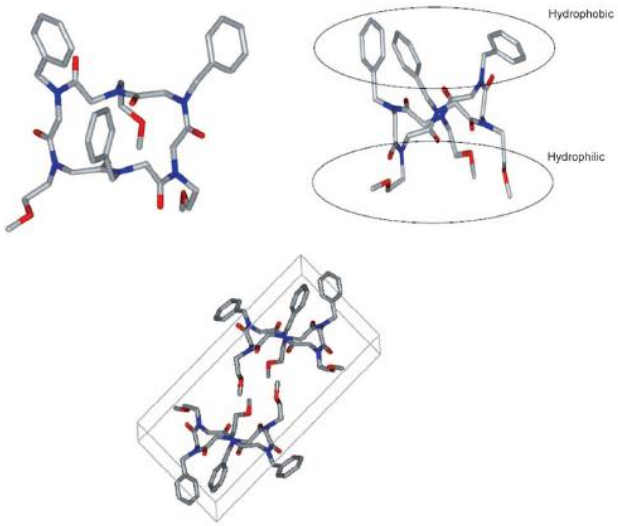

Figure 3.2. Crystal structure of cyclic hexamer **102**.[31]

In the crystalline state, the packing of the cyclic hexamer appears to be directed by two dominant interactions. The unit cell (figure **3.2**, bottom) contains a pair of molecules, in which the polar groups establish contacts between the two macrocycles. The interface between each unit cell is defined predominantly by aromatic interactions between the hydrophobic side chains. X-ray crystallography of peptoid octamer **103** reveals structure that retains many of the same general features as observed in the hexamer (figure **3.3**).

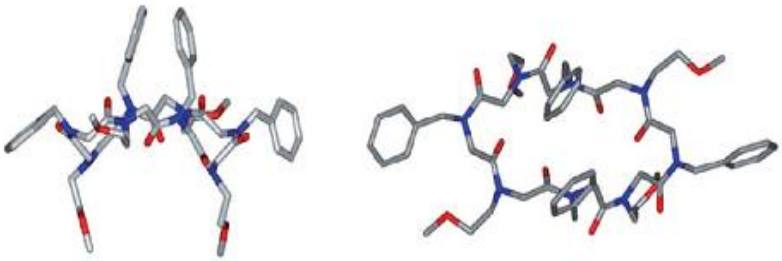

Figure 3.3. Cyclic octamer **103**.[7] Top: Equatorial view relative to the cyclic backbone. Bottom: Axial view, backbone dimensions 8.0 x 4.8 Å.

The unit cell within the crystal contains four molecules (figure **3.4**). The macrocycles are assembled in a hierarchical manner, and associate by stacking of the oligomer backbones. The stacks interlock to form sheets, and finally the sheets are sandwiched to form the three-dimensional lattice. It is notable that in the stacked assemblies, the cyclic backbones overlay in the axial direction, even in the absence of hydrogen bonding.

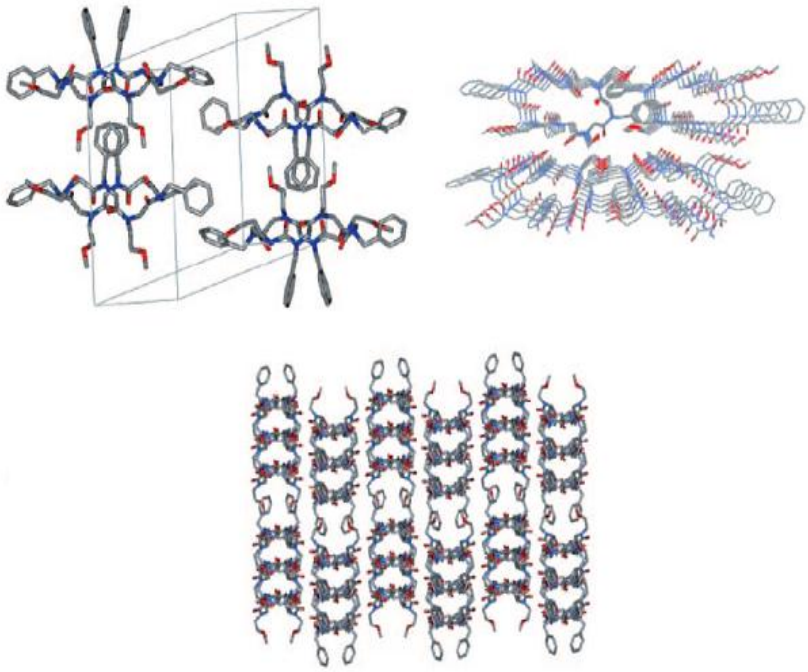

Figure 3.4. Cyclic octamer **103**. Top: The unit cell contains four macrocycles. Middle: Individual oligomers form stacks. Bottom: The stacks arrange to form sheets, and sheets are propagated to form the crystal lattice.

Cyclic α and β-peptides, by contrast, can form stacks organized through backbone hydrogen-bonding networks [81-82]. Computational and structural analyses for a cyclic peptoid trimer **30**, tetramer **31**, and hexamer **32** (figure **3.5**) were also reported by my research group[83].

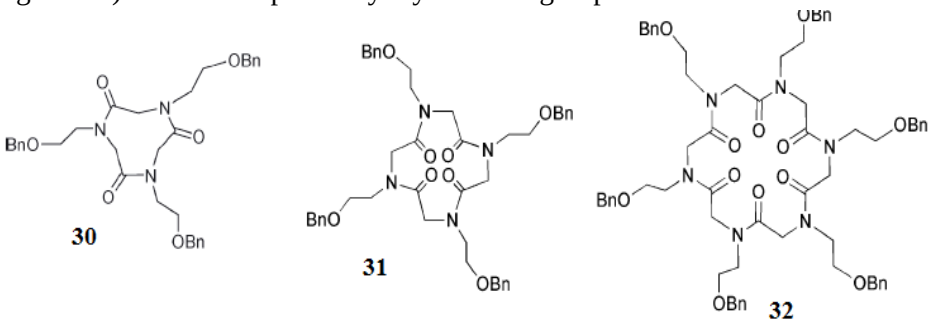

Figure 3.5. Trimer **30**, tetramer **31**, and hexamer **32** were also reported by my research group.

Theoretical and NMR studies for the trimer **30** suggested the backbone amide bonds to be present in the cis form. The lowest energy conformation for the tetramer **31** was calculated to contain two cis and two trans amide bonds, which was confirmed by X-ray crystallography. Interestingly, the cyclic

[81] J. D. Hartgerink, J. R. Granja, R. A. Milligan, M. R. Ghadiri, *J. Am. Chem. Soc.* **1996**, 118, 43–50.
[82] F. Fujimura, S. Kimura, *Org. Lett.* **2007**, 9, 793 – 796.
[83] N. Maulucci, I. Izzo, G. Bifulco, A. Aliberti, C. De Cola, D. Comegna, C. Gaeta, A. Napolitano, C. Pizza, C. Tedesco, D. Flot, F. De Riccardis, *Chem. Commun*. **2008**, 3927 –3929.

hexamer **32** was calculated and observed to be in an all-trans form subsequent to the coordination of sodium ions within the macrocycle. Considering the interesting results achieved in these cases, we decided to explore influences of chains (benzyl- and metoxyethyl) in the cyclopeptoids' backbone, when we have just benzyl groups and metoxyethyl groups. So, we have synthesized three different molecules: a *N*-benzyl cyclohexapeptoid **56**, a *N*-benzyl cyclotetrapeptoid **57**, a *N*-metoxyethyl cyclohexapeptoid **58** (figure **3.6**).

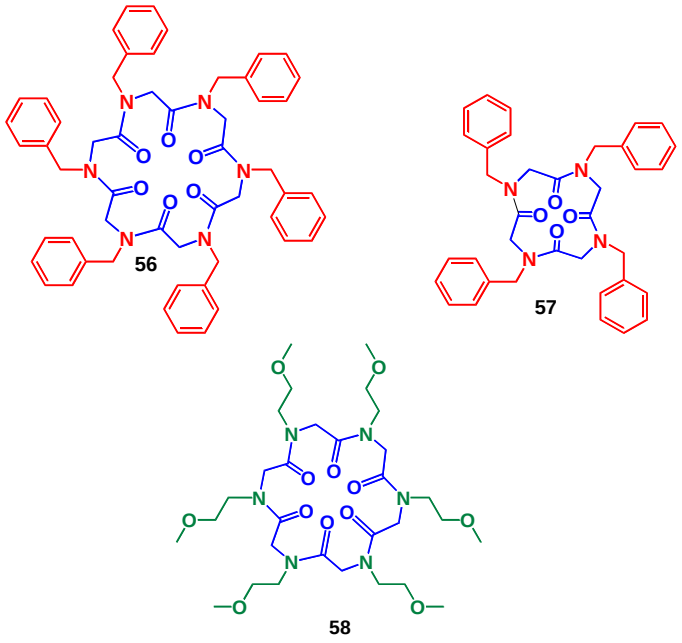

Figure 3.6. *N*-Benzyl-cyclohexapeptoid **56**, *N*-benzyl-cyclotetrapeptoid **57** and *N*-metoxyethyl-cyclohexapeptoid **58**.

3.2 Results and discussion

3.2.1 Chemistry

The synthesis of linear hexa- (**104**) and tetra- (**105**) *N*-benzyl glycine oligomers and of linear hexa-*N*-metoxyethyl glycine oligomer (**106**), was accomplished on solid-phase (2-chlorotrityl resin) using the "sub-monomer" approach,[84] (scheme **3.1**).

[84] R. N. Zuckermann, J. M. Kerr, B. H. Kent, and W. H. Moos, *J. Am. Chem. Soc.*, **1992**, 114, 10646.

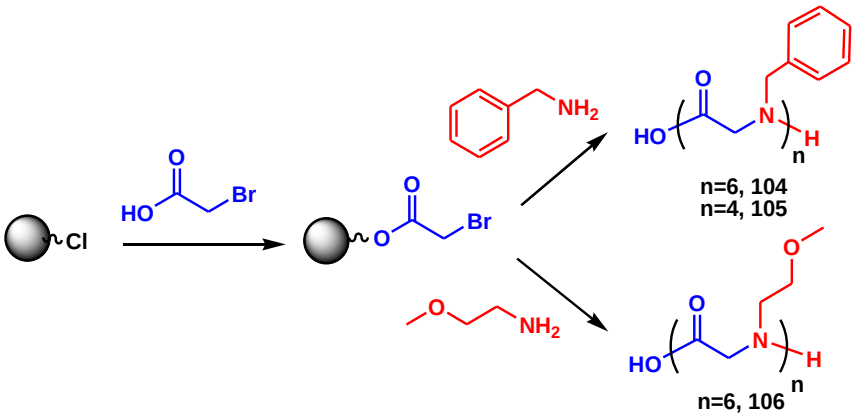

Scheme 3.1. "Sub-monomer" approach for the synthesis of linear tetra- (**104**) and hexa- (**105**) *N*-benzyl glycine oligomers and of linear hexa-*N*-metoxyethyl glycine oligomers (**106**).

All the reported compounds were successfully synthesized as established by mass spectrometry, with isolated crude yields between 60 and 100% and purities greater than 90 % by HPLC analysis.[85]

Head-to-tail macrocyclization of the linear *N*-substituted glycines were realized in the presence of PyBop in DMF (figure **3.7**).

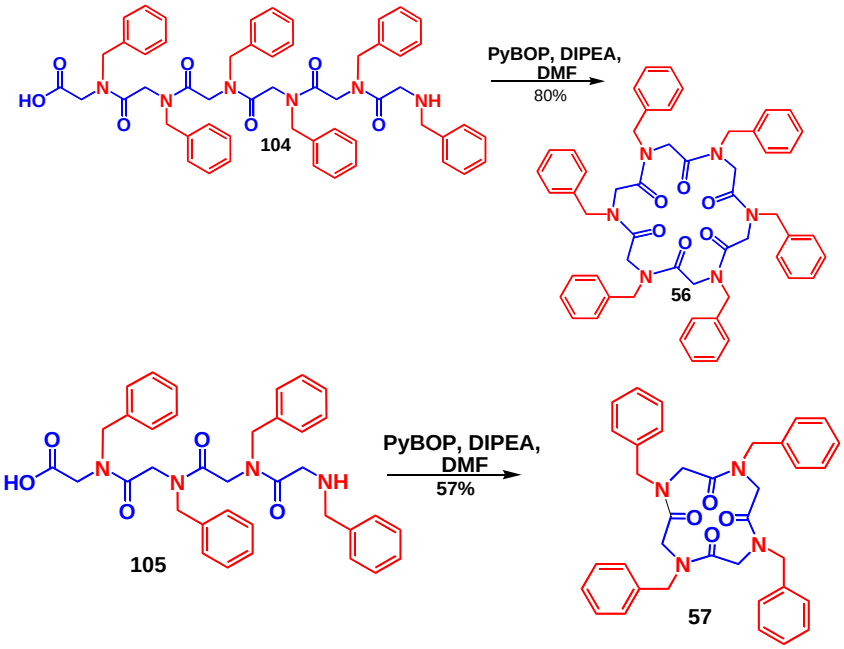

[85] Analytical HPLC analyses were performed on a Jasco PU-2089 quaternary gradient pump equipped with an MD-2010 plus adsorbance detector using C_{18} (Waters, Bondapak, 10 µm, 125Å, 3.9 × 300 mm), reversed phase columns.

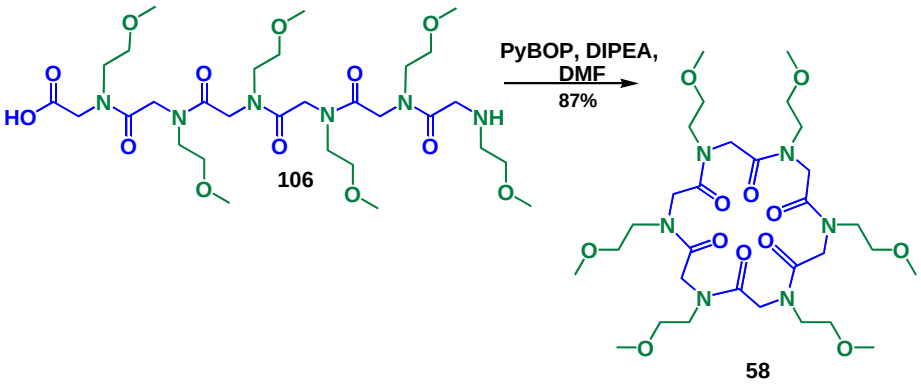

Figure 3.7. Cyclization of oligomers **104**, **105** and **106.**

Several studies in model peptide sequences have shown that incorporation of *N*-alkylated amino acid residues can improve intramolecular cyclization[86a-b-c]. By reducing the energy barrier for interconversion between amide *cisoid* and *transoid* forms, such sequences may be prone to adopt turn structures, facilitating the cyclization of linear peptides.[87] Peptoids are composed of *N*-substituted glycine units, and linear peptoid oligomers have been shown to readily undergo *cis*/*trans* isomerization. Therefore, peptoids may be capable of efficiently sampling greater conformational space than corresponding peptide sequences,[88] allowing peptoids to readily populate states favorable for condensation of the N- and C-termini. In addition, macrocyclization may be further enhanced by the presence of a terminal

secondary amine, as these groups are known to be more nucleophilic than corresponding primary amines with similar p*K*a's, and thus can exhibit greater reactivity.[89]

3.2.2 Structural Analysis

Compounds **56, 57** and **58** were crystallized and subjected to an X-ray diffraction analysis. For the X-ray crystallographic studies were used different crystallization techniques, like as:

1. slow evaporation of solutions;
2. diffusion of solvent between two liquids with different densities;
3. diffusion of solvents in vapor phase;
4. *seeding*.

The results of these tests are reported, respectively, in the tables **3.1**, **3.2** and **3.3** above:

[86] a) Blankenstein, J.; Zhu, J. P. *Eur. J. Org. Chem.* **2005**, 1949-1964. b) Davies, J. S. *J. Pept. Sci.* **2003**, *9*, 471-501. c) Dale, J.; Titlesta, K. *J. Chem. Soc.*,*Chem. Commun.* **1969**, 656-659.

[87] Scherer, G.; Kramer, M. L.; Schutkowski, M.; Reimer, U.; Fischer, G. *J. Am. Chem. Soc.* **1998**, *120*, 5568-5574.

[88] Patch, J. A.; Kirshenbaum, K.; Seurynck, S. L.; Zuckermann, R. N. In *Pseudo-peptides in Drug DeVelopment*; Nielson, P. E., Ed.; Wiley-VCH: Weinheim, Germany, **2004**; pp 1-35.

[89] (a) Bunting, J. W.; Mason, J. M.; Heo, C. K. M. *J. Chem. Soc., Perkin Trans. 2* **1994**, 2291-2300. (b) Buncel, E.; Um, I. H. *Tetrahedron* **2004**, *60*, 7801-7825.

Table 3.1. Results of crystallization of cyclopeptoid **56.**

#	SOLVENT 1	SOLVENT 2	Technique	Results
1	$CHCl_3$		Slow evaporation	Crystalline precipitate
2	$CHCl_3$	CH_3CN	Slow evaporation	Precipitate
3	$CHCl_3$	AcOEt	Slow evaporation	Crystalline precipitate
4	$CHCl_3$	Toluene	Slow evaporation	Precipitate
5	$CHCl_3$	Hexane	Slow evaporation	Little crystals
6	$CHCl_3$	Hexane	Diffusion in vapor p	Needlelike crystals
7	$CHCl_3$	Hexane	Diffusion in vapor p	Prismatic crystals
8	$CHCl_3$	Hexane	Diffusion in vapor p th *seeding*	Needlelike crystals
9	$CHCl_3$	Acetone	Slow evaporation	Crystalline precipitate
10	$CHCl_3$	AcOEt	Diffusion in vapor phase	Crystals
11	$CHCl_3$	Water	Slow evaporation	Precipitate

Table 3.2. Results of crystallization of cyclopeptoid **57.**

#	SOLVENT 1	SOLVENT 2	SOLVENT 3	Technique	Results
1	CH_2Cl_2			Slow evaporation	Prismatic crystals
2	$CHCl_3$			Slow evaporation	Precipitate
3	$CHCl_3$	AcOEt	CH_3CN	Slow evaporation	Crystalline Aggregates
4	$CHCl_3$	Hexane		Slow evaporation	Little crystals

Table 3.3. Results of crystallization of cyclopeptoid **58.**

#	SOLVENT 1	SOLVENT 2	SOLVENT 3	Technique	Results
1	$CHCl_3$			Slow evaporation	Crystals
2	$CHCl_3$	CH_3CN		Slow evaporation	Precipitate
3	AcOEt	CH_3CN		Slow evaporation	Precipitate
5	AcOEt	CH_3CN		Slow evaporation	Prismatic crystals
6	CH_3CN	i-PrOH		Slow evaporation	Little crystals
7	CH_3CN	MeOH		Slow evaporation	Crystalline precipitate
8	Esano	CH_3CN		Diffusion between two phases	Precipitate
9	CH_3CN				Crystallin precipitate

Trough these crystallizations, we had some crystals suitable for the analysis. Conditions **#6** and **#7** (compound **56**, table **3.1**), gave two types of crystals (structure **56A** and **56B**, figure **3.8**)

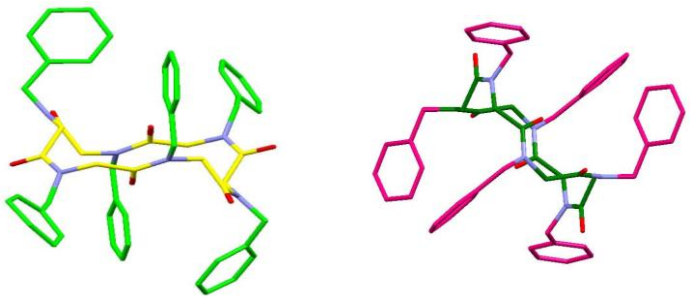

56A **56B**

Figure 3.8. Structures of *N*-Benzyl-cyclohexapeptoid **56A** and **57B.**

For compound **57**, condition **#1** (table **3.2**)**,** gave prismatic crystals (figure **3.9**).

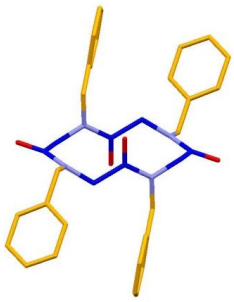

57

Figure 3.9. Structures of *N*-Benzyl-cyclotetrapeptoid **57.**

For compound **58**, condition **#5** (table **3.2**)**,** gave prismatic colorless crystals (figure **3.10**).

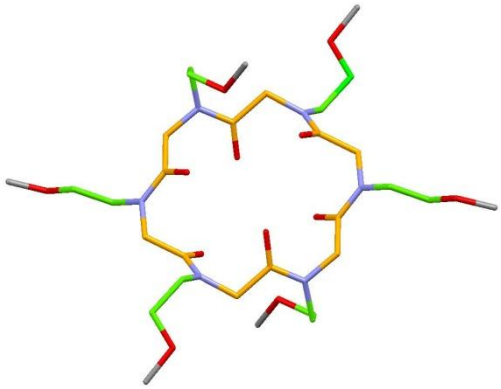

58

Figure 3.10. Structures of *N*-metoxyethyl-cyclohexapeptoid **58.**

Table 3.4 reports the crystallographic data for the resolved structures **56A**, **56B**, **57** and **58**.

Compound	**56A**	**56B**	**57**	**58**
Formula	$C_{54}H_{54}N_6O_6 \cdot 2H_2O$	$C_{54}H_{54}N_6O_6$	$C_{36}H_{36}N_4O_4$	$C_{30}H_{54}N_6O_{12}$
P.M. (g mol^{-1})	919.03	883.03	588.69	513.36
Dim. crist. (mm)	0.7 x 0.2 x 0.1	0.2 x 0.3 x 0.0	0.3 x 0.3 x 0.07	0.3 x 0.1x 0.05
Source	Rotating anode	Rotating anode	Rotating anode	Rotating anode
λ (Å)	1.54178	1.54178	1.54178	1.54178
Cristalline syste	monoclinic	triclinic	orthorhombic	triclinic
Space group	*C2/c*	*P 1*	*Pbca*	*P 1*
***a* (Å)** ***b* (Å)** ***c* (Å)** **α (°)** **β (°)** **γ (°)**	45.73(7) 9.283(14) 23.83(4) 105.97(4)	9.240(12) 11.581(13) 11.877(17) 109.06(2) 101.62(5) 92.170(8)	10.899(3) 10.055(3) 27.255(7)	8.805(3) 11.014(2) 12.477(2) 70.97(2) 77.347(16) 89.75(2)
***V* (Å^3)**	9725(27)	1169(3)	2986.9(14)	1113.1(5)
Z	8	1	4	2
D_{calc} (g cm^{-3})	1.206	1.254	1.309	1.532

μ (cm^{-1})	0.638	0.663	0.692	2.105
Total reflection	7007	2779	2253	2648
Observed reflecti on ($I>2\sigma_I$)	4883	1856	1985	1841
R_1 ($I>2\sigma_I$)	0.1345	0.0958	0.0586	0.1165
R_w	0.4010	0.3137	0.2208	0.3972

3.2.3 Structural analysis of N-Benzyl-cyclohexapeptoid 56A.

Initially, single crystals of *N*-benzylcyclohexapeptoid **56** were formed by slow evaporation of solvents (chloroform/hexane=1/0.5). Optimal conditions of crystallization were in chloroform, trough vapor phase diffusion of hexane (external solvent) and with seeding. These techniques gave air stable needlelike crystals (**34A**).

The crystals show a monoclinic crystalline cell with the following parameters: a = 45.73(7) Å, b = 9.283(14) Å, c = 23.83(4) Å, β = 105.97(4)°, V = 9725(27) $Å^3$, $C_{2/c}$ space group. Eight molecules of **56** and 4 molecules of water were present in the elementary cell. Water molecules are on a binary symmetry axis and they formed a bridge trough a hydrogen bond with a carbonyl group of cyclopeptoids, between two molecules of equivalent cyclopeptoids. These water molecules formed a water channel (figure **3.11**). The peptoid backbone of **56A** showed an overall rectangular form, with four *cis* amide bonds reside at each corner, with two *trans* amide bonds were present on two opposite sides.

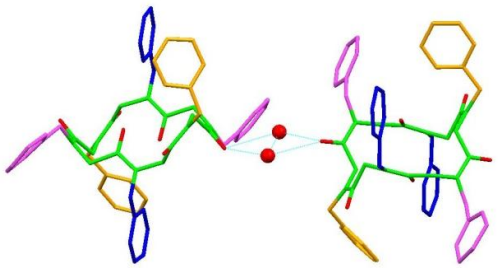

56A

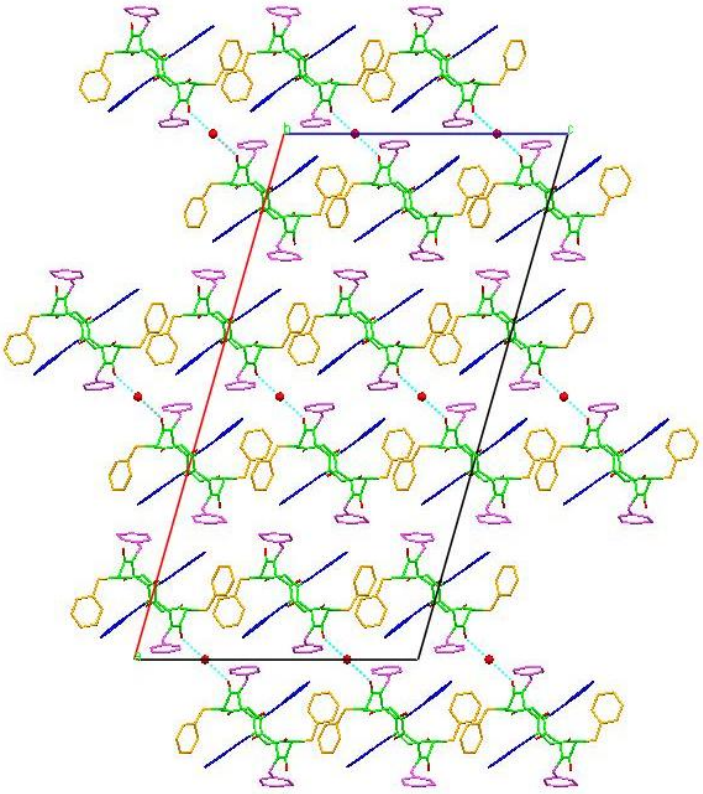

View along the axis ***b***

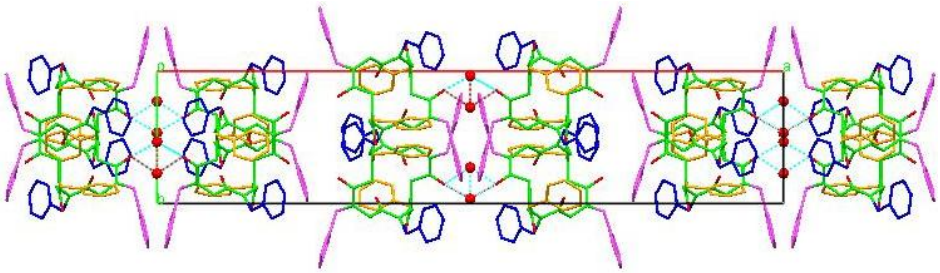

View along the axis ***c***

Figure 3.11. Hydrogen bond between water and two equivalent cyclopeptoids. Blue and pink benzyl group are pseudo parallel to each other, while yellow benzyl group are pseudo perpendicular to each other.

3.2.4 Structural analysis of N-Benzyl-cyclohexapeptoid 56B.

Cyclohexamer **56** was formed two different crystals (**#6** and **#7**, table **3.1**). In condition **#7** it formed prismatic crystals and showed a triclinic structure (**56B**). The cell parameters were: a = 9.240(12)Å, b = 11.581(13)Å, c = 11.877(17)Å, α = 109.06(2)°, β = 101.62(5)°, γ = 92.170(8)°, V = 1169(3) Å^3, the space group is: *P1*.

Just cyclopeptoid **56B** was into the cell and crystallographic gravity centre was coincident with inversion centre.

Monoclinic (**56A**) and Triclinic (**56B**) structures of cyclopeptoid **56** showed the same backbone, but benzyl groups had a different orientation. In figure **3.12** is showed the superposition of two structures.

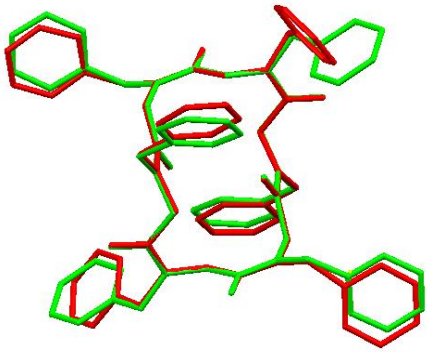

Figure 3.12. superposition of two structures **56A** and **56B**.

Triclinic crystalline cell [a = 9.240(12)Å, b = 11.581(13)Å, c = 11.877(17)Å, α = 109.06(2)°, β = 101.62(5)°, γ = 92.170(8)°] is been compared with monoclinic cell [a = 45.73(7) Å, b = 9.283(14) Å, c = 23.83(4) Å, β = 105.97(4)°], and we could see a new triclinic cell similar to the first, if we applied the following operation on triclinic cell.

$$\begin{pmatrix} a' \\ b' \\ c' \end{pmatrix} = \begin{pmatrix} 0 & 1 & 0 \\ 0 & 0 & 1 \\ 1 & 0 & 0 \end{pmatrix} \begin{pmatrix} a \\ b \\ c \end{pmatrix} = \begin{pmatrix} b \\ c \\ a \end{pmatrix}$$

a = 11.877(17)Å, b = 9.240(12)Å, c = 11.581(13)Å, α = 92.170(8)°, β 109.06(2)°, γ= 101.62(5)°, so a_M=4 a_T, b_M=b_T e c_M=2c_T.

The triclinic cell was considered a distortion of the monoclinic cell. In figure **3.13** were reported the structure of **56B.**

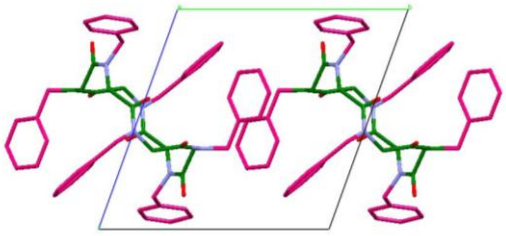

View along the axis ***a***

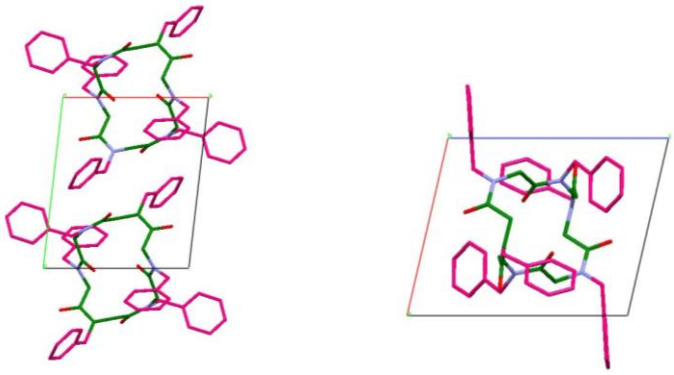

View along the axis ***b*** View along the axis ***c***

Figure 3.13. Crystalline structure of **56B**.

3.2.5 Structural analysis of *N*-Benzyl-cyclotetra peptoid 57.

Cyclotetramer **57** was obtained by slowly evaporation of solvent (CH_2Cl_2) as colorless prismatic and stable crystals (figure **3.14**). They presented an orthorhombic crystalline cell [a = 10.899(3) Å, b = 10.055(3) Å, c = 27.255(7) Å, V = 2986.9(14) Å^3] and they belonged to space group *Pbca*.

X-Ray structure of **57** showed a cis-trans-cis-trans (*ctct)* stereochemical arrangement; benzyl group were parallel to each other, and two of these were pseudo-equatorial (figure **3.14**).

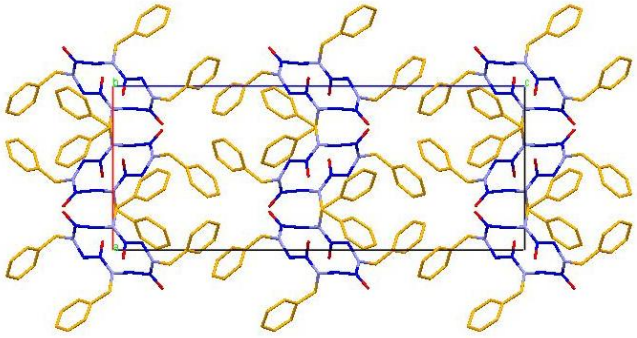

View along the axis ***b***

Figure 3.14. Crystalline structure of **57.**

3.2.6 Structural analysis of *N*-metoxyethyl-cyclohexapeptoid 58.

Single crystal (**58**) was obtained in slowly evaporation of solvent (AcOEt/ACN) as colorless prismatic and stable crystals. They were present triclinic crystalline cell with parameters cell: a = 8.805(3) Å, b = 11.014(2) Å, c = 12.477(2) Å, α = 70.97(2)°, β = 77.347(16)°, γ = 89.75(2)°, V = 1113.1(5) Å^3 and they belonged to space group *P1*.

^{1}H-NMR studies confirmed the presence of a complex species of **58** and it was analyzed by X-ray method (figure **3.15**).

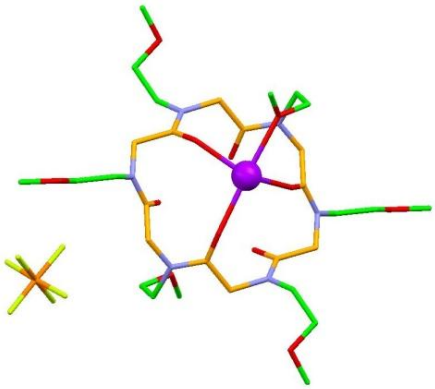

Figure 3.15. X-ray structure of **58.**

The structure obtained, showed a unique all-*trans* peptoid bond configuration, with the carbonyl groups alternately pointing toward the sodium cation and forcing the N-linked side chains to assume an alternate pseudo-equatorial arrangement. X-ray showed the presence of an anion (hexafluorophosphate), too. Hexafluorophosphate is present as counterion of the coupling agent (PyBop). The structure of **58** was described like a coordination polymer, in fact two sodium atoms (figure **3.16**) were coordinated with a cyclopeptoid, and this motif was repeat along the axis **a**.

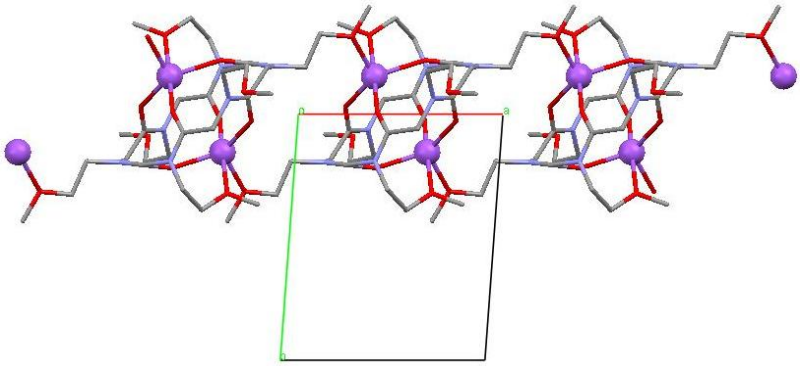

(a)

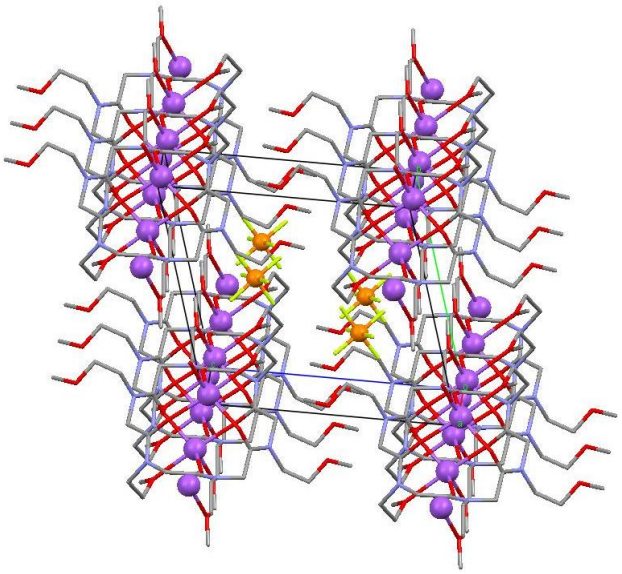

(b)

Figure 3.16. (a) View along the axis **a; (b)** perspective view of the rows in the crystalline cell of **58.**

3.3 X-ray analysis on powder of 56A and 56B.

Polymorphous crystalline structures of **56A** and **56B** were analyzed to confirm analogy between polymorphous species. Crystals were obtained by tests **#6** and **#7** (table **3.1**) and were ground in a mortar until powder. The powder was put into capillaries (0.05 mm) and X-ray spectra were acquired in a range of 4°-45° of 2ζ. X-ray spectra have confirmed crystallinity of the sample, as well as his polymorphism (figure **3.17**).

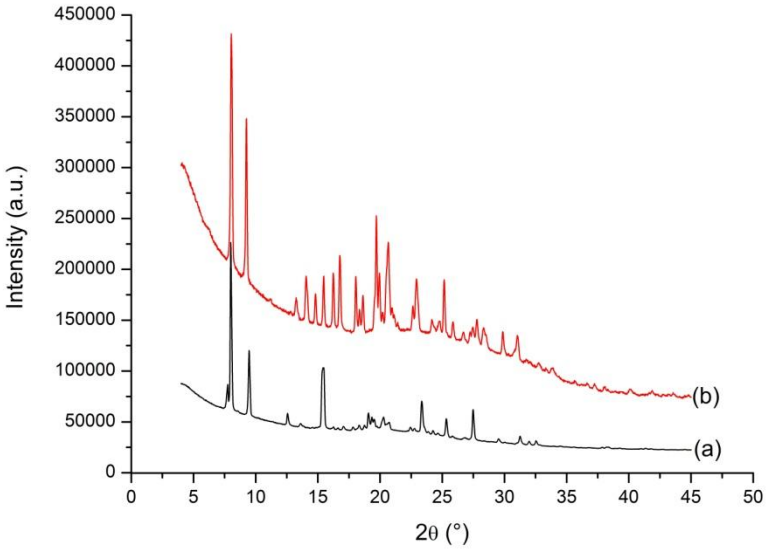

Figure 3.17. Diffraction profiles for **56A** (a) and **56B** (b).

Diffraction profiles acquired, were indexed using data on the monoclinic and triclinic unit cell. In particular, on the left of spectra, peaks were similar for both polymorphs. Instead, on the right of spectra, were present diffraction peaks typical of one of two species.

3.4 Conclusions

In this chapter, the synthesis and structural characterization of three cyclopeptoids (**56**, **57** and **58**) were reported.

For compound **56**, two different polymorph structures were isolated (**56A** and **56B**); crystalline structure of **56A** shows a monoclinic cell and a water channel. Instead, crystalline structure of **56B**, presents a triclinic cell without water channel. Backbone's conformation of **56A** and **56B** is similar (*cctcct*), but benzyl groups' conformation is different. X-ray analysis on powders of **56A** and **56B**, has confirmed the non coexistence of the monoclinic and triclinic structures in the same sample. *N*-benzylcyclotetrapeptoid **57** presents an orthorhombic cell and a conformation *ctct.*

Finally, *N*-metoxyethylcyclohexapeptoid **58**, has been isolated as sodium ion complex. The crystalline structure consists of rows of cyclopeptoids and sodium ions, hexafluophosphate ions are in the gaps. Backbone's conformation results to be all trans (*tttttt*) and sodium ions are coordinated with secondary interactions to the oxygens of carbonyl groups and to the oxygens of methoxy groups.

3.5 Experimental section

3.5.1 General Methods.

All reactions involving air or moisture sensitive reagents were carried out under a dry argon or nitrogen atmosphere using freshly distilled solvents. Tetrahydrofuran (THF) was distilled from $LiAlH_4$ under argon. Toluene and CH_2Cl_2 were distilled from CaH_2. Glassware was flame-dried (0.05 Torr) prior to use. When necessary, compounds were dried in vacuo over P_2O_5 or by azeotropic removal of water with toluene under reduced pressure. Starting materials and reagents purchased from commercial suppliers were generally used without purification unless otherwise mentioned. Reaction temperatures were measured externally; reactions were monitored by TLC on Merck silica gel plates (0.25 mm) and visualized by UV light, I_2, or by spraying with H_2SO_4-$Ce(SO_4)_2$, phosphomolybdic acid or ninhydrin solutions and drying. Flash chromatography was performed on Merck silica gel 60 (particle size: 0.040-0.063 mm) and the solvents employed were of analytical grade. Yields refer to chromatographically and spectroscopically (^{1}H- and ^{13}C-NMR) pure materials. The NMR spectra were recorded on Bruker DRX 400, (^{1}H at 400.13 MHz, ^{13}C at 100.03 MHz), Bruker DRX 250 (^{1}H at 250.13 MHz, ^{13}C at 62.89 MHz), and Bruker DRX 300 (^{1}H at 300.10 MHz, ^{13}C at 75.50 MHz) spectrometers. Chemical shifts (δ) are reported in ppm relatively to the residual solvent peak ($CHCl_3$, δ = 7.26, $^{13}CDCl_3$, δ: = 77.0; CD_2HOD, δ = 3.34, $^{13}CD_3OD$, δ = 49.0) and the multiplicity of each signal is designated by the following abbreviations: s, singlet; d, doublet; t, triplet; q, quartet; quint, quintuplet; m, multiplet; br, broad. Coupling costants (*J*) are quoted in Hz. Homonuclear decoupling, COSY-45 and DEPT experiments completed the full assignment of each signal. Elemental analyses were performed on a CHNS-O FlashEA apparatus (Thermo Electron Corporation) and are reported in percent abundance. High resolution ESI-MS spectra were performed on a Q-Star Applied Biosystem mass spectrometer. ESI-MS analysis in positive ion mode was performed using a Finnigan LCQ Deca ion trap mass spectrometer (ThermoFinnigan, San Josè, CA, USA) and the mass spectra were acquired and processed using the Xcalibur software provided by Thermo Finnigan. Samples were dissolved in 1:1 CH_3OH/H_2O, 0.1 % formic acid, and infused in the ESI source by using a syringe pump; the flow rate was 5 μl/min. The capillary voltage was set at 4.0 V, the spray voltage at 5 kV, and the tube lens offset at -40 V. The capillary temperature was 220 °C. HPLC analyses were performed on a Jasco BS 997-01 series,

equipped with a quaternary pumps Jasco PU-2089 Plus, and an UV detector Jasco MD-2010 Plus. The resulting residues were purified by semipreparative reverse-phase C18 (Waters, Bondapak, 10 μm, 125Å, 7.8 × 300 mm).

3.5.2 Synthesis

Linear peptoid oligomers **104, 105** and **106** were synthesized using a sub-monomer solid-phase approach[11]. In a typical synthesis 2-chlorotrityl chloride resin (2,α-dichlorobenzhydryl-polystyrene crosslinked with 1% DVB; 100–200 mesh; 1.2 mmol/g, 600 mg, 0.720 mmol) was swelled in dry DMF (6 mL) for 45 min and washed twice with dry DCM (6 mL).

The first sub-monomer was attached onto the resin by adding 120 mg (1.2 eq, 0.86 mmol) of bromoacetic acid in dry DCM (6 mL) and 502 μL of DIPEA (4.0 mmol) on a shaker platform for 40 min at room temperature, followed by washing with dry DCM (6 mL) and then with DMF (6 x 6 mL). To the bromoacetylated resin was added a DMF solution (1 M, 7 mL) of the desired amine (benzylamine -10 eq, 772 mg, 7.20 mmol- or methoxyethylamine -10 eq, 541 mg, 620 μl, 7.20 mmol- the commercially available [Aldrich]) the mixture was left on a shaker platform for 30 min at room temperature, then the resin was washed with DMF (6 x 6 mL). Subsequent bromoacetylation reactions were accomplished by reacting the aminated oligomer with a solution of bromoacetic acid in DMF (1.2 M, 6 mL) and 1.23 mL of DIC for 40 min at room temperature. The filtered resin was washed with DMF (6 x 6 mL) and treated again with the amine in the same conditions reported above. This cycle of reactions was iterated until the target oligomer was obtained (hexa- **104** and tetralinears **105** and **106** peptoids).

The cleavage was performed by treating twice the resin, previously washed with DCM (6 x 6 mL), with 6 mL of 20% HFIP in DCM (v/v) on a shaker platform at room temperature for 30 min and 5 min, respectively. The resin was then filtered away and the combined filtrates were concentrated in vacuo. The final products were dissolved in 50% acetonitrile in HPLC grade water and analysed by RP-HPLC (purity >95% for all the oligomers, conditions: 5% to 100% B in 30 min [A: 0.1% TFA in water, B: 0.1% TFA in acetonitrile], flow: 1.0 mL/min, 220 nm. C18 reversed-phase analytical column [Waters, μBondapak, 10 lm, 125 Å, 3.9 mm x 300 mm]) and ESI mass spectrometry. The linear oligomers **75**, **76** and **77** were subjected to the cyclization reaction without further purification.

✓ *Compound **104**: m/z* (ES) 901 (MH^+); (HRES) MH^+, found 901.4290 $C_{54}H_{57}N_6O_7^+$ requires 901.4289. 100 %.

✓ *Compound **105:** m/z* (ES) 607 (MH^+); (HRES) MH^+, found 607.2925 $C_{36}H_{39}N_4O_5^+$ requires 606.2920. 100 %.

✓ *Compound **106:** m/z* (ES) 709 (MH^+); (HRES) MH^+, found 709.3986 $C_{30}H_{57}N_6O_{13}^+$ requires 709.3984. 100 %.

3.5.3 General cyclization reaction (synthesis of 56, 57 and 58)

A solution of the linear peptoid (**104**, **105** and **106**), previously co-evaporated three times with toluene, was prepared under nitrogen in dry DMF (20 mL).

✓ Linear **104** (37 mg, 0.0611 mmol) was dissolved in DMF dry (5 mL) and the mixture was added drop-wise by syringe pump in 2 h to a stirred solution of PyBop (127 mg, 4 eq, 0.244 mmol) and DIPEA (49 mg, 6.2 eq, 66 µl, 0.319 mmol) in dry DMF (15 mL) at room temperature in anhydrous atmosphere.

✓ Linear **105** (300 mg, 0.333 mmol) was dissolved in DMF dry (20 mL) and the mixture was added drop-wise by syringe pump in 2 h to a stirred solution of PyBop (4.0 eq, 692 mg, 1.37 mmol) and DIPEA (6.0 eq, 360 µl, 2.06 mmol) in dry DMF (20 mL) at room temperature in anhydrous atmosphere.

✓ Linear **106** (1224 mg, 0.316 mmol) was dissolved in DMF dry (20 mL) and the mixture was added drop-wise by syringe pump in 2 h to a stirred solution of PyBop (655 mg, 4 eq, 1.26 mmol) and DIPEA (254 mg, 6.2 eq, 342 µl, 1.96 mmol) in dry DMF (85 mL) at room temperature in anhydrous atmosphere.

After 12 h the resulting mixtures were concentrated in vacuo, diluted with CH_2Cl_2 (20 mL) and a solution of HCl (1 N, 20 mL). The single mixture was extracted with CH_2Cl_2 (2 x 20 mL) and the combined organic phases were washed with water (12 mL), dried over anhydrous Na_2SO_4, filtered and concentrated in vacuo.

All cyclic products were dissolved in 50% acetonitrile in HPLC grade water and analysed by RP-HPLC (purity >85% for all the cyclic oligomers).

Eluition conditions: 5%-100% B in 30 min [A: 0.1% TFA in water, B: 0.1% TFA in acetonitrile], flow: 1.0 mL/min, 220 nm. C18 reversed-phase analytical column [Waters, lBondapak, 10 lm, 125 Å, 3.9 mm x 300 mm] and ESI mass spectrometry (zoom scan technique).

The crude residues (**56**, **57** and **58**) were purified by HPLC on a C18 reversed-phase preparative column, conditions: 20%-100% B in 40 min [A: 0.1% TFA in water, B: 0.1% TFA in acetonitrile], flow: 2.0 mL/min, 220 nm. The samples were dried in a falcon tube under low pressure.

✓ *Compound **56:*** δ_H (300.10 MHz $CDC1_3$) 7.15 (30 H, m, H Ar); 4.40 (12H, br., -NCHHCO, -CH_2Ph), 3.80 (4H, br., -CH_2Ph), 3.38 (8H, m., -CH_2Ph). 80%, *m/z* (ES) 883 (MH^+); (HRES) MH^+, found 883.4110 $C_{54}H_{55}N_6O_6^+$ requires 882.4105. **HPLC**: t_R: 19.9 min.

✓ *Compound **57:*** δ_H (250 MHz, $CDCl_3$) 7.23 (20 H, br. H Ar), 5.55 (2 H, br. d., *J* 14 Hz, -NCHHCO), 5.40 (2 H, br. d., *J* 14.5 Hz, -NCHHCO), 4.40 (6 H, m., *J* 17 Hz, -CH_2Ph), 3.72 (2 H, br. d., *J* 14.2 Hz, -NCHHCO), 3.50 (4 H, br. d., *J* 14.5 Hz, -NCHHCO, -CH_2Ph). δ_C (75 MHz, $CDCl_3$) 168.94 (CO x 2), 167.78 (CO x 2), 135,72 (C_q-Ar x 2), 135,15 (C_q-Ar x 2), 128.91 (C-Ar x 8), 128.56 (C-Ar x 4), 127.82 (C-Ar x 4), 127.52 (C-Ar x 4), 50.29 (C x 2), 49.30 (C x 2), 48.82 (C x 2), 47.14 (C x 2). 57%, *m/z* (ES) 589 (MH^+); (HRES) MH^+, found 589.2740 $C_{36}H_{37}N_4O_4^+$ requires 589.2737. **HPLC**: t_R: 18.0 min.

✓ *Compound **58:*** δ_H (250 MHz, $CDCl_3$) 4.63 (3 H, br. d., *J* 17 Hz, -NCHHCO), 3.88 (3 H, br. d., *J* 17 Hz, -NCHHCO), 3.48 (48 H, m., -NCHHCO, -$CH_2CH_2OCH_3$). δ_C (400 MHz, $CDCl_3$, mixture of rotamers) 171. 5, 171.0, 179.6, 170.1, 170.0, 169.8, 169.7, 169.5, 169.3, 169.1, 168.9, 168.7, 168.2, 168.1, 71.7, 71.5, 71.4, 71.3, 71.0, 70.8, 70.6 (bs), 70.2 (bs), 70.0 (bs),, 69.8 (bs),69.5 (bs), 69.3 (bs), 69.1 (bs), 68.8 (bs), 68.7 (bs), 59.1 (bs), 58.9 (bs), 58.6 (bs), 58.2 (bs), 53.4 (bs), 52.4 (bs), 52.2 (bs), 50.9 (bs), 50.7 (bs), 50.4 (bs), 50.3 (bs), 50.2 (bs), 49.9 (bs), 49.1 (bs), 48.7 (bs), 48.4 (bs), 48.3 (bs),

48.0 (bs), 47.6 (bs),, 47.4 (bs),47.0 (bs), 46.8 (bs),, 46.6 (bs), 45.9 (bs), 45.5 (bs), 43.3 (bs). 87%, *m/z* (ES) 691 (MH^+); (HRES) MH^+, found 691.3810 $C_{30}H_{55}N_6O_{12}^+$ requires 691.3800. **HPLC**: t_R: 11.8 min.

3.5.4 General method of X-ray analysis

X-ray analysis were made with Bruker D8 ADVANCE utilized glass capillaries Lindemann and diameters of 0.5 mm. CuKα was used as radiations with wave length collimated (1.5418 Å) and parallelized using Göbel Mirror. Ray dispersion was minimized with collimators (0.6 - 0.2 - 0.6) mm. Below, I report diffractometric on powders analysis of **56A** and **56B.**

✓ *X-ray analysis on powders obtained by crystallization tests.*

Crystals were obtained by crystallization **#6** of **56,** they were ground into a mortar and introduced into a capillary of 0.5 mm. Spectra was registered on rotating capillary between $2\zeta = 4°$ and $2\zeta = 45°$, the measure was performed in a range of 0.05° with a counting time of 3s. In a similar way, was analyzed crystal **#7** of **56**.

✓ *X-ray analysis on single crystal of **56A**.*

56A was obtained by **#6** table **3,** in chloroform with diffusion in vapor phase of hexane (extern solvent) and subsequently with seeding. These crystals were needlelike and air stable. A crystal of dimension of 0.7 x 0.2 x 0.1 mm was pasted on a glass fiber and examined to room temperature with a diffractometer for single crystal Rigaku AFC11, and with a detector CCD Saturn 944 using a rotating anode of Cu and selecting a wave length CuKα (1.54178 Å). Elementary cell was monoclinic with parameters a = 45.73(7) Å, b = 9.283(14) Å, c = 23.83(4) Å, β = 105.97(4)°, V = 9725(27) Å^3, Z=8 and belonged to space group $C_{2/c}$.

Data reduction

7007 reflections were measured, 4883 were strong ($F^2 > 2\sigma(F^2)$). Data were corrected, for Lorentz and polarization effects. The linear absorption coefficient for CuKα was 0.638 cm^{-1} without correction.

Resolution and refinement of the structure

Resolution program was called SIR2002[90] and it was based on representations theory for evaluation of the structure semivariant in 1, 2, 3 and 4 phases. It is more based on multiple solution technique and on selection of most probable solutions technique, too. The structure was refined with least-squares techniques using the program SHELXL97[91]

Function minimized with refinement is:

$$\Sigma w(F_0^2 - F_c^2)^2$$

considering all reflections, even the weak.

The disagreement index that was optimized is:

$$wR_2 = \frac{\Sigma_i w_i \left| F_{i0}^2 - F_{ic}^2 \right|}{\Sigma_i w_i F_{i0}^2}$$

[90] SIR92: A. Altomare *et al. J. Appl. Cryst.* **1994**, 27,435

[91] G. M. Sheldrick, "A program for the Refinement of Crystal Structure from Diffraction Data", Universität Göttingen **1997**.

It was based on squares of structure factors, typically reported together the index R_1:

$$R_1 = \frac{\Sigma_i \left| F_{i0} - F_{ic} \right|}{\Sigma_i F_{i0}}$$

Considering only strong reflections ($I>2\sigma(I)$).

The corresponding disagreement index R_{W2}, calculating all the reflections is 0.4, while R_1 is 0.13. For thermal vibration was used an anisotropic model. Hydrogen atoms were collocated in canonic positions and were included into calculations.

Rietveld analysis

Rietveld method represents a structural refinement technique and it use the continue diffraction profile of a spectrum on powders.[92]

Refinement procedure consists in least-squares techniques using GSAS[93] like program.

This analysis was conducted on diffraction profile of monoclinic structure **34A.** Atomic parameters, of structural model of single crystal, were used without refinement. Peaks profile was defined by a pseudo Voigt function, combining it with a special function, which consider asymmetry. This asymmetry derives by axial divergence.[94] The background was modeled manually, using GUFI[95] like program. Data were refined for parameters cell, profile and zero shift. Similar procedure was used for triclinic structure **56B.**

✓ *X-ray analysis on single crystal of **56B**.*

56B was obtained by **#7** table **3.1,** by chloroform with diffusion in vapor phase of hexane (extern solvent). These crystals were colorless, prismatic and air stable. A crystal (dimension: 0.2 x 0.3 x 0.08 mm) was pasted on a glass fiber and was examined to room temperature with a diffractometer for single crystal Rigaku AFC11, and with a detector CCD Saturn 944 using a rotating anode of Cu and selecting a wave length CuKα (1.54178 Å). Elementary cell was triclinic with parameters a = 9.240(12) Å, b = 11.581(13) Å, c = 11.877(17) Å, α = 109.06(2)°, β = 101.62(5)°, γ = 92.170(8)°, V = 1169(3) Å^3 Z = 1 and belonged to space group P_1.

Data reduction

2779 reflections were measured, 1856 were strong ($F^2 > 2\sigma (F^2)$). Data were corrected, for Lorentz and polarization effects. The linear absorption coefficient for CuKα was 0.663 cm^{-1} without correction.

Resolution and refinement of the structure

---

[92] A**.** Immirzi, *La diffrazione dei cristalli*, Liguori Editore prima edizione italiana, Napoli **2002**.

[93] A. C. Larson and R. B. Von Dreele, *GSAS General Structure Analysis System*, LANL Report LAUR 86 – 748, Los Alamos National Laboratory, Los Alamos, USA **1994**.

[94] P. Thompson, D. E. Cox and J. B. Hasting, *J. Appl. Crystallogr.*,**1987**, 20; 79, L. W. Finger, D. E. Cox and A. P. Jephcoat, *J. Appl. Crystallogr.*, **1994**, 27, 892.

[95] R. E. Dinnebier and L. W. Finger, *Z. Crystallogr. Suppl.*, **1998**, 15, 148; present on: www.fkf.mpg.del/Xray/html/body_gufi_software.html.

The corresponding disagreement index R_{W2}, calculating all the reflections is 0.31, while R_1 is 0.09. For thermal vibration was used an anisotropic model. Hydrogen atoms were collocated in canonic positions and included into calculations.

✓ *X-ray analysis on single crystal of **57**.*

57 was obtained by **#1** table **3.2,** by slowly evaporation of dichloromethane. These crystals were colorless, prismatic and air stable. A crystal of dimension of 0.3 x 0.3 x 0.07 mm was pasted on a glass fiber and was examined to room temperature with a diffractometer for single crystal Rigaku AFC11, and with a detector CCD Saturn 944 using a rotating anode of Cu and selecting a wave length CuKα (1.54178 Å). Elementary cell is triclinic with parameters *a* = 10.899(3) Å, *b* = 10.055(3) Å, *c* = 27.255(7) Å, *V* = 2986.9(14) $Å^3$, Z=4 and belongs to space group P*bca*.

Data reduction

2253 reflections were measured, 1985 were strong ($F^2 > 2\sigma(F^2)$). Data were corrected, for Lorentz and polarization effects. The linear absorption coefficient for CuKα was 0.692 cm^{-1} without correction.

Resolution and refinement of the structure

The corresponding disagreement index R_{W2}, calculating all the reflections is 0.22, while R_1 is 0.05. For thermal vibration is used an anisotropic model. Hydrogen atoms were collocated in canonic positions and included into calculations.

✓ *X-ray analysis on single crystal of **58**.*

58 was obtained by **#5** table **5,** by slowly evaporation of ethyl acetate/acetonitrile. These crystals were colorless, prismatic and air stable. A crystal (dimension: 0.3 x 0.1 x 0.05mm) was pasted on a glass fiber and was examined to room temperature with a diffractometer for single crystal Rigaku AFC11, and with a detector CCD Saturn 944 using a rotating anode of Cu and selecting a wave length CuKα (1.54178 Å).

Elementary cell was triclinic with parameters *a* = 8.805(3) Å, *b* = 11.014(2) Å, *c* = 12.477(2) Å, *α* = 70.97(2)°, *β* = 77.347(16)°, *γ* = 89.75(2)°, *V* = 1113.1(5) $Å^3$, Z=2 and belonged to space group P*1*.

Data reduction

2648 reflections were measured, 1841 were strong ($F^2 > 2\sigma(F^2)$). Data were corrected, for Lorentz and polarization effects. The linear absorption coefficient for CuKα was 2.105 cm^{-1} without correction.

Resolution and refinement of the structure

The corresponding disagreement index R_{W2}, calculating all the reflections is 0.39, while R_1 is 0.11. For thermal vibration was used an anisotropic model. Hydrogen atoms were collocated in canonic positions and included into calculations.

Chapter 4

4. Cationic cyclopeptoids as potential macrocyclic nonviral vectors

4.1 Introduction

Viral and nonviral gene transfer systems have been under intense investigation in gene therapy for the treatment and prevention of multiple diseases[96]. Nonviral systems potentially offer many advantages over viral systems, such as ease of manufacture, safety, stability, lack of vector size limitations, low immunogenicity, and the modular attachment of targeting ligands[97]. Most nonviral gene delivery systems are based on cationic compounds— either cationic lipids[2] or cationic polymers[98]— that spontaneously complex with a plasmid DNA vector by means of electrostatic interactions, yielding a condensed form of DNA that shows increased stability toward nucleases.

Although cationic lipids have been quite successful at delivering genes *in vitro*, the success of these compounds *in vivo* has been modest, often because of their high toxicity and low transduction efficiency.

A wide variety of cationic polymers have been shown to mediate *in vitro* transfection, ranging from proteins [such as histones[99] and high mobility group (HMG) proteins[100]] and polypeptides (such as polylysine[3,101], short synthetic peptides[102,103], and helical amphiphilic peptides[104,105]) to synthetic polymers (such as polyethyleneimine[106], cationic dendrimers[107,108], and glucaramide polymers[109]). Although the efficiencies of gene transfer vary with these systems, a large variety of cationic structures are effective. Unfortunately, it has been difficult to study systematically the effect of polycation structure on transfection activity.

---

[96] Mulligan, R. C. (1993) *Science* **260,** 926–932.
[97] Ledley, F. D. (1995) *Hum. Gene Ther.* **6,** 1129–1144.
[98] Wu, G. Y. & Wu, C. H. (1987) *J. Biol. Chem.* **262,** 4429–4432
[99] Fritz, J. D., Herweijer, H., Zhang, G. & Wolff, J. A *Hum. Gene Ther.* **1996**, **7,** 1395–1404.
[100] Mistry, A. R., Falciola, L., L. Monaco, Tagliabue, R., Acerbis, G., Knight, A., Harbottle, R. P., Soria, M., Bianchi, M. E., Coutelle, C. & Hart, S. L. *BioTechniques*, **1997**, 22**,** 718–729.
[101] Wagner, E., Cotten, M., Mechtler, K., Kirlappos, H. & Birnstiel, M. L. *Bioconjugate Chem.* **1991**, 2**,** 226–231.
[102]Gottschalk, S., Sparrow, J. T., Hauer, J., Mims, M. P., Leland, F. E., Woo, S. L. C. & Smith, L. C. *Gene Ther.* **1996,** 3, 448–457.
[103] Wadhwa, M. S., Collard, W. T., Adami, R. C., McKenzie, D. L. & Rice, K. G. *Bioconjugate Chem.* **1997,** 8**,** 81–88.
[104] Legendre, J. Y., Trzeciak, A., Bohrmann, B., Deuschle, U., Kitas, E. & Supersaxo, A. *Bioconjugate Chem.* **1997**, 8, 57–63.
[105] Wyman, T. B., Nicol, F., Zelphati, O., Scaria, P. V., Plank, C. & Szoka, F. C., Jr. *Biochemistry* **1997**, 36**,** 3008–3017.
[106] Boussif, O., Zanta, M. A. & Behr, J.-P. *Gene Ther.* **1996**, 3, 1074–1080.
[107] Tang, M. X., Redemann, C. T. & Szoka, F. C., Jr. *Bioconjugate Chem.* **1996,** 7, 703–714
[108] Haensler, J. & Szoka, F. C., Jr. *Bioconjugate Chem.* **1993,** 4, 372–379.
[109] Goldman, C. K., Soroceanu, L., Smith, N., Gillespie, G. Y., Shaw, W., Burgess, S., Bilbao, G. & Curiel, D. T. *Nat. Biotech.* **1997,** 15**,** 462–466.

Since the first report in 1987[110], cell transfection mediated by cationic lipids (Lipofection, figure **4.1**) has become a very useful methodology for inserting therapeutic DNA into cells, which is an essential step in gene therapy[111].

Several scaffolds have been used for the synthesis of cationic lipids, and they include polymers,[112] dendrimers,[113] nanoparticles,[114] "gemini" surfactants,[115] and, more recently, macrocycles.[116]

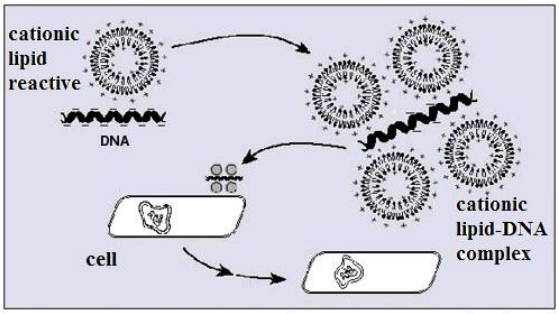

Figure 4.1. Cell transfection mediated by cationic lipids

It is well-known that oligoguanidinium compounds (polyarginines and their mimics, guanidinium modified aminoglycosides, etc.) efficiently penetrate cells, delivering a large variety of cargos.[16b,117]

Ungaro et al. reported[21c] that calix[*n*]arenes bearing guanidinium groups directly attached to the aromatic nuclei (upper rim) are able to condense plasmid and linear DNA and perform cell transfection in a way which is strongly dependent on the macrocycle size, lipophilicity, and conformation. Unfortunately, these compounds are characterized by low transfection efficiency and high cytotoxicity

[110] Felgner, P. L.; Gadek, T. R.; Holm, M.; Roman, R.; Chan, H. W.; Wenz, M.; Northrop, J. P.; Ringold, G. M.; Danielsen, M. *Proc. Natl. Acad. Sci. U.S.A.* **1987**, *84*, 7413–7417.

[111] (a) Zabner, J. *Ad*V. *Drug. Deli*V*ery Re*V. **1997**, *27*, 17–28. (b) Goun, E. A.; Pillow, T. H.; Jones, L. R.; Rothbard, J. B.; Wender, P. A. *ChemBioChem* **2006**, *7*, 1497–1515. (c) Wasungu, L.; Hoekstra, D. *J. Controlled Release* **2006**, *116*, 255–264. (d) Pietersz, G. A.; Tang, C.-K.; Apostolopoulos, V. *Mini-Re*V. *Med. Chem.* **2006**, *6*, 1285–1298.

[112] (a) Haag, R. *Angew. Chem., Int. Ed.* **2004**, *43*, 278–282. (b) Kichler, A. *J. Gene Med.* **2004**, *6*, S3–S10. (c) Li, H.-Y.; Birchall, J. *Pharm. Res.* **2006**, *23*, 941–950.

[113] (a) Tziveleka, L.-A.; Psarra, A.-M. G.; Tsiourvas, D.; Paleos, C. M. *J. Controlled Release* **2007**, *117*, 137–146. (b) Guillot-Nieckowski, M.; Eisler, S.; Diederich, F. *New J. Chem.* **2007**, *31*, 1111–1127.

[114] (a) Thomas, M.; Klibanov, A. M. *Proc. Natl. Acad. Sci. U.S.A.* **2003**, *100*, 9138–9143. (b) Dobson, J. *Gene Ther.* **2006**, *13*, 283–287. (c) Eaton, P.; Ragusa, A.; Clavel, C.; Rojas, C. T.; Graham, P.; Dura´n, R. V.; Penade´s, S. *IEEE T. Nanobiosci.* **2007**, *6*, 309–317.

[115] (a) Kirby, A. J.; Camilleri, P.; Engberts, J. B. F. N.; Feiters, M. C.; Nolte, R. J. M.; So¨derman, O.; Bergsma, M.; Bell, P. C.; Fielden, M. L.; Garcı´a Rodrı´guez, C. L.; Gue´dat, P.; Kremer, A.; McGregor, C.; Perrin, C.; Ronsin, G.; van Eijk, M. C. P. *Angew. Chem., Int. Ed.* **2003**, *42*, 1448–1457. (b) Fisicaro, E.; Compari, C.; Duce, E.; D'Onofrio, G.; Ro´z˙ycka- Roszak, B.; Woz´niak, E. *Biochim. Biophys. Acta* **2005**, *1722*, 224–233.

[116] (a) Srinivasachari, S.; Fichter, K. M.; Reineke, T. M. *J. Am. Chem. Soc.* **2008**, *130*, 4618–4627. (b) Horiuchi, S.; Aoyama, Y. *J. Controlled Release* **2006**, *116*, 107–114. (c) Sansone, F.; Dudic`, M.; Donofrio, G.; Rivetti, C.; Baldini, L.; Casnati, A.; Cellai, S.; Ungaro, R. *J. Am. Chem. Soc.* **2006**, *128*, 14528–14536. (d) Lalor, R.; DiGesso, J. L.; Mueller, A.; Matthews, S. E. *Chem. Commun.* **2007**, 4907–4909.

[117] (a) Nishihara, M.; Perret, F.; Takeuchi, T.; Futaki, S.; Lazar, A. N.; Coleman, A. W.; Sakai, N.; Matile, S. *Org. Biomol. Chem.* **2005**, *3*, 1659–1669. (b) Takeuchi, T.; Kosuge, M.; Tadokoro, A.; Sugiura, Y.; Nishi, M.; Kawata, M.; Sakai, N.; Matile, S.; Futaki, S. *ACS Chem. Biol.* **2006**, *1*, 299–303. (c) Sainlos, M.; Hauchecorne, M.; Oudrhiri, N.; Zertal-Zidani, S.; Aissaoui, A.; Vigneron, J.-P.; Lehn, J.-M.; Lehn, P. *ChemBioChem* **2005**, *6*, 1023–1033. (d) Elson-Schwab, L.; Garner, O. B.; Schuksz, M.; Crawford, B. E.; Esko, J. D.; Tor, Y. *J. Biol. Chem.* **2007**, *282*, 13585–13591. (e) Wender, P. A.; Galliher, W. C.; Goun, E. A.; Jones, L. R.; Pillow, T. *Ad*V. *Drug Re*V. **2008**, *60*, 452–472.

especially at the vector concentration required for observing cell transfection (10-20 μM), even in the presence of the helper lipid DOPE (dioleoyl phosphatidylethanolamine).[16c,118]

Interestingly, Ungaro et al. found that attaching guanidinium (figure **4.2, 107**) moieties at the phenolic OH groups (lower rim) of the calix[4]arene through a three carbon atom spacer results in a new class of cytofectins[16].

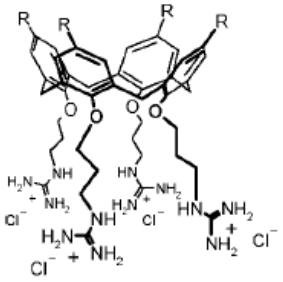

R= t-Bu;107/a
R= H; 107/b
R= Hex; 107/c

Figure 4.2. Calix[4]arene like a new class of cytofectines.

One member of this family (figure **4.2**), when formulated with DOPE, performed cell transfection quite efficiently and with very low toxicity, surpassing a commercial lipofectin, widely used for gene delivery. Ungaro et al reported in a communication[119] the basic features of this new class of cationic lipids in comparison with a nonmacrocyclic (gemini-type, **108**) model compound (figure **4.3**).

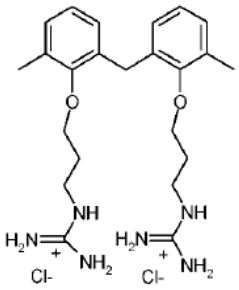

108

Figure 4.3. Nonmacrocyclic cationic lipids, gemini-type.

The ability of compounds **107 a-c** and **108** to bind plasmid DNA pEGFP-C1 (4731 bp) was assessed through gel electrophoresis and ethidium bromide displacement assays[11]. Both experiments evidenced that the macrocyclic derivatives **107 a-c** bind to plasmid more efficiently than **108**. To fully understand the structure–activity relationship of cationic polymer delivery systems, Zuckermann[120] examined a set of cationic *N*-substituted glycine oligomers (NSG peptoids) of defined length and sequence. A diverse set of peptoid oligomers, composed of systematic variations in main-chain length, frequency of cationic

[118] (a) Farhood, H.; Serbina, N.; Huang, L. *Biochim. Biophys. Acta* **1995**, *1235*, 289–295.

[119] Bagnacani V., Sansone F., Donofrio G., Baldini L., Casnati A., Ungaro R. *Org. Lett.*, **2008,** Vol. *10*, No. 18, 3953-3959**.**

[120] J. E. Murphy, T. Uno, J. D. Hamer, F. E. Cohen, V. Dwarki, R. N. Zuckermann *Proc. Natl. Acad. Sci. Usa* **1998,** Vol. 95, Pp. 1517–1522, Biochemistry.

side chains, overall hydrophobicity, and shape of side chain, were synthesized. Interestingly, only a small subset of peptoids were found to yield active oligomers. Many of the peptoids were capable of condensing DNA and protecting it from nuclease degradation, but only a repeating triplet motif (cationic-hydrophobic-hydrophobic) was found to have transfection activity. Furthermore, the peptoid chemistry lends itself to a modular approach to the design of gene delivery vehicles; side chains with different functional groups can be readily incorporated into the peptoid, and ligands for targeting specific cell types or tissues can be appended to specific sites on the peptoid backbone. These data highlight the value of being able to synthesize and test a large number of polymers for gene delivery. Simple analogies to known active peptides (e.g., polylysine) did not directly lead to active peptoids. The diverse screening set used in this article, revealed that an unexpected specific triplet motif was the most active transfection reagent. Whereas, some minor changes lead to improvement in transfection, other minor changes abolished the capability of the peptoid to mediate transfection. In this context, they speculate that whereas the positively charged side chains interact with the phosphate backbone of the DNA, the aromatic residues facilitate the packing interactions between peptoid monomers. In addition, the aromatic monomers are likely to be involved in critical interactions with the cell membrane during transfection. Considering the interesting results reported, we decided to investigate on the potentials of cyclopeptoids in the binding with DNA and the possible impact of the side chains (cationic and hydrophobic) towards this goal. Therefore, we have synthesized the three cyclopeptoids reported in figure **4.4** (**62, 63** and **64**) which show a different ratio between the charged and the nonpolar side chains.

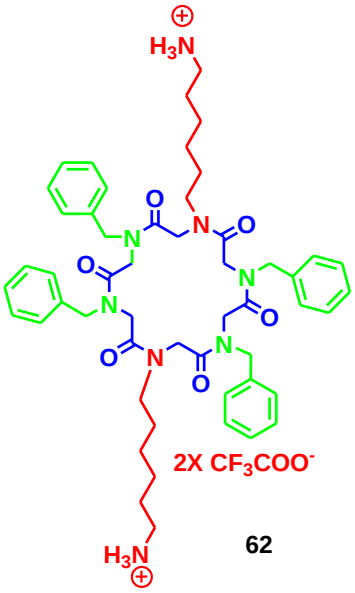

62

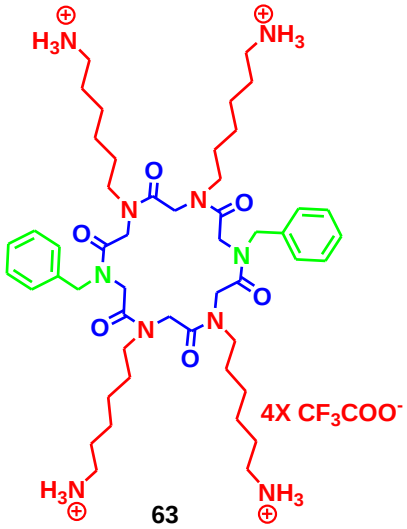

63

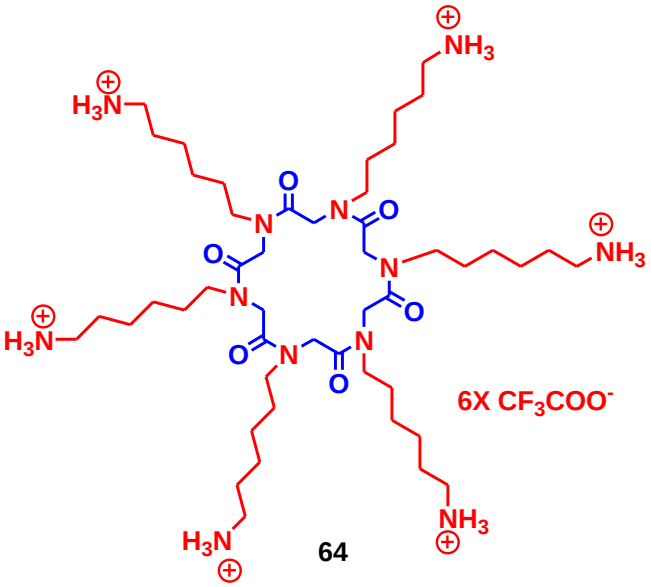

Figure 4.4. Dicationic cyclohexapeptoid **62,** tetracationic cyclohexapeptoid **63**, hexacationic cyclohexapeptoid **64.**

4.2 Results and discussion

4.2.1 Synthesis

In order to obtain our targets first step was the synthesis of the amine submonomer *N*-*t*-Boc-1,6-diaminohexane **110** as reported in scheme **4.1**[121].

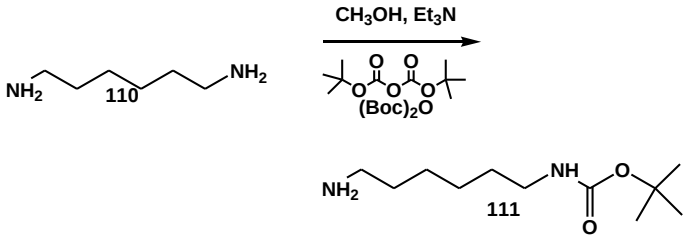

Scheme 4.1. *N*-Boc protection.

The synthesis of the three *N*-protected linear precursors (**112, 113** and **114**, scheme **4.2**) was accomplished on solid-phase (2-chlorotrityl resin) using the "sub-monomer" approach.

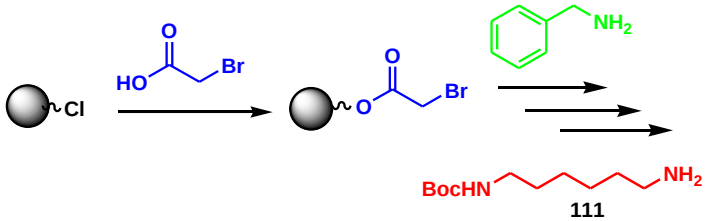

[121] Krapcho, A. P. & Kuell, C. S. *Synth. Commun* **1990**, *20*, 2559–2564.

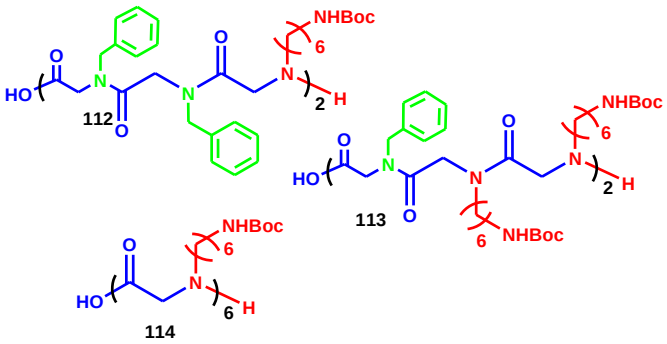

Scheme 4.2. "Sub-monomer" approach for the synthesis of hexa-linears (**112, 113** and **114).**

Head-to-tail macrocyclizations of the linear *N*-substituted glycines were realized in the presence of HATU in DMF, according to our previous results.[122] Cyclization of oligomers **112**, **113** and **114** proved to be quite efficient (**115, 116** and **117** were characterized with HPLC and EI-MS, scheme **4.3**).

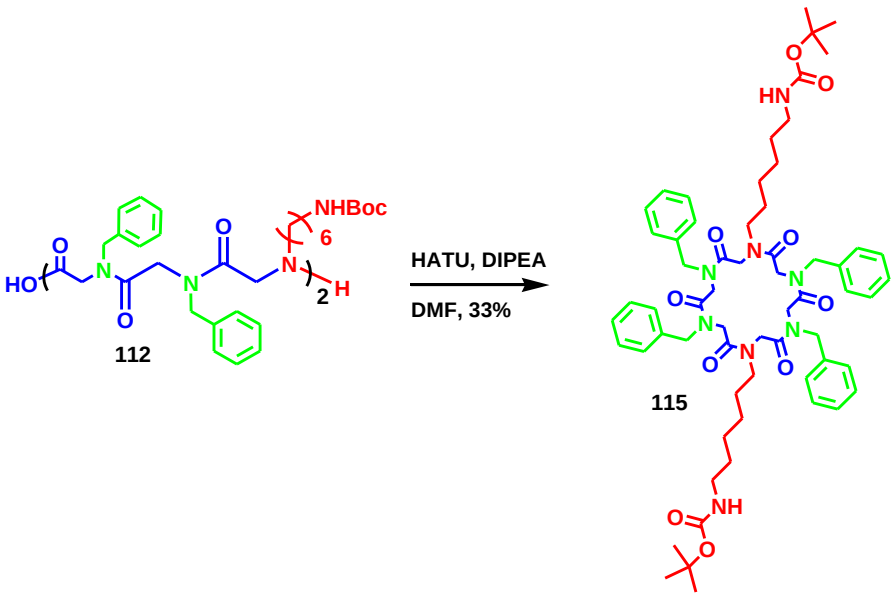

[122] N. Maulucci, I. Izzo, G. Bifulco, A. Aliberti, C. De Cola, D. Comegna, C. Gaeta, A. Napolitano, C. Pizza, C. Tedesco, D. Flot, F. De Riccardis, *Chem. Commun*. **2008**, 3927 –3929.

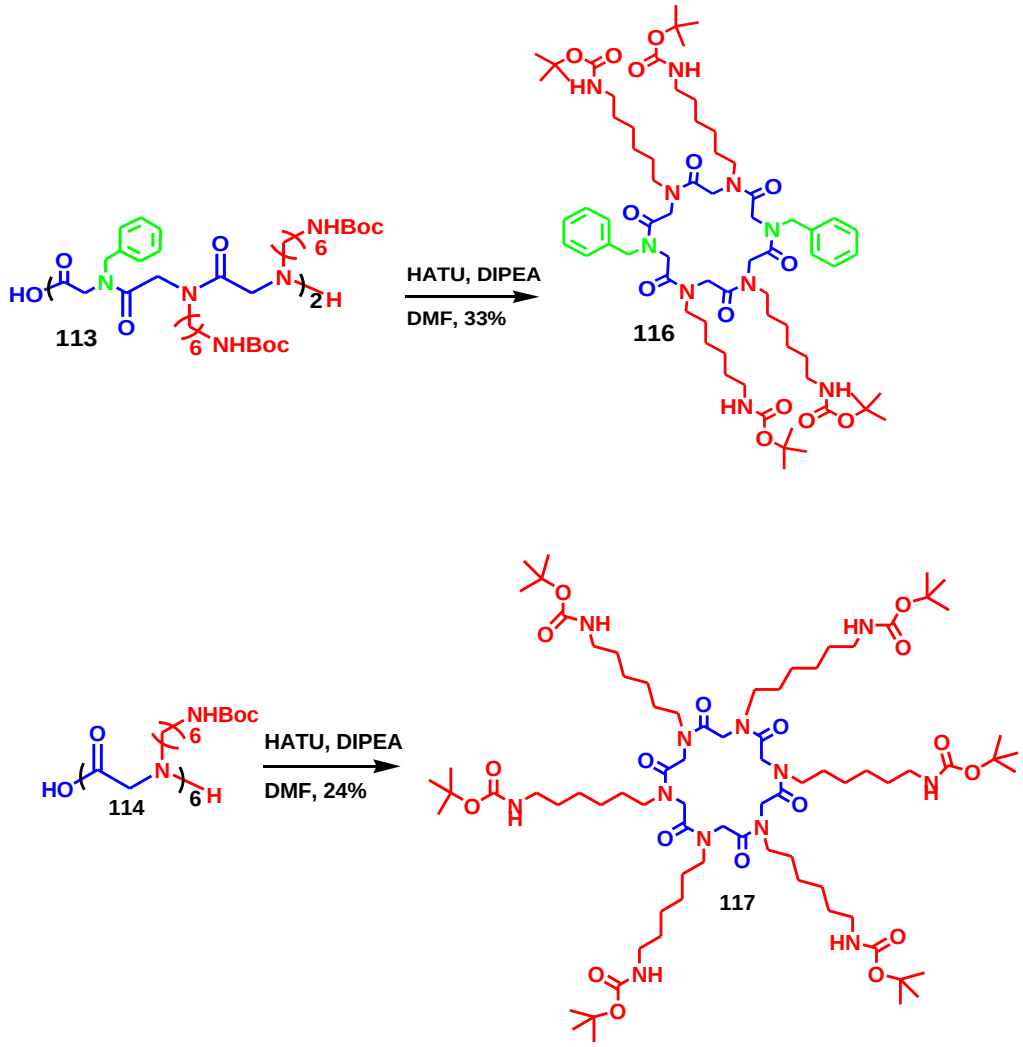

Scheme 4.3. Protected cyclopeptoids **115**, **116** and **117.**

All cyclic products were deprotected with 33% TFA in CH_2Cl_2 to give quantitative yields of cyclopeptoids **62**, **63** and **64**.

4.2.2 Biological tests.

In collaboration with Donofrio's group, biological activity evaluation was performed. All cyclopeptoids synthesized for this study should complex spontaneously plasmid DNA, owing to an extensive network of electrostatic interactions. The binding of the cationic peptoid to plasmid DNA should result in neutralization of negative charges in the phosphate backbone of DNA. This interaction can be measured by the inability of the large electroneutral complexes obtained to migrate toward the cathode during electrophoresis on agarose gel. The ability of peptoids to complex with DNA was evaluated by incubating peptoids with plasmid DNA at a 3:1 (+/-) charge ratio and analyzing the complexes by agarose gel electrophoresis. Peptoids tested in this experiment were not capable of completely retarding the migration of DNA into the gel. In this experiment, cyclopeptoids **62**, **63** and **64** failed to retard the migration of DNA into the gel. Therefore, the spacing of charged residues on the

peptoid backbone as well as the degree of hydrophobicity of the side chains have a dramatic effect on the ability to form homogenous complexes with DNA in high yield.

4.3 Conclusions

In this project three different cyclopeptoids **62, 63** and **64,** decorated with cationic side chains, were synthetized. Biological evaluation demonstrated that they were not able to act as DNA vectors. A possible reason of these results could be that spatial orientation (see in chapter 3) of the side chains in cyclopeptoids did not assure the correct coordination and the binding with DNA.

4.4 Experimental section

4.4.1 Synthesis

✓ *Compound **111***

Di-*tert*-butyl carbonate (0.4 eq., 7.51g, 0.034 mmol) was added to 1,6-diaminohexane (10 g, 0.086 mmol) in CH_3OH/Et_3N (9/1) and the reaction was stirred overnight. The solvent was evaporated and the residue was dissolved in DCM (20 mL) and extracted using a saturated solution of $NaHCO_3$ (20 mL). Then water phase was washed with DCM (3 · 20 ml). The combined organic phase was dried over Mg_2SO_4 and concentrated in vacuo to give a pale yellow oil. The compound was purified by flash chromatography ($CH_2Cl_2/CH_3OH/NH_3$ 2.0M solution in ethyl alcohol, from: 100/0/0.1 to 70/30/0.1) to give **81** (0.51 g, 30%) as a yellow light oil; [Found: C, 61.1; H, 11.2; N, 12.9; O,14.8. $C_{11}H_{24}N_2O_2$ requires C, 61.07; H, 11.18; N, 12.95; O, 14.79%]; R_f (98/2/0.1, $CH_2Cl_2/CH_3OH/NH_3$ 2.0M solution in ethyl alcohol) 0.63; δ_H (250 MHz, $CDCl_3$) 4.84 (brs, 1H, N*H*-Boc), 2.97-2.94 (bq, 2H, CH_2-NH-Boc, *J* = 7.5 MHz), 2.56-2.51 (t, 2H, CH_2NH$_2$, *J* 7.0 MHz), 1.8 (brs, 2H, NH_2), 1.30 (s, 9H, (CH_3)$_3$); 1.30-1.18 (m, 8H, CH_2); *m/z* (ES) 217 (MH^+); (HRES) MH^+, found 217.1920. $C_{11}H_{25}N_2O_2^+$ requires 217.1916.

4.4.2 General procedures for linear oligomers 112, 113 and 114.

Linear peptoid oligomers **112, 113** and **114** were synthesized using a sub-monomer solid-phase approach[11]. In a typical synthesis 2-chlorotrityl chloride resin (2,α-dichlorobenzhydryl-polystyrene crosslinked with 1% DVB; 100–200 mesh; 1.33 mmol/g, 400 mg, 0.532 mmol) was swelled in dry DMF (4 mL) for 45 min and washed twice with dry DCM (4 mL).

The first sub-monomer was attached onto the resin by adding 120 mg (1.2 eq, 0.63 mmol) of bromoacetic acid in dry DCM (4 mL) and 370 μL of DIPEA (2.10 mmol) on a shaker platform for 40 min at room temperature, followed by washing with dry DCM (4 mL) and then with DMF (4 x 4 mL). To the bromoacetylated resin was added a DMF solution (1 M, 5.3 mL) of the desired amine (benzylamine -10 eq- or **111** -10 eq-) the mixture was left on a shaker platform for 30 min at room temperature, then the resin was washed with DMF (4 x 4 mL). Subsequent bromoacetylation reactions were accomplished by reacting the aminated oligomer with a solution of bromoacetic acid in DMF (1.2 M, 5.3 mL) and 823 μL of DIC for 40 min at room temperature. The filtered resin was washed with DMF (4 x 4 mL) and treated again with the amine in the same conditions reported above. This cycle of reactions was iterated until the target oligomer was obtained (**112**, **113** and **114** peptoids). The cleavage was performed by treating twice the resin, previously washed with DCM (6 x 6 mL), with 4 mL of 20% HFIP in DCM (v/v) on a shaker platform at room temperature for 30 min and 5 min, respectively. The

resin was then filtered away and the combined filtrates were concentrated in vacuo. The final products were dissolved in 50% acetonitrile in HPLC grade water and analysed by RP-HPLC (purity >95% for all the oligomers, conditions: 5% to 100% B in 30 min [A: 0.1% TFA in water, B: 0.1% TFA in acetonitrile], flow: 1.0 mL/min, 220 nm. C18 reversed-phase analytical column [Waters, μBondapak, 10 μm, 125 Å, 3.9 mm x 300 mm]) and ESI mass spectrometry. The linear oligomers **112**, **113** and **114** were subjected to the cyclization reaction without further purification.

✓ *Compound **112:*** t_R:19.6 min; *m/z* (ES) 1119 (MH^+); (HRES) MH^+, found 1119.6485 $C_{62}H_{87}N_8O_{11}^+$ requires 1119.6489. 100%.

✓ *Compound **113:*** t_R:19.0 min; *m/z* (ES) 1338 (MH^+); (HRES) MH^+, found 1337.8690 $C_{70}H_{117}N_{10}O_{15}^+$ requires 1337.8694. 100%.

✓ *Compound **114:*** t_R:21.0 min; *m/z* (ES) 1556 (MH^+); (HRES) MH^+, found 1556.0910 $C_{78}H_{147}N_{12}O_{19}^+$ requires 1556.0900. 100%.

4.4.3 General cyclization reaction (synthesis of 115, 116 and 117)

A solution of the linear peptoid (**112**, **113** and **114**), previously co-evaporated three times with toluene, was prepared under nitrogen in dry DMF (20 mL).

✓ Linear **112** (1.0 eq., 104 mg, 0.093 mmol) was dissolved in DMF dry (10 mL) and the mixture was added drop-wise by syringe pump in 2 h to a stirred solution of HATU (3.1 eq., 112.0 mg, 0.29 mmol) and DIPEA (6.0 eq., 97 μl, 0.55 mmol) in dry DMF (20 mL) at room temperature in anhydrous atmosphere.

✓ Linear **113** (1.0 eq., 217.0 mg, 0.162 mmol) was dissolved in DMF dry (10 mL) and the mixture was added drop-wise by syringe pump in 2 h to a stirred solution of HATU (3.1 eq., 191.1 mg, 0.50 mmol) and DIPEA (6.0 eq, 174.6 μl, 1.00 mmol) in dry DMF (20 mL) at room temperature in anhydrous atmosphere.

✓ Linear **114** (1.0 eq., 112.0 mg, 0.072 mmol) was dissolved in DMF dry (10 mL) and the mixture was added drop-wise by syringe pump in 2 h to a stirred solution of HATU (3.1 eq, 84.7 mg, 0.223 mmol) and DIPEA (6.2 eq, 76 μl, 0.43 mmol) in dry DMF (20 mL) at room temperature in anhydrous atmosphere.

After 12 h the resulting mixtures were concentrated in vacuo, diluted with CH_2Cl_2 (20 mL) and a solution of HCl (0.1 N, 20 mL). The single mixture was extracted with CH_2Cl_2 (2 x 20 mL) and the combined organic phases were washed with water (12 mL), dried over anhydrous Na_2SO_4, filtered and concentrated in vacuo.

All protected cyclic **115**, **116** and **117** were dissolved in 50% acetonitrile in HPLC grade water and analysed by RP-HPLC (purity >85% for all the cyclic oligomers, conditions: 5%-100% B in 30 min [A: 0.1% TFA in water, B: 0.1% TFA in acetonitrile], flow: 1.0 mL/min, 220 nm. C18 reversed-phase analytical column [Waters, μBondapak, 10 μm, 125 Å, 3.9 mm x 300 mm]) and ESI mass spectrometry (zoom scan technique).

The crude residues were purified by HPLC on a C18 reversed-phase preparative column, conditions: 20%-100% B in 40 min [A: 0.1% TFA in water, B: 0.1% TFA in acetonitrile], flow: 2.0 mL/min, 220 nm. The samples were dried in a falcon tube under low pressure.

✓ *Compound **115:*** δ_H (400 MHz, CD_3CN:$CDCl_3$ (9:1), mixture of conformers) 7.34-7.06 (m, 20H, *H*-Ar), 5.19 (br s, 2H, N*H*), 4.80-3.60 (m, 20H, NCH_2Ph, -COCH_2N- overlapped), 3.33-3.09 (m, 4H, -CH_2N), 3.02-2.96 (m, 4H, -CH_2NHBoc), 1.38 (br s, 18 H, C(CH_3)$_3$); 1.38-1.17 (m, 16 H, (CH_2)$_4$); 33%, *m/z* (ES) 1101 (MH^+); (HRES) MH^+, found 1101.3785. $C_{62}H_{85}N_8O_{10}^+$ requires 1101.3780. **HPLC**: t_R: 20.6 min.

✓ *Compound **116:*** δ_H (400 MHz, CD_3OD, mixture of conformers) 7.46-7.32 (m, 10H, *H*-Ar), 4.90-3.20 (m, 24H, NCH_2Ph, -COCH_2N- -CH_2N overlapped with HDO e MeOD), 3.07-2.84 (m, 8H, -CH_2NHBoc), 1.48 (br s, 36 H, C(CH_3)$_3$); 1.72-1.17 (m, 32 H, (CH_2)$_4$). δ_C (100 MHz, $CDCl_3$, mixture of conformers) 170.6, 169.0, 168.9, 1586.3, 156.1, 155.8, 155.7, 144.4, 143.4, 143.3, 140.8, 140.7, 136.2, 136.0, 127.9, 127.5, 127.4, 126.9, 126.4, 124.5, 119.4, 81.7, 81.6, 67.5, 67.0, 66.0, 65.9, 59.8, 50.4, 50.0, 49.9, 48.7, 48.3, 46.7, 46.6, 39.0, 27.4, 20.5. 33%, *m/z* (ES) 1319 (MH^+); (HRES) MH^+, found 1319.7130. $C_{70}H_{115}N_{10}O_{14}^+$ requires 1319.7128. **HPLC**: t_R: 21.2 min.

✓ *Compound **117:*** δ_H (250 MHz, CD_3OD, mixture of conformers) 4.90-3.20 (m, 24H, -COCH_2N-,-CH_2N overlapped with HDO e MeOD), 3.10-2.85 (m, 12H, -CH_2NHBoc), 1.44 (br s, 54 H, C(CH_3)$_3$); 1.72-1.20 (m, 48 H, (CH_2)$_4$). δ_C (62.5 MHz, CD_3OD , mixture of conformers) 173.5 (bs), 172.3 (bs), 171.9 (bs), 171.7 (bs), 171.2 (bs), 170.9 (bs), 170.6 (bs), 170.2 (bs), 158.5, 79.7, 50.6 (bs) , 50.0 - 48.0 (overlapped with MeOD), 41.2, 40.6 (bs), 30.9, 29.7 (bs), 29.4 (bs), 28.8, 27.6 (bs). 24%, *m/z* (ES) 1538 (MH^+); (HRES) MH^+, found 1538.0480. $C_{78}H_{145}N_{12}O_{18}^+$ requires 1538.0476. **HPLC**: t_R: 22.5 min.

4.4.4 General deprotection reaction (synthesis of 62, 63 and 64)

Protected cyclopeptoids **115** (34 mg, 0.030 mmol), **116** (38.9 mg, 0.029 mmol) and **117** (26 mg, 0.017mmol)**,** were dissolved in a mixture of DCM and TFA (9/1, 4 mL) and the reaction was stirred for two hours. After, products were precipitated in cold Ethyl Ether (20 mL) and centrifuged. Solids were recuperated with a quantitative yield.

✓ *Compound **62:*** δ_H (250 MHz, MeOD, mixture of conformers) 7.38-7.01 (m, 20H, *H*-Ar), 4.80 - 3.30 (m, 24H, NCH_2Ph, -COCH_2N, -CH_2N overlapped with HDO and MeOD), 3.00-2.83 (m, 4H, -C$H_2NH_3^+$), 1.75 -1.30 (m, 16 H, (CH_2)$_4$); δ_C (75 MHz, MeOD, mixture of conformers) 174.2 (bs), 172.1 (bs), 171.5 (bs), 171.1 (bs), 171.0 (bs), 162.2 (bs, CF_3*C*OO-), 138.2 (bs), 138.0 (bs), 137.5 (bs), 137.1 (bs), 131.1 (bs), 130.2, 129.7, 129.3, 129.0, 128.6, 128.3, 127.0, 54.8, 53.8, 52.8, 52.1 (bs), 50.8 (bs), 50.6, 49.8-48.1 (overlapped with MeOD), 40.6, 30.7, 28.5, 28.1, 27.1, 24.2. m/z (ES) 916 (MH^+); (HRES) MH^+, found 916.1800. $C_{53}H_{72}N_8O_6^{3+}$ requires 916.1797.

✓ *Compound **63:*** δ_H (300 MHz, CD_3OD, mixture of conformers) δ: 7.44-7.31 (m, 10H, *H*-Ar), 4.90 - 3.30 (m, 24H, NCH_2Ph, -COCH_2N, -CH_2N overlapped with HDO and MeOD), 3.00-2.83 (m,

8H, -C*H*$_2$NH$_3^+$), 1.75 -1.30 (m, 32 H, (C*H*$_2$)$_4$). m/z (ES) 923 (MH^+); (HRES) MH^+, found 923.2792. $C_{50}H_{87}N_{10}O_6^{5+}$requires 923.2792.

✓ *Compound **64:*** δ_H (300 MHz, CD_3OD, mixture of conformers) δ: 4.90-3.16 (m, 24H, -COC*H*$_2$N-, -C*H*$_2$N overlapped with HDO and MeOD), 3.10-2.89 (m, 12H, -C*H*$_2$NH$_3^+$), 1.72-1.25 (m, 48 H, (C*H*$_2$)$_4$. m/z (ES) 943 (MH^+); (HRES) MH^+, found 943.3978. $C_{48}H_{103}N_{12}O_6^{7+}$ requires 943.3970.

4.4.5 DNA preparation and storage.

Plasmid DNA was purified through cesium chloride gradient centrifugation (T. Maniatis, E.F. Fritsch, J. Sambrook, in Molecular Cloning: A Laboratory Manual, 2nd edition, Cold Spring Harbor Laboratory: New York, 1989). A stock solution of the plasmid 0.350 M in milliQ water (Millipore Corp., Burlington, MA) was stored at -20 °C.

4.4.6 Electrophoresis mobility shift assay (EMSA)

Binding reactions were performed in a final volume of 14 µL with 10 µl of 20 mM Tris/HCl pH 8, 1 µL of plasmid (1 µg of pEGFP-C1) and 3 µL of compound **62**, **63** and **64** at different final concentrations, ranging from 25 to 200 µM. Binding reaction was left to take place at room temperature for 1 h; 5 µL of 1 g/mL in H_2O of glycerol was added to each reaction mixture and loaded on a TA (40 mM Tris–Acetate) 1% agarose gel. At the end of the binding reaction 1 L (0.01 mg) of ethidium bromide solution is added. The gel was run for 2.5 h in TA buffer at 10 V/cm. EDTA was omitted from the buffers because it competes with DNA in the reaction.

Chapter 5

5. *Complexation with Gd(III) of carboxyethyl cyclopeptoids as possible contrast agents in MRI.*

5.1 Introduction

Tomography of magnetic resonance (Magnetic Resonance Imaging, MRI) has gained great importance in the last three decades in medicinal diagnostics as an imaging technique with a superior spatial resolution and contrast. The most important advantage of MRI over the competing radio-diagnostic methods such as X-Ray Computer Tomography (CT), Single-Photon Emission Computed Tomography (SPECT) or Positron Emission Tomography (PET) is definitely the absence of harmful high-energy radiations. Moreover, MRI often represents the only reliable diagnostic method for, *e.g.*cranial abnormalities or multiple sclerosis[123]. In the course of time, it was found that in some examinations of, *e.g.* the gastrointestinal tract or cerebral area, the information obtained from a simple MRI image might not be sufficient. In these cases, the administration of a suitable contrast enhancing agent (CA) proved to be extremely useful. Quite soon, it was verified that the most capable class of CAs could be some compounds containing paramagnetic metal ions.

These drugs would be administered to a patient in order to (1) improve the image contrast between normal and diseased tissue and/or (2) indicate the status of organ function or blood flow[124]. The image intensity in ^{1}H NMR imaging, largely composed of the NMR signal of water protons, depend on the nuclear relaxation times. Complexes of paramagnetic transition and lanthanide ions, which can decrease the relaxation times of nearby nuclei *via* dipolar interactions, have received attention as potential contrast agents. Paramagnetic contrast agents are an integral part of this trend: they are unique among diagnostic agents. In tissue, these agents are not visualized directly on the NMR image but are detected indirectly by virtue of changes in proton relaxation behavior. Moreover, the expansion of these agents offers interesting challenges for investigators in the chemical, physical, and biological sciences[1]. These comprise the design and synthesis of stable, nontoxic, and tissue-specific metal complexes and the quantitative understanding of their effect on nuclear relaxation behavior in solution and in tissue. Physical principles of MRI rely on the monitoring of the different distribution and properties of water in the examined tissue and also on a spatial variation of its proton longitudinal (T_1) and transversal (T_2) magnetic relaxation times[125]. All CAs can be divided (according to the site of action) into extracellular, organ-specific and blood pool agents. Historically, the chemistry of the T_1-CAs has been explored more extensively as the T_1 relaxation time of diamagnetic water solutions is typically five-times longer than T_2 and, consequently easier to be shortened[1]. From the chemical point of view, T_1-CAs are complexes of paramagnetic metal ions, such as Fe(III), Mn(II) or Gd(III), with suitable organic ligands.

Gadolinium (III) is an optimal relaxation agents for its high paramagnetism (seven unpaired electrons) and for its properties in term of electronic relaxation[126]. The presence of paramagnetic Gd

[123] P. Hermann, J. Kotek, V. Kubìcek and I. Lukes *Dalton Trans.*, **2008**, 3027–3047.
[124] Randall E. Lauffer *Chem. Rev.* **1987**, *87*, 901-927.
[125] *The Chemistry of Contrast Agents in Medical Magnetic Resonance Imaging*, ed. A. E. Merbach, and E. Tòth, John Wiley & Sons, Chichester (England), **2001**.
[126] S. Aime, M. Botta, M. Fasano and E. Terreno *Chemical Society Reviews*, **1998**, *27*, 19-29.

(III) complexes causes a dramatic enhancement of the water proton relaxation rates and then allows to add physiological information to the impressive anatomical resolution commonly obtained in the uncontrasted images.

Other general necessities of contrast agent for MRI are low toxicity, rapid excretion after administration, good water solubility and low osmotic potential of the solutions clinically used. However, the main problem of the medical utilizations of heavy metal ions like the Gd(III) ion is a significant toxicity of their "free" (aqua-ion) form. Thus, for clinical use of gadolinium(III), it must be bound in a complex of high stability and, even more importantly, it must show a long term resistance to a transmetallation/transchelation loss of the Gd(III) ion. High chelate stability is essential for lanthanide complexes in medicine because lanthanide ions have known toxicity via their interaction with Ca(II) binding sites. So, the preferred metal complexes, in addition to showing high thermodynamic (and possibly kinetic) stability, should present at least one water molecule in their inner coordination sphere, in rapid exchange with the bulk solvent, in order to affect strongly the relaxation of all solvent protons.

The Gd (III) chelate efficiency is commonly evaluated *in vitro* by the measure of its relaxivity (r_1), that, for commercial contrast agents as Magnevist (DTPA, **118**), Doratem (DOTA, **119**), Prohance (HP-DO3A, **120**) and Omniscan (DTPA-BMA, **121**), (figure **5.1**) is around 3.4-3.5 $mM^{-1}s^{-1}$ (20 MHz and 39°C).[2]

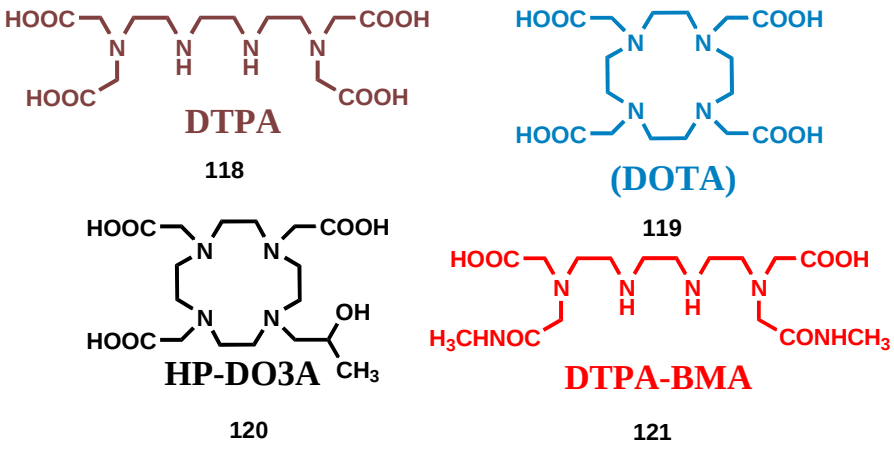

Figure 5.1. Commercial contrast agents.

The observed water proton longitudinal relaxation rate in a solution containing a paramagnetic metal complex is given by the sum of three contributions (eq. **5.1**)[2-127], where R_1^w is the water relaxation rate in the absence of the paramagnetic compound, R_{1p}^{is} represents the contribution due to exchange of water molecules from the inner coordination sphere of the metal ion to the bulk water and R_{1p}^{os} is the contribution of solvent molecules diffusing in the outer coordination sphere of the paramagnetic center. The overall paramagnetic relaxation enhancement ($R^{is}_{1p} + R^{os}_{1p}$) referred to a 1 mm concentration of a given Gd(III) chelate is called its relaxivity[2].

The inner sphere contribution is directly proportional to the molar concentration of the complex-Gd, to the number of water molecules coordinated to the paramagnetic center, *q*, and inversely proportional

[127] a) J. A. Peters, J. Huskens and D. J. Raber, *Prog. NMR Spectrosc.*, **1996**, *28*, 283. b) S. H. Koenig and R. D. Brown III, *Prog. NMR Spectrosc.*, **1990**, ***22***, 487.

to the sum of the mean residence lifetime, τ_M, of the coordinate water protons and their relaxtion time, T_{1M} (eq. **5.2**).

$$R_1^{obs} = R_1^o + R_{1p}^{is} + R_{1p}^{os} \qquad \text{Eq. 5.1}$$

$$R_{1p}^{is} = \frac{q[C]}{55.5(T_{1M} + \tau_M)} \qquad \text{Eq. 5.2}$$

The latter parameter is directly proportional to the sixth power of the distance between the metal center and the coordinated water protons (r) and depends on the molecular reorientational time, τ_R, of the chelate, on the electronic relaxation times, T_{iE}, (i=1 , 2), of the unpararied electrons of the metal and on the applied magnetic field strength itself (eq. **5.3** and **5.4**).

$$\frac{1}{T_{1M}} = \frac{2}{15}\left(\frac{\mu_0}{4\pi}\right)^2 \frac{\hbar^2 \gamma_s^2 \gamma_H^2}{r_{GdH}^6} S(S+1)\left(\frac{3\tau_{c1}}{1+\omega_H^2\tau_{c1}^2} + \frac{7\tau_{c2}}{1+\omega_s^2\tau_{c2}^2}\right) \qquad \text{Eq. 5.3}$$

$$\frac{1}{\tau_{ci}} = \frac{1}{\tau_R} + \frac{1}{\tau_M} + \frac{1}{\tau_{Ei}} \qquad \text{Eq. 5.4}$$

For resume all parameters:

- q is the number of water molecules coordinated to the metal ion;
- t_M is their mean residence lifetime;
- T_{1M} is their longitudinal relaxation time;
- S is the electron spin quantum number;
- γ_S and γ_H are the electron and the proton nuclear magnetogyric ratios;
- $r_{Gd–H}$ is the distance between the metal ion and the protons of the coordinated water molecules;
- ω_H and ω_S are the proton and electron Larmor frequencies, respectively;
- t_R is the reorientational correlation time;
- τ_{S1} and τ_{S2} are the longitudinal and transverse electron spin relaxation times.

The dependence of $R^{is}{}_{1p}$ and $R^{os}{}_{1p}$ on magnetic field is very significant, because the analysis of the magnetic field dependence permits the determination of the major parameters characterizing the relaxivity of Gd (III) chelate.

A significant step for the design and the characterization of more efficient contrast agents is represented by the investigation of the relationships between the chemical structure and the factors determining the ability to enhance the water protons relaxation rates. The overall relaxivity can be correlated with a set of physico-chemical parameters, which characterize the complex structure and dynamics in solution. Those that can be chemically tuned, are of primary importance in the ligand design (figure **5.2**)[1].

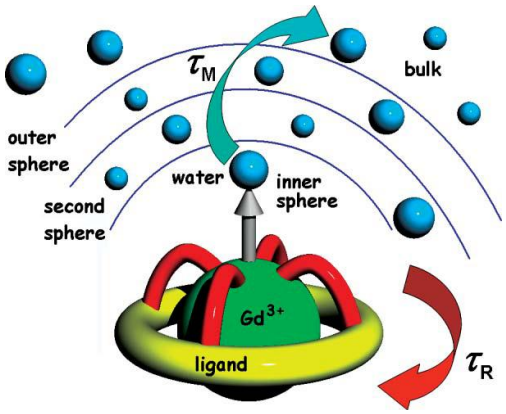

Figure 5.2. Model of Gd(III)-based contrast agent in solution.

Therefore, considering the importance of the contrast agents based on Gd (III), the cyclopeptoids complexing ability of sodium and the analogy between ionic ray of sodium (1.02 Å) and gadolinium (0.94 Å), the design and the synthesis of cyclopeptoids as potential Gd(III) chelates were realized. Consequently, taking inspiration from the commercial CAs, three different cyclopeptoids (figure **5.3**: **65**, **66** and **67**) containing polar and soluble side chains, were prepared and their complexing ability of Gd (III) was evaluated in collaboration with Prof. S. Aime at the University of Torino.

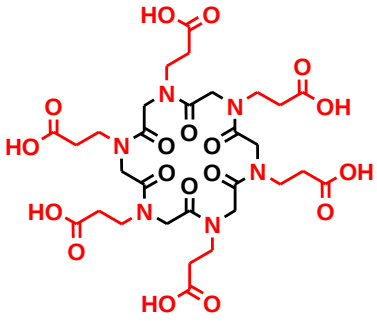

65

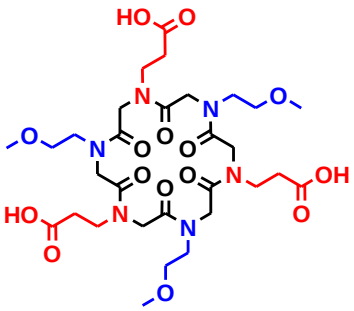

66

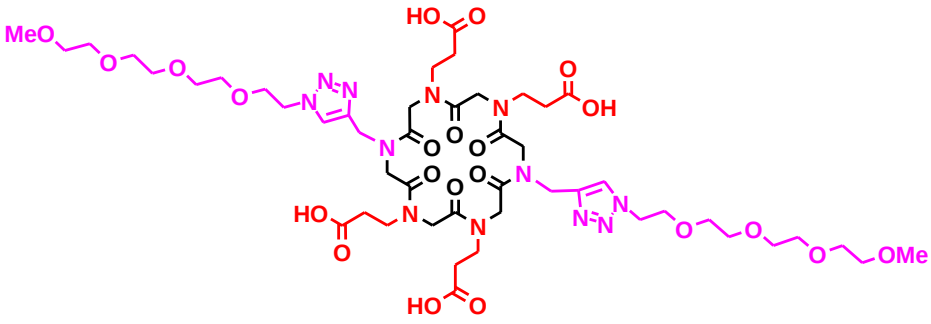

67

Figure 5.3. Hexacarboxyethyl cyclohexapeptoid **65**, Tricarboxyethyl ciclohexapeptoid **66** and tetracarboxyethyl cyclopeptoid **67**.

5.2 Lariat ether and click chemistry.

Cyclopeptoid **67** reminds a lariat ether. Lariat ethers are macrocyclic polyether compounds having one or more donor-group-bearing sidearms. Sidearms can be attached either to carbon (carbon-pivot lariat ethers) or to nitrogen (nitrogen-pivot lariat ethers). When more than one sidearm is attached, the number of them is designated using standard prefixes and the Latin word bracchium, which means arm.

A two-armed compound is thus a bibracchial lariat ether (abbreviated as BiBLE). Cations such as Na^+, Ca^{2+}, and NH^{4+} are strongly bound by these ligands[128].

We have expanded the lariat ethers concept to cyclopeptoids as well as macrocycles and we have included molecules having sidearms that contain a donor group. These sidearms were incorporated into the cyclic skeleton with a practical and rapid method: the "click chemistry". It consists in a chemistry tailored to generate substances quickly and reliably by joining small units together. Of the reactions comprising the click universe, the "perfect" example is the Huisgen 1,3-dipolar cycloaddition[129] of alkynes to azides to form 1,4-disubsituted-1,2,3-triazoles (scheme **5.1**). The copper(I)-catalyzed reaction is mild and very efficient, requiring no protecting groups, and no purification in many cases.[130] The azide and alkyne functional groups are largely inert towards biological molecules and aqueous environments, which allows the use of the Huisgen 1,3-dipolar cycloaddition in target guided synthesis[131] and activity-based protein profiling. The triazole has similarities to the ubiquitous amide moiety found in nature, but unlike amides, is not susceptible to cleavage. Additionally, they are nearly impossible to oxidize or reduce.

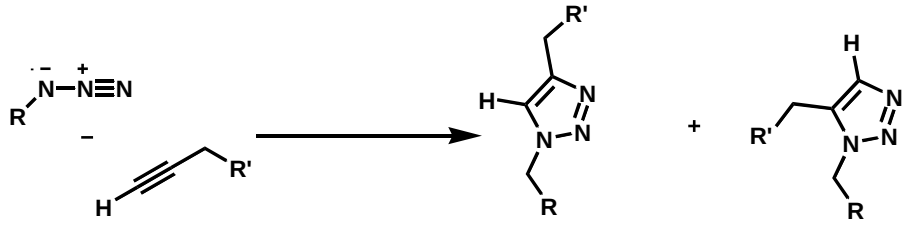

Scheme 5.1. Huisgen 1,3-dipolar cycloaddition.

Cu(II) salts in presence of ascorbate is used for preparative synthesis of 1,2,3-triazoles, but it is problematic in bioconjugation applications. However, tris[(1-benzyl-1*H*-1,2,3-triazol-4-yl)methyl]amine, has been shown to effectively enhance the copper-catalyzed cycloaddition without damaging biological scaffolds.[132]

Therefore, an important intermediate has been a cyclopeptoid containing two alkyne groups in the sidearms chains (**122**, figure **5.4**).

---

[128] G.W. Gokel, K. A. Arnold, M. Delgado, L. Echeverria, V. J. Gatto, D. A. Gustowski, J. Hernandez, A. Kaifer, S. R. Miller, and L. Echegoyen *Pure & Appl. Chem.,* **1988**, *60*, 461-465**.**

[129] For recent reviews, see: (a) Kolb, H. C.; Sharpless, K. B. *Drug Discovery Today* **2003**, *8*, 1128. (b)Kolb, H. C. et al. *Angew. Chem. Int. Ed.* **2001**, *40*, 2004.

[130] (a) Rostovtsev, V. V. et al. *Angew. Chem. Int. Ed.***2002**, *41*, 2596. (b) Tornøe, C. W. et al. *J. Org. Chem.* **2002**, *67*, 3057.

[131] (a) Manetsch, R. et al. *J. Am. Chem. Soc.***2004**, *126*, 12809. (b) Lewis, W. G. et al.*Angew. Chem. Int. Ed.* **2002**, *41*, 1053.

[132] Zhang, L. et al. *J. Am. Chem. Soc.* **2005**,*127*, 15998.

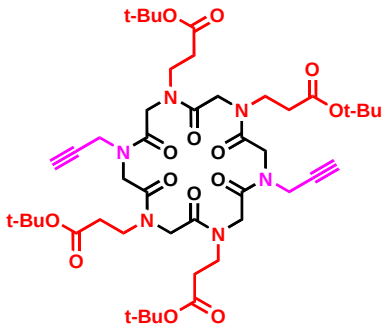

122

Figure 5.4. Cyclopeptoid intermediate.

5.3 Results and discussion

5.3.1 Synthesis

Initially, the synthesis of the linear precursors was accomplished through solid-phase mixed approach (“submonomer” and ‘‘monomer’’ approach) consisting in an alternate attachment of the *N*-fluorenylmethoxycarbonyl,*N*’-carboxymethyl-β-alanine, (**126**, scheme **5.2**), and a two step construction of monomers remnant, added to the resin in standard conditions.

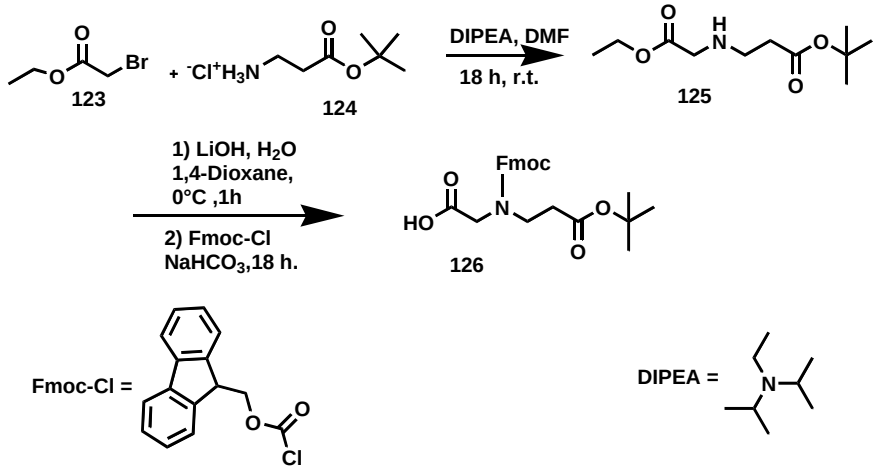

Scheme 5.2. Synthesis of monomer *N*-fluorenylmethoxycarbonyl,*N*’- carboxymethyl-β-alanine.

DIC and HATU-induced couplings and chemoselective deprotections yielded the required oligomers **127, 128**, and **129** (figure **5.5**).

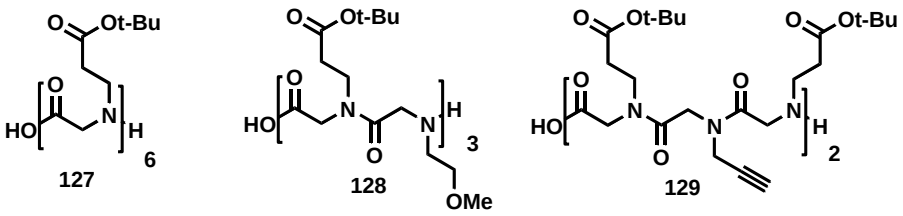

Figure 5.5. Linear cyclopeptoids.

All linear compounds were successfully synthesized as established by mass spectrometry, with isolated crude yields between 62 and 70% and purities greater than 90 % by HPLC. Head-to-tail macrocyclizations of the linear protect *N*-substituted glycines were realized in the presence of HATU in DMF, according to our precedent results (figure **5.6**).[133]

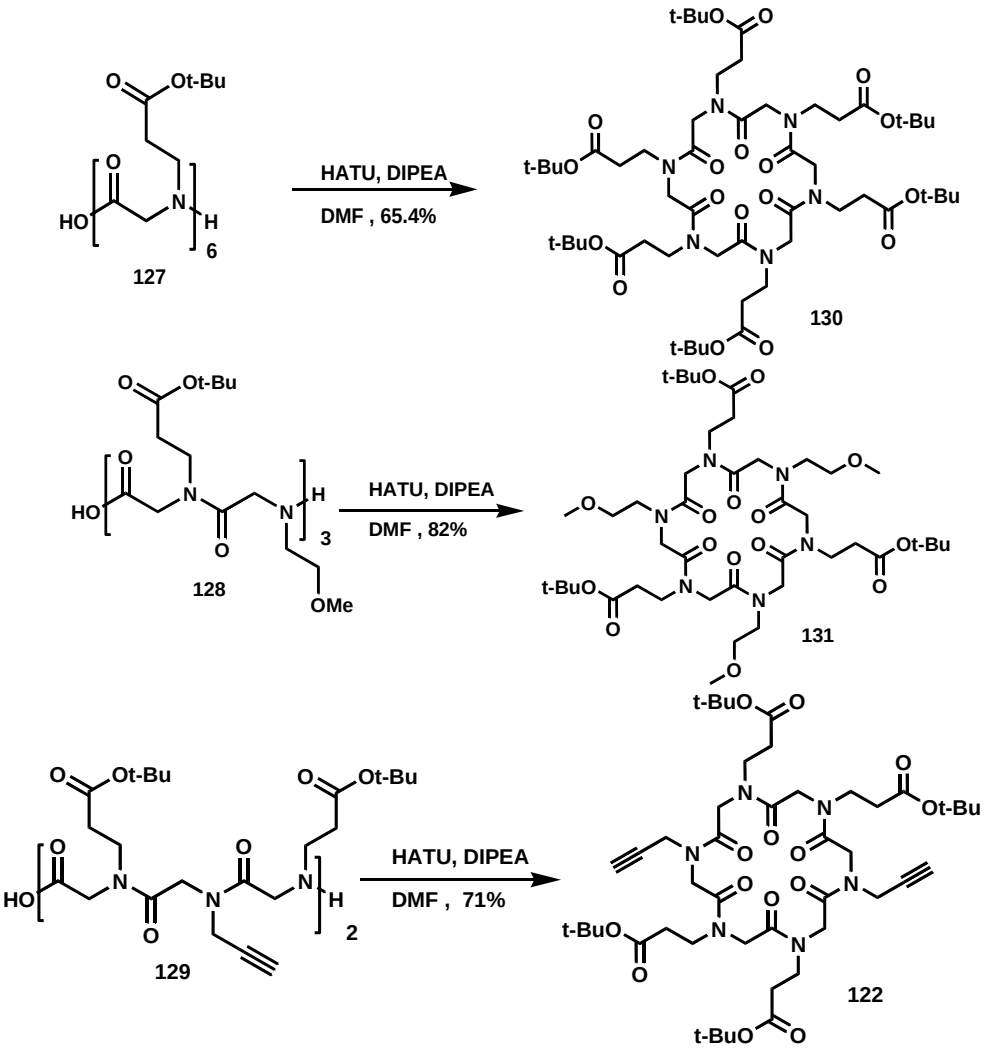

Figure 5.6. Synthesis of Protected cyclopeptoids.

The Boc-protected cyclic precursors (**130** and **131**) were deprotected with trifluoroacetic acid (TFA), to afford **65** and **66**. While, Boc-protected cyclic **122** was reacted with azide **132,** through click chemistry to afford protected cyclic **133** (figure **5.7**).

[133] Maulucci I., Izzo I., Bifulco G., Aliberti A., De Cola C., Comegna D., Gaeta C., Napolitani A., Pizza C., Tedesco C., Flot D., De Riccardis F., *Chem Commun* **2008**, 3927-3929.

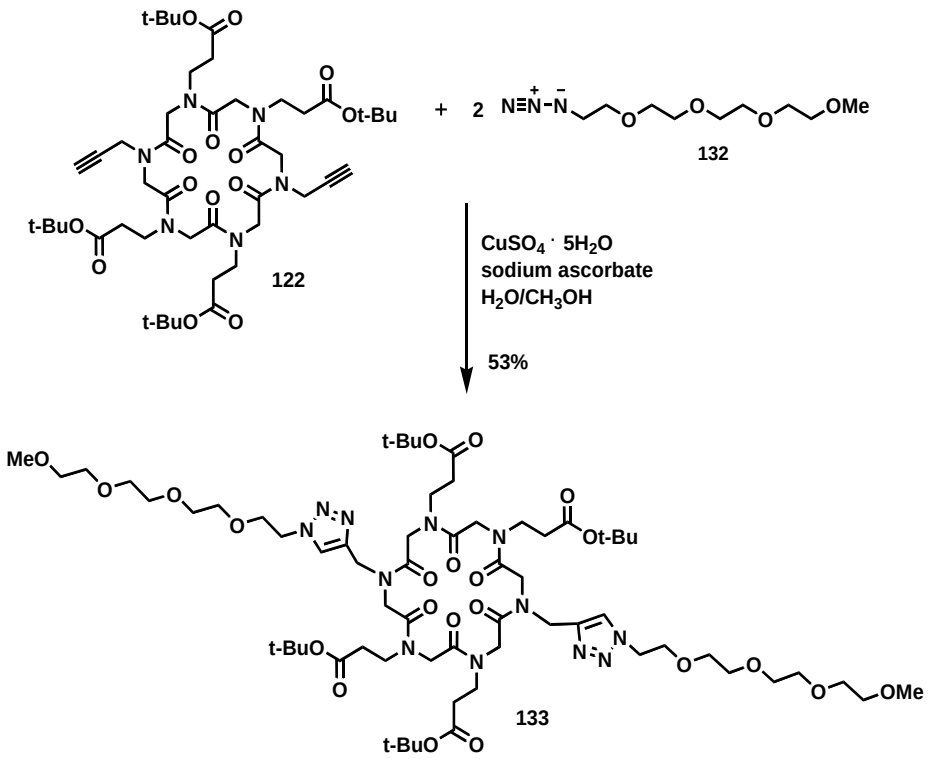

Figure 5.7. Click chemistry reaction.

Finally, cyclopeptoid **133** was deprotected, in presence of trifluoroacetic acid (TFA) in CH_2Cl_2, to afford **67.**

5.3.2. Stability evaluation of 65 and 66 as metal complexes.

The degree of toxicity of a metal chelate is related to its *in vivo* degree of dissociation before excretion.

The relaxation rate of the cyclopeptoid solutions (~2 mM), was evaluated. Cyclopeptoids **65** and **66** were titrated with a solution of $GdCl_3$ (11.2 mM) to establish their purity (pH=7, 25°C and 20 MHz, figure **5.7**).

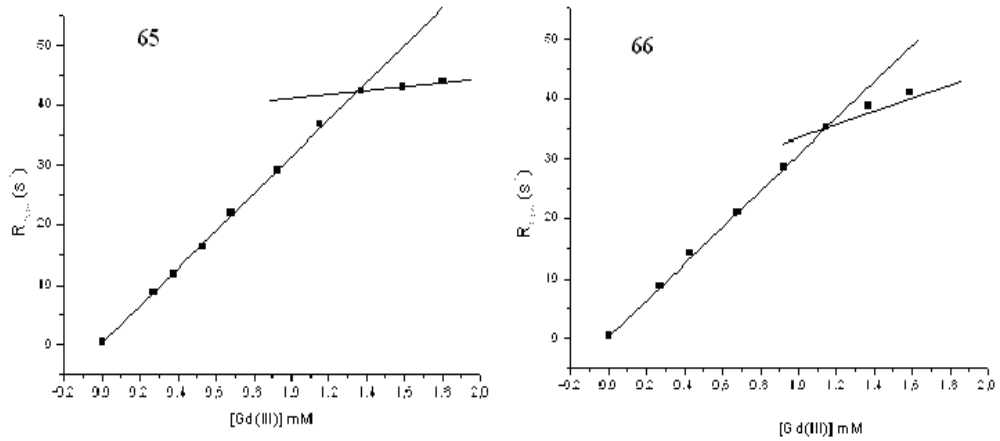

Figure 5.8. Titration of cyclopeptoids **65** and **66** with $GdCl_3$.

The relaxation rate linearly increased adding Gd(III). Its pendence represents the relaxivity (R_{1p}) of complex Gd-**65** and Gd-**66**. When Gd(III) was added in excess, the line changes its pendence and followes the relaxivity increase typical of Gd aquaion (R_{1p}= 13 $mM^{-1}s^{-1}$).

$$R_{1oss} = R_{1W} + r_{1p}[Gd\text{-}CP] \qquad \text{Eq. 5.5}$$

CP = cyclopeptoid

R_{1W} is the water relaxation rate in absence of the paramagnetic compound (= 0.38). Purity was been of 73% and 56% for **65** and **66**, respectively. From these data, we calculated the complexes relaxivity, which was 31.5 $mM^{-1}s^{-1}$ e 25.3 $mM^{-1}s^{-1}$ for Gd-**65** and Gd-**66**, respectively. These values resulted higher, when compared with the commercial contrast agents (~4-5 $mM^{-1}s^{-1}$).

By measuring solvent longitudinal relaxation rates over a wide range of magnetic fields with a field-cycling spectrometer that rapidly switches magnetic field strength over a range corresponding to proton Larmor frequencies of 0.01–70 MHz, we calculate important relaxivity parameters. The data points represent the so-called nuclear magnetic relaxation dispersion (NMRD), profile that can be adequately fitted to yield the values of the relaxation parameters (figure **5.9**).

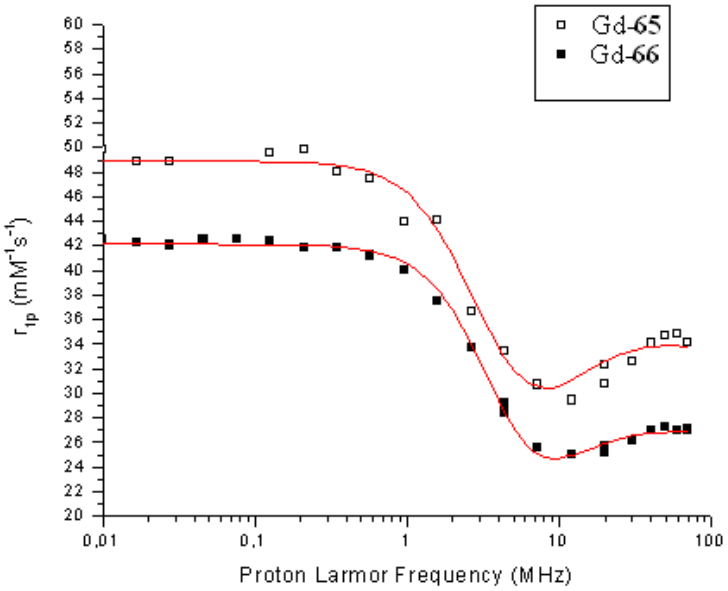

Figure 5.9. $1/T_1$ NMRD profiles for Gd-**65** and Gd-**66**

The efficacy of the CA, measured as the ability of its 1 mM solution to increase the longitudinal relaxation R_1 (=$1/T_1$) of water protons, is called relaxivity and labeled r_1. According to the well established Solomon-Boembergen-Morgan theory and its improvement, called generalized SBM[134], the relaxivity parameters (see eq. **5.1-5.4**) were evaluated and reported into table **5.1**.

[134] E. Strandeberg, P. O. Westlund *J. Magn. Reson., Ser. A,* **1996,** *122*, 179-191.

Table 5.1. Parameters determined by SBM theory.

	Δ^2 (s^{-2})	τ_v (ps)	τ_M (s)	τ_R (ps)	q	q_{ass}
Gd-**65**	2.1×10^{19}	27.5	1×10^{-8}	280	3	15
Gd-**66**	2.8×10^{19}	22.5	1×10^{-8}	216	3	14

Electronic relaxation parameters (Δ^2 e τ_v) were similar for complexes Gd-**65** and Gd-**66** and comparable to commercial contrast agents.

From the data reported (see **q** and $\mathbf{q_{ass}}$) appears that Gd-**65** and Gd-**66** complexes coordinate directly (in the inner sphere, see figure **5.2**) 3 water molecules and about 14-15 water molecules in the second coordination sphere.

Finally, we have also tested the stability of the complex Gd-**65** in solution using EDTA as competitor ($\log K_{EDTA}$=17.35) in a titration (figure **5.10**, increased EDTA amounts into Gd-**65** solution, 0.918 mM, pH 7). Being stability constant of Gd-EDTA complex known, and once knew Gd-**65** relaxivity, it was possible to fit these experimental data and obtain stability constant of the examined complex.

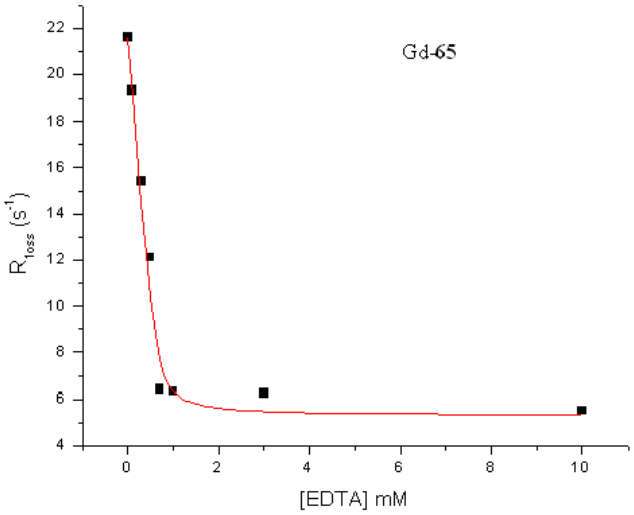

Figure 5.10. Tritation profile of Gd-**65** with EDTA**.**

The stability constant was determinated to be $\log K_{Gd\text{-}65}$ = 15.95 resulting too low for possible *in vivo* applications. The stability studies for the complexes Gd-**66** and Gd-**67** are in progress.

5.4 Experimental section

5.4.1 Synthesis

✓ *Compound **125***

To a solution of β-alanine hydrochloride **124** (3.0 g, 16.5 mmol) in DMF dry (5 mL), DIPEA (5.74 mL, 33.0 mmol) and ethyl bromoacetate (0.93 mL, 8.25 mmol) were added. The reaction mixture was stirred overnight, concentrated *in vacuo*, dissolved in CH_2Cl_2 (20 mL) and washed with brine solution. The aqueous layer was extracted with CH_2Cl_2 (three times). The combined organic phases were dried over $MgSO_4$, filtered and the solvent evaporated *in vacuo* to give a crude material **125** (3.0 g, 100 %, yellow oil), which was used in the next step without purification. δ_H (300.10 MHz, $CDCl_3$) 1.31 (3H, t, *J*

9.0 Hz, C<u>H</u>$_3$CH$_2$), 1.47 (9H, s, C(C<u>H</u>$_3$)$_3$), 2.74 (2H, t, *J* 6.0 Hz, NHCH$_2$C<u>H</u>$_2$CO), 3.09 (2H, t, *J* 9.0 Hz, NHC<u>H</u>$_2$CH$_2$CO), 3.65 (2H, s, C<u>H</u>$_2$NHCH$_2$CH$_2$CO), 4.26 (2H, q, *J* 15.0 Hz); δ_C (75.50 MHz, $CDCl_3$) 14.01, 27.97, 33.50, 44.30, 49.14, 60.41, 81.44, 168.88, 170.77. *m/z* (ES) 232 (MH^+); (HRES) MH^+, found 232.1552. $C_{11}H_{22}NO_4^+$ requires 232.1549.

✓ *Compound **126***

To a solution of **125** (3.0 g, 13.0 mmol) in 1,4-dioxane (30 mL) at 0°C, LiOH•H_2O (0.587 g, 14.0 mmol) in H_2O (30 mL) was added. After two hours, $NaHCO_3$ (1.42 g, 9.9 mmol) and Fmoc-Cl (4.33 g, 9.9 mmol) were added. The reaction mixture was stirred overnight. Subsequently, $KHSO_4$ (until pH= 3) was added and concentrated *in vacuo*, dissolved in CH_2Cl_2 (20 mL). The aqueous layer was extracted with CH_2Cl_2 (three times). The combined organic phases were dried over $MgSO_4$, filtered and the solvent evaporated *in vacuo* to give a crude material (5.8 g g, yellow oil), which was purified by flash chromatography (CH_2Cl_2/CH_3OH, from: 100/0 to 80/20, 0.1% ACOH) to give **126** (50 mg, 30%). δ_H (300.10 MHz, $CDCl_3$, mixture of rotamers) 1.44 (9H, s, C(C<u>H</u>$_3$)$_3$), 2.32 (1.2H, t, *J* 6.4 Hz, NHCH$_2$C<u>H</u>$_2$CO, rot. a) 2.58 (0.8H, t, *J* 6.0 Hz, NHCH$_2$C<u>H</u>$_2$CO, rot. b), 3.45 (1.2H, t, *J* 6.3 Hz, NHC<u>H</u>$_2$CH$_2$CO, rot. a), 3.59 (0.8H, t, *J* 5.9 Hz, NHC<u>H</u>$_2$CH$_2$CO, rot. b), 4.05 (0.8H, s, C<u>H</u>$_2$NHCH$_2$CH$_2$CO, rot. b), 4.13 (1.2H, s, C<u>H</u>$_2$NHCH$_2$CH$_2$CO, rot. a), 4.20 (0.4H, t, *J* 6.0 Hz, CH$_2$C<u>H</u>Fmoc, rot. b), 4.28 (0.6H, t, *J* 6.0 Hz, CH$_2$C<u>H</u>Fmoc, rot. a), 4.45 (1.2H, d, *J* 6.3 Hz, C<u>H</u>$_2$CHFmoc, rot. b), 4.55 (0.8H, d, *J* 6.0 Hz, C<u>H</u>$_2$CHFmoc, rot. a), 7.19-7.44 (4H, m, Ar. (Fmoc)), 7.53 (0.8H, d, *J* 7.3 Hz, Ar. (Fmoc), rot. b), 7.59 (1.2H, d, *J* 7.3 Hz, Ar. (Fmoc), rot. a), 7.73 (0.8H, t, *J* 7.3 Hz, Ar. (Fmoc), rot. b), 7.78 (1.2H, t, *J* 7.3 Hz, Ar. (Fmoc), rot. a). δC (62.89 MHz, $CDCl_3$, mixture of rotamers) 27.90, 34.42, 34.60, 44.38, 45.09, 47.03 (× 2), 49.71, 49.99, 67.59, 80.87, 119.84, 124.70 (× 2), 125.16 (× 2), 126.91, 127.00, 127.59 (× 2), 128.08, 128.89, 141.19, 143.62, 155.63, 156.24, 171.11, 171.61, 174.88, 175.04. *m/z* (ES) 454 (MH^+); (HRES) MH^+, found 454.229. $C_{26}H_{32}NO_6^+$ requires 454.223.

5.4.2 Linear compounds 127, 128 and 129.

Linear peptoids **127, 128** and **129**, were synthesized by alternating submonomer and monomer solid-phase method using standard manual Fmoc solid-phase peptide synthesis protocols. Typically 0.20 g of 2-chlorotrityl chloride resin (Fluka; 2,α-dichlorobenzhydryl-polystyrene crosslinked with 1% DVB; 100-200 mesh; 1.20 mmol/g) was swelled in dry DCM (2 mL) for 45 min and washed twice in dry DCM (2 mL). To the resin, monomer **126** (68 mg, 0.16 mmol) and DIPEA (0.11 mL, 0.64 mmol) in dry DCM (2 mL) were added and putted on a shaker platform for 1h and 15 min at room temperature, washes with dry DCM (3 × 2mL) and then with DMF (3 × 2 mL) followed. The resin was capped with a solution of DCM/CH_3OH/DIPEA. The Fmoc group was deprotected with 20% piperidine/DMF (v/v, 3 mL) on a shaker platform for 3 min and 7 min respectively, followed by extensive washes with DMF (3 × 3 mL), DCM (3 × 3 mL) and DMF (3 × 3 mL). Subsequently, for compound **130**, the resin was incubated with a solution of monomers **126** (0.64 mmol), HATU (0.24 g, 0.62 mmol), DIPEA (220 μL, 1.28 mmol) in dry DMF (2 mL) on a shaker platform for 1 h, followed by extensive washes with DMF (3 × 2 mL), DCM (3 × 2 mL) and DMF (3 × 2 mL). For compounds **128** and **129**, instead, bromoacetylation reactions were accomplished by reacting the oligomer with a solution of bromoacetic acid (690 mg, 4.8 mmol) and DIC (817 μL, 5.28 mmol) in DMF (4 mL) on a shaker platform 40 min at

room temperature. Subsequent specific amine was added (methoxyethyl amine: 0.17 mL, 2.0 mmol or propargyl amine: 0.15 mL, 2.4 mmol).

Chloranil test was performed and once the coupling was complete the Fmoc group was deprotected with 20% piperidine/DMF (v/v, 3 mL) on a shaker platform for 3 min and 7 min respectively, followed by extensive washes with DMF (3 × 3 mL), DCM (3 × 3 mL) and DMF (3 × 3 mL). The yields of loading step and of the following coupling steps were evaluated interpolating the absorptions of dibenzofulvene-piperidine adduct (λmax = 301, ε = 7800 M-1 cm-1), obtained in Fmoc deprotection step (the average coupling yield was 63-70%).

The synthesis proceeded until the desired oligomer length was obtained. The oligomer-resin was cleaved in 4 mL of 20% HFIP in DCM (v/v). The cleavage was performed on a shaker platform for 30 min at room temperature the resin was then filtered away. The resin was treated again with 4 mL of 20% HFIP in DCM (v/v) for 5 min, washed twice with DCM (3 mL), filtered away and the combined filtrates were concentrated in vacuo. The final products were dissolved in 50% ACN in HPLC grade water and analysed by RP-HPLC and ESI mass spectrometry.

✓ *Compound **127:*** t_R: 18.1 min; *m/z* (ES) 1129 (MH^+); (HRES) MH^+, found 1129. 6500 $C_{54}H_{93}N_6O_{19}^+$ requires 1129.6425. 80%.

✓ *Compound **128:*** t_R: 15.1 min; *m /z* (ES) 919 (MH^+); (HRES) MH^+, found 919.5248 $C_{42}H_{75}N_6O_{16}^+$ requires 919.5240. 75%

✓ *Compound **129:*** t_R: 16.5 min; *m/z* (ES) 945 (MH^+); (HRES) MH^+, found 949.5138 $C_{43}H_{73}N_6O_{15}^+$ requires 949.5134. 85%

5.4.3 General cyclization reaction (synthesis of 130, 131 and 122)

A solution of the linear peptoid (**127**, **128** and **129**), previously co-evaporated three times with toluene, was prepared under nitrogen in dry DMF (20 mL).

✓ Linear **127** (0.110 g, 0.097 mmol) was dissolved in DMF dry (8 mL) and the mixture was added drop-wise by syringe pump in 2 h to a stirred solution of HATU (0.15 g, 0.39 mmol) and DIPEA (0.10 mL, 0.60 mmol) in dry DMF (25 mL) at room temperature in anhydrous atmosphere.

✓ Linear **128** (0.056 g, 0.061 mmol) was dissolved in DMF dry (5 mL) and the mixture was added drop-wise by syringe pump in 2 h to a stirred solution of HATU (0.093 g, 0.244 mmol) and DIPEA (0.065 mL, 0.38 mmol) in dry DMF (15 mL) at room temperature in anhydrous atmosphere.

✓ Linear **129** (0.050 g, 0.053 mmol) was dissolved in DMF dry (4.5 mL) and the mixture was added drop-wise by syringe pump in 2 h to a stirred solution of HATU (0.080 g, 0.211 mmol) and DIPEA (0.057 mL, 0.333 mmol) in dry DMF (13.5 mL) at room temperature in anhydrous atmosphere.

After 12 h the resulting mixtures were concentrated in vacuo, diluted with CH_2Cl_2 (20 mL) and a solution of HCl (0.1 N, 20 mL). The single mixture was extracted with CH_2Cl_2 (2 x 20 mL) and the combined organic phases were washed with water (12 mL), dried over anhydrous Na_2SO_4, filtered and concentrated in vacuo.

All cyclic products were dissolved in 50% acetonitrile in HPLC grade water and analysed by RP-HPLC (purity >85% for all the cyclic oligomers).

Eluition conditions: 5%-100% B in 30 min [A: 0.1% TFA in water, B: 0.1% TFA in acetonitrile], flow: 1.0 mL/min, 220 nm. C18 reversed-phase analytical column [Waters, lBondapak, 10 lm, 125 Å, 3.9 mm x 300 mm]) and ESI mass spectrometry (zoom scan technique).

The crude residues (**130**, **131** and **122**) were purified by HPLC on a C18 reversed-phase preparative column, conditions: 20%-100% B in 40 min [A: 0.1% TFA in water, B: 0.1% TFA in acetonitrile], flow: 2.0 mL/min, 220 nm. The samples were dried in a falcon tube under low pressure.

✓ *Compound **130**:* δ_H (300.00 MHz, $CDCl_3$, mixture of conformers) 1.44 (54H, br s, $C(C\underline{H}_3)_3$), 2.54-3.58 (24H, m, $C\underline{H}_2C\underline{H}_2COO$t-Bu), 3.94-4.50 (12H, m, $C\underline{H}_2$ intranular). δ_C (62.89 MHz, $CDCl_3$, mixture of conformers) 27.99, 29.63, 33.20, 33.72, 34.02, 34.15, 34.74, 43.80, 44.33, 44.58, 45.04, 45.31, 45.55, 45.72, 45.94, 46.76, 47.56, 47.74, 48.58, 48.96, 49.77, 50.04, 50.37, 51.02, 52.77, 53.23, 53.40, 80.58, 81.41, 167.65, 167.76, 167.93, 168.19, 168.32, 168.56, 168.86, 168.90, 169.02, 169.15, 169.28, 169.38, 169.51, 169.93, 170.27, 170.38, 170.62, 170.69, 170.78, 170.91, 170.96, 171.14, 171.34, 171.39, 171.58, 171.67, 171.74, 171.87. 65%, m/z (ES) 1111 (MH^+); (HRES) MH^+, found 1111.6395. $C_{54}H_{91}N_6O_{18}^+$ requires 1111.6390. **HPLC**: t_R 20.05 min.

✓ *Compound **130** with sodium picrate:* δ_H (400 MHz, CD_3CN:$CDCl_3$ 9:1, 25 °C, soluzione 4.0 mM) 1.44 (54H, s, $C(C\underline{H}_3)_3$), 2.56 (12H, t, *J* 8.0 Hz, $CH_2C\underline{H}_2COO$*t*-Bu), 3.47 (6H, m, $CH\underline{H}CH_2COO$*t*-Bu), 3.61 (6H, m, $C\underline{H}HCH_2COO$*t*-Bu), 3.92 (6H, d, *J* 16.0 Hz, -OCC$\underline{H}$HN, pseudoequatorial), 4.61 (6H, d, *J* 20.0 Hz, -OCCH$\underline{H}$N, pseudoaxial), 8.77 (3H, s, Picrate). δ_C (100 MHz, CD_3CN:$CDCl_3$ 9:1, 25 °C, solution 4.0 mM) 28.46, 34.78, 45.50, 50.20, 82.27, 127.24, 128.22, 143.10, 170.15, 171.73.

✓ *Compound **131**:* δ_H (400.10 MHz, $CDCl_3$, mixture of conformers) 1.43-146 (54H, br s, $C(C\underline{H}_3)_3$), 3.25-3.60 (33H, m, $C\underline{H}_2C\underline{H}_2COO$*t*-Bu e $C\underline{H}_2C\underline{H}_2OC\underline{H}_3$), 3.94-4.65 (12H, m, $C\underline{H}_2$ intranular). δ_C (62.89 MHz, $CDCl_3$, mixture of conformers) 29.13, 29.33, 29.56, 35.01, 35.41, 45.17, 46.35, 47.20, 49.62, 49.92, 50.61, 53.97, 59.93, 60.26, 72.80, 81.95, 81.10, 82.69, 114.01, 118.00, 160.61, 160.72, 170.01, 170.75, 171.21, 171.45, 171.90, 172.19, 172.45, 172.88, 173.10. 82%, m/z (ES) 901 (MH^+); (HRES) MH^+, found 901.5138. $C_{42}H_{73}N_6O_{15}^+$ requires 901.5134. **HPLC**: t_R 15.05 min.

✓ *Compound **131** with sodium picrate:* δ_H (400 MHz, CD_3CN:$CDCl_3$ 9:1, solution 4.0 mM) 1.44 (27H, s, $C(C\underline{H}_3)_3$), 2.56 (6H, t, *J* 8.0 Hz, $CH_2C\underline{H}_2COO$*t*-Bu), 3.32 (9H, s, $CH_2CH_2OC\underline{H}_3$), 3.47-3.70 (18H, m, $C\underline{H}HCH_2COO$*t*-Bu e $CH\underline{H}CH_2COO$*t*-Bu e $C\underline{H}_2C\underline{H}_2OCH_3$), 3.81 (3H, d, *J* 16.7 Hz, -OCC$\underline{H}$HN, pseudoequatorial), 3.89 (3H, d, *J* 17.0 Hz, -OCC$\underline{H}$HN, pseudoequatorial) 4.64 (3H, d, *J* 16.7 Hz, -OCCH$\underline{H}$N, pseudoaxial), 4.68 (3H, d, *J* 16.6 Hz, -OCCH$\underline{H}$N, pseudoaxial), 8.74 (3H, s, Picrate).

✓ *Compound **122**:* δ_H (400.10 MHz, $CDCl_3$, mixture of conformers) 1.43-144 (36H, br s, $C(C\underline{H}_3)_3$), 2.15-2.80 (10H, m, $CH_2C\underline{H}_2COO$t-Bu e $CH_2CC\underline{H}$), 3.50-4.65 (24H m, $C\underline{H}_2CCH$, $C\underline{H}_2$ intranular e $C\underline{H}_2CH_2COO$t-Bu). (62.89 MHz, $CDCl_3$, mixture of conformers) 27.87, 29.50, 33.59, 34.16, 36.53, 36.71, 36.98, 43,78, 44.02, 44.21, 44.37, 45.09, 46.87, 47.55, 47.67, 47.80, 48.66, 49.03, 49.25, 49.91, 50.16, 50.53, 50.91, 52.97, 53.29, 72.36, 72.50, 72.86, 80.56, 81.27, 81.36, 157.86, 158.63, 167.20, 168.05, 168.51, 168.89, 170.26, 171.00, 171.51, 171.52. 71%, m/z (ES) 931 (MH^+); (HRES) MH^+, found 931.5029. $C_{46}H_{71}N_6O_{14}^+$ requires 931.5028. **HPLC**: t_R 18.00 min.

5.4.4 Synthesis of 133 by click chemistry.

Compound **122** (0.010 g, 0.011 mmol) was dissolved in CH_3OH (55 μL) and compound **132** (0.015 g 0.066 mmol) was added and the reaction was stirred for 15 minutes. Subsequent, a solution of $CuSO_4$ penta hydrate (0.001 g, 0.0044 mmol) and sodium ascorbate (0.0043 g, 0.022 mmol) in water (110 μL) was slowly added. The reaction was stirred overnight. After, at the solution H_2O (0.3 ml) was added and the single mixture was extracted with CH_2Cl_2 (2 x 20 mL) and the combined organic phases were washed with water (12 mL), dried over anhydrous Na_2SO_4, filtered and concentrated in vacuo. The crude residue **133** was purified by HPLC on a C18 reversed-phase preparative column, conditions: 20%-100% B in 40 min [A: 0.1% TFA in water, B: 0.1% TFA in acetonitrile], flow: 2.0 mL/min, 220 nm. The samples were dried in a falcon tube under low pressure (53 %). δ_H (400.10 MHz, $CDCl_3$, mixture of conformers) 1.42 (36H, br s, $C(C\underline{H}_3)_3$), 2.54 (8H, m, $CH_2C\underline{H}_2COOt$-Bu), 3.30-5.05 (62H, m, $C\underline{H}_2CH_2COOt$-Bu, $NC\underline{H}_2C{=}CH$, $C\underline{H}_2$ etilen-glicole, $C\underline{H}_2$ intranulari e $OC\underline{H}_3$,), 7.90 (2H, m, C=C$\underline{H}$). δ_C (100.03 MHz, $CDCl_3$, mixture of conformers) 14.02, 22.56, 28.04, 29.62, 31.93, 32.99, 33.73, 42.27, 43.01, 44.48, 45.01, 45.64, 48.38, 48.91, 49.44, 50.60, 53.34, 58.92, 69.15, 69.99, 70.52, 71.89, 80.54, 80.69, 80.80, 80.92, 81.36, 113.87, 116.40, 124.16, 124.35, 124.46, 124.65, 124.74, 125.32, 125.47, 142.21, 158.91, 159.41, 159.52, 168.72, 169.54, 171.40, 170.55, 171.00, 171.20, 171.31. m/z (ES) 1397 (MH^+); (HRES) MH^+, found 1397.7780. $C_{64}H_{109}N_{12}O_{22}^+$ requires 1397.7779. **HPLC**: t_R 18.30 min.

5.4.5 General deprotection reaction (synthesis of 65, 66 and 67)

Protected cyclopeptoids **130** (0.058 g, 0.052mmol), **131** (0.018 g, 0.020 mmol) and **122** (0.010 g, 0.0072 mmol)**,** were dissolved in a mixture of *m*-cresol and TFA (1/9, 1.3 mL for **130**, 0.5 mL for **131**, 0.18 mL for **122**) and the reaction was stirred for one hour. After, products were precipitated in cold Ethyl Ether (20 mL) and centrifuged. Solids were recuperated with a quantitative yield.

✓ *Compound **65**:* δ_H (300.00 MHz, $CDCl_3$, mixture of conformers) 1.44 (54H, br s, $C(C\underline{H}_3)_3$), 2.54-3.58 (24H, m, $C\underline{H}_2C\underline{H}_2COOt$-Bu), 3.94-4.50 (12H, m, $C\underline{H}_2$ intranular). δ_c (62.89 MHz, $CDCl_3$, mixture of conformers) 27.99, 29.63, 33.20, 33.72, 34.02, 34.15, 34.74, 43.80, 44.33, 44.58, 45.04, 45.31, 45.55, 45.72, 45.94, 46.76, 47.56, 47.74, 48.58, 48.96, 49.77, 50.04, 50.37, 51.02, 52.77, 53.23, 53.40, 80.58, 81.41, 167.65, 167.76, 167.93, 168.19, 168.32, 168.56, 168.86, 168.90, 169.02, 169.15, 169.28, 169.38, 169.51, 169.93, 170.27, 170.38, 170.62, 170.69, 170.78, 170.91, 170.96, 171.14, 171.34, 171.39, 171.58, 171.67, 171.74, 171.87. m/z (ES) 775 (MH^+); (HRES) MH^+, found 775.2638. $C_{30}H_{43}N_6O_{18}^+$ requires 775.2635. **HPLC**: t_R 4.05 min.

✓ *Compound **65** with sodium picrate:* δ_H (400.10 MHz, CD_3CN/D_2O/MeOD=2/1/1, spettro 1.5:1 complesso) 2.60 (12H, m, $CH_2C\underline{H}_2COOH$), 3.40 (6H, m, C$\underline{H}$HCH_2COOH, overlapped with water signal), 3.54 (6H, m, CH$\underline{H}$CH_2COOH), 3.85 (6H, d, *J* 16.5 Hz, -OCC$\underline{H}$HN, pseudoequatorial), 4.72 (6H, d, *J* 17.1 Hz, -OCCH$\underline{H}$N, pseudoaxial), 8.68 (3H, s, Picrate).

✓ *Compound **66:*** δ_H (300.00 MHz, $CDCl_3$, mixture of rotamers) 3.24-4.80 (45H, complex signal, $C\underline{H}_2C\underline{H}_2OC\underline{H}_3$, $C\underline{H}_2C\underline{H}_2COOH$, $C\underline{H}_2$ intranular). δ_c (62.89 MHz, CD_3CN:MeOD=9:1, mixture of rotamers) 14.59, 31.43 32.14, 32.58, 43.59, 44.00, 44.60, 45.04, 45.74, 49.31, 49.69, 50.04, 57.57, 57.77, 57,85, 58.02, 58.29, 65.51, 69.42, 69.57, 70.11, 70.21, 70.35, 168.70, 168.91, 168.98, 169.34, 169.45, 169.57, 169.87, 169.97, 170.35, 170.83, 171.10, 171.60, 171.82, 172.75, 172.98, 173.18,

173.30. m/z (ES) 733 (MH^+); (HRES) MH^+, found 733.3259. $C_{30}H_{49}N_6O_{15}^+$ requires 733.3256. **HPLC**: t_R 8.43 min.

✓ *Compound **66** with sodium picrate:* δ_H (300.00 MHz, $CDCl_3$, mixture of rotamers) 2.61 (6H, br s, $CH_2C\underline{H}_2COOH$, overlapped with water signal), 3.30 (9H, s, $CH_2CH_2OC\underline{H}_3$), 3.50-3.60 (18H, m, $CH\underline{H}CH_2COOH$, $C\underline{H}HCH_2COOH$ e $C\underline{H}_2C\underline{H}_2OCH_3$), 3.77 (3H, d, *J* 21.0 Hz, -OCC$\underline{H}$HN, pseudoequatorial), 3.84 (3H, d, *J* 21.0 Hz, -OCC$\underline{H}$HN, pseudoequatorial), 4.64 (3H, d, *J* 15.0 Hz, -OCCH$\underline{H}$N, pseudoaxial), 4.83 (3H, d, *J* 15.0 Hz, -OCCH$\underline{H}$N, pseudoaxial), 8.68 (3H, s, picrate).

✓ *Compound **67:*** δ_H (400.10 MHz, $CDCl_3$, mixture of rotamers) 2.99-3.07 (8H, m, $CH_2C\underline{H}_2COOt$-Bu), 3.70 (6H, s, $OC\underline{H}_3$), 3.80-5.50 (56H, m, $C\underline{H}_2CH_2COOt$-Bu, $NC\underline{H}_2C{=}CH$, $C\underline{H}_2$ ethyleneglicol, $C\underline{H}_2$ intranular), 7.90 (2H, m, C=C$\underline{H}$). **HPLC**: t_R 10.13 min.

Chapter 6

6. Cyclopeptoids as mimetic of natural defensins.

6.1 Introduction

The efficacy of antimicrobial host defense in animals can be attributed to the ability of the immune system to recognize and neutralize microbial invaders quickly and specifically. It is evident that innate immunity is fundamental in the recognition of microbes by the naive host.[135] After the recognition step, an acute antimicrobial response is generated by the recruitment of inflammatory leukocytes or the production of antimicrobial substances by affected epithelia. In both cases, the host's cellular response includes the synthesis and/or mobilization of antimicrobial peptides that are capable of directly killing a variety of pathogens.[136] For mammals there are two main genetic categories for antimicrobial peptides: cathelicidins and defensins[2].

Defensins are small cationic peptides that form an important part of the innate immune system. Defensins are a family of evolutionarily related vertebrate antimicrobial peptides with a characteristic β-sheet-rich fold and a framework of six disulphide-linked cysteines[3]. Hexamers of defensins create voltage-dependent ion channels in the target cell membrane causing permeabilization and, ultimately, cell death.[137] Three defensin subfamilies have been identified in mammals: α-defensins, β-defensins, and the cyclic θ-defensins (figure **6.1**)[138].

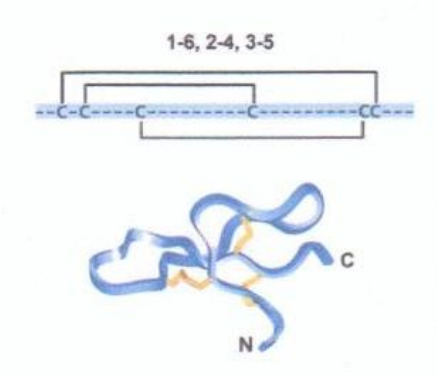

α-defensin

[135] Hoffmann J. A., Kafatos F. C., Janeway C. A ., Ezekowitz R. A. *Science*, **1999**, *284*, 1313-1318.
[136] Selsted M. E, and Ouelette A. J. *Nature immunol.*, **2005**, 6, 551-557.
[137] a) Kagan, B.L., Selsted, M.E., Ganz, T. Lehrer, R.I. *Proc. Natl Acad. Sci. USA*, **1990**, *87*, 210–214. b) Wimley, W.C., Selsted, M.E. White, S.H. *Protein Sci*., **1994**, *3*, 1362–1373.
[138] Ganz, T. *Science*, **1999**, *286*, 420–421.

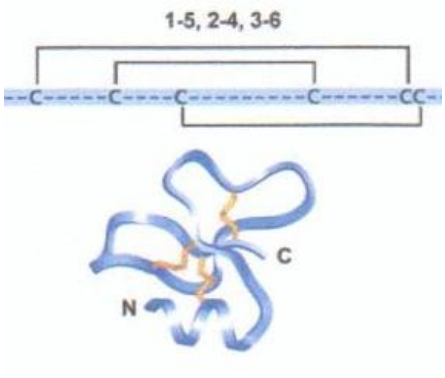

β-defensin

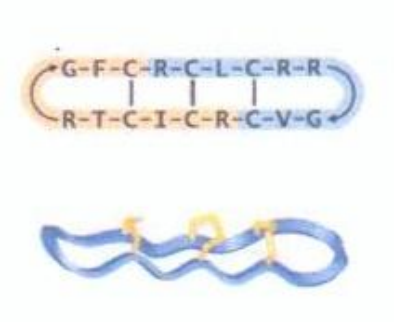

θ-defensin

Figure 6.1. Defensins profiles.

Defensins show broad anti-bacterial activity[139] as well as anti-HIV properties[140]. The anti-HIV-1 activity of α-defensins was recently shown to consist of a direct effect on the virus, combined with a serum-dependent effect on infected cells[141]. Defensins are constitutively produced by neutrophils[142] or produced in the Paneth cells of the small intestine.

Given that no gene for θ-defensins has been discovered, it is thought that θ-defensins is a proteolytic product of one or both of α-defensins and β-defensins. α-defensins and β-defensins are active against *Candida albicans* and are chemotactic for T-cells, whereas θ-defensins is not[143]. α-Defensins and β-defensins have recently been observed to be more potent than θ-defensins against the Gram negative bacteria *Enterobacter aerogenes* and *Escherichia coli* as well as the Gram positive *Staphylococcus aureus* and *Bacillus cereus*[9]. Considering that peptidomimetics are much stable and better performing than peptides *in vivo*, we have supposed that peptoids' backbone could mimic natural defensins. For this reason we have synthesized some peptoids with sulphide side chains (figure **6.2,** block **I**, **II**, **III** and **IV**), and explored the conditions for disulfide bond formation.

[139] a) Ghosh, D., Porter, E., Shen, B., Lee, S.K., Wilk, D., Drazba, J., Yadav, S.P., Crabb, J.W., Ganz, T. Bevins, C.L. *Nat. Immunol.,* **2002**, *3*, 583–590.b) Salzman, N.H., Ghosh, D., Huttner, K.M., Paterson, Y. Bevins, C.L. *Nature*, **2003**, *422*, 522–526.

[140] a) Zhang, L., Yu, W., He, T., Yu, J., Caffrey, R.E., Dalmasso, E.A., Fu, S., Pham, T., Mei, J., Ho, J.J. *Science*, **2002**, *298*, 995–1000. b) 7. Zhang, L., Lopez, P., He, T., Yu, W. Ho, D.D. *Science*, **2004**, *303*, 467.

[141] Chang, T.L., Vargas, J.J., Del Portillo, A. Klotman, M.E. *J. Clin. Invest*., **2005**, *115*, 765–773.

[142] Yount, N.Y., Wang, M.S., Yuan, J., Banaiee, N., Ouellette, A.J. Selsted, M.E. . *J. Immunol.*, **1995**, *155*, 4476–4484.

[143] Lehrer, R.I., Ganz, T., Szklarek, D. Selsted, M.E. *J. Clin. Invest*., **1988**, *81*, 1829–1835.

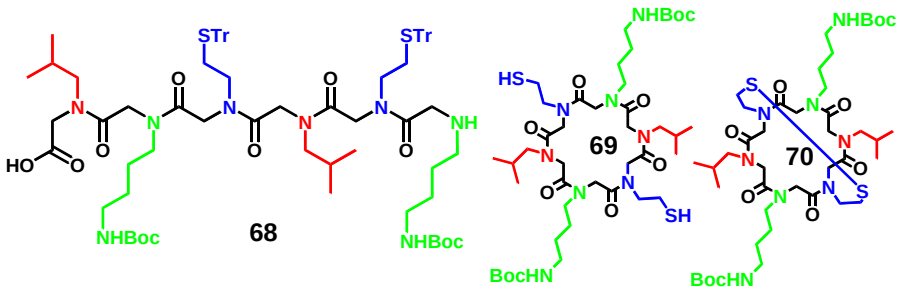

Figure 6.2, block I. Structures of the hexameric linear (**68**) and corresponding cyclic **69** and **70.**

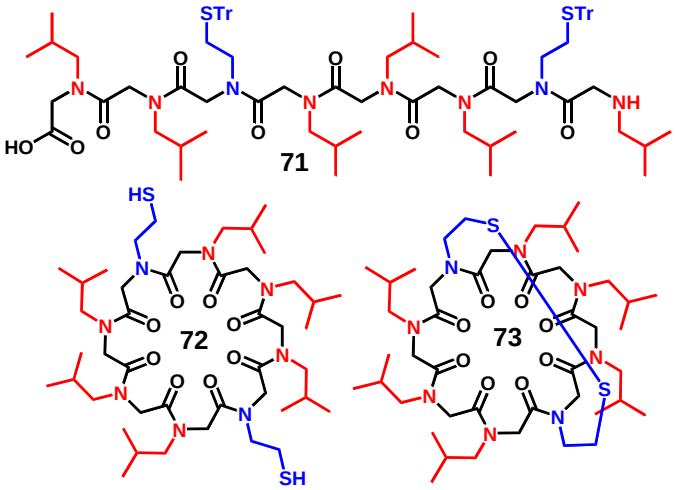

Figure 6.2, block II. Structures of octameric linear (**71**) and corresponding cyclic **72** and **73**

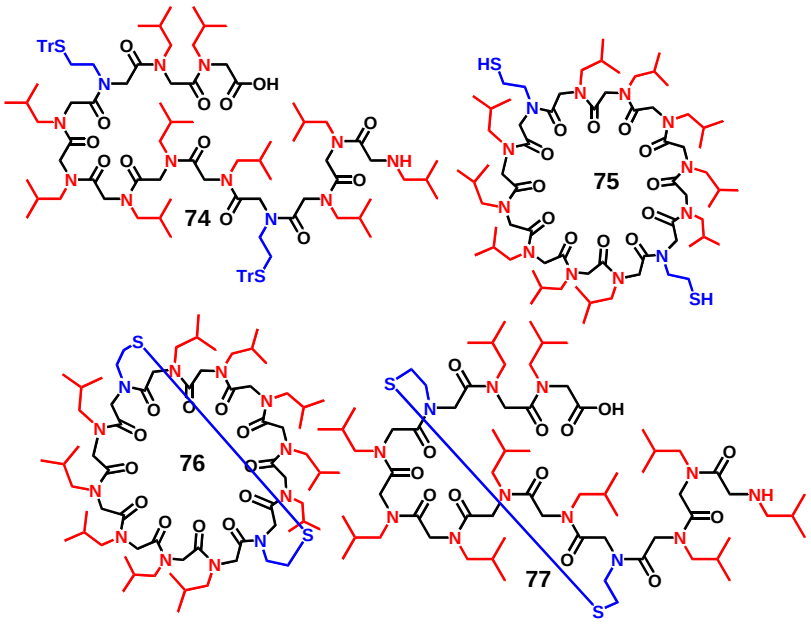

Figure 6.2, block III. Structures of linear (**74**) and corresponding cyclic **75, 76** and **77**

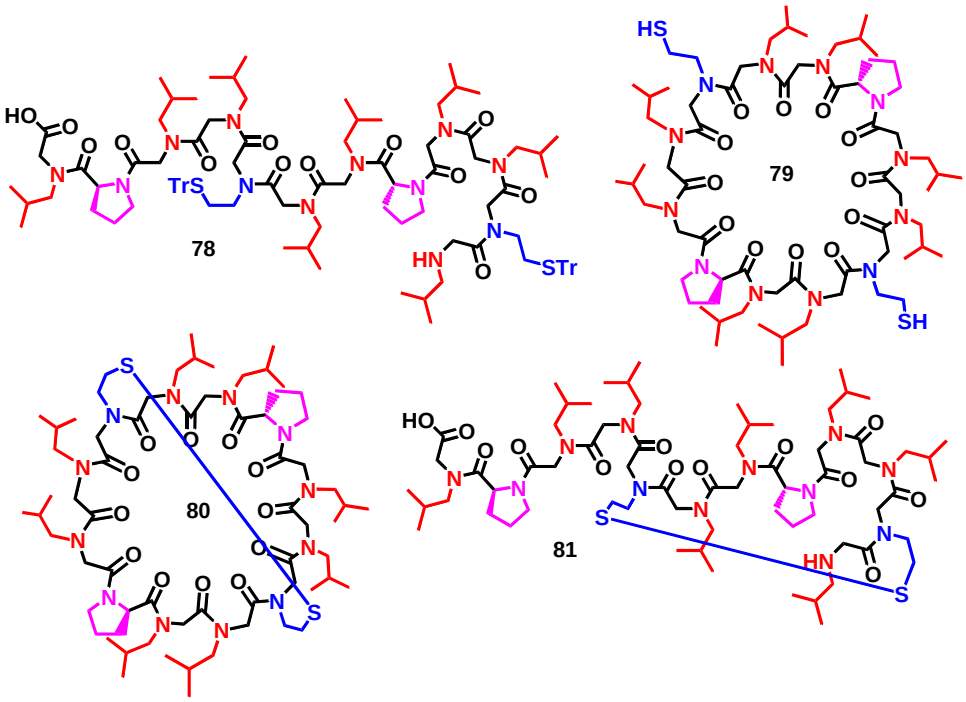

Figure 6.2, block IV. Structures of dodecameric linear diprolinate (**78**) and corresponding cyclic **79, 80** and **81.**

Disulfide bonds play an important role in the folding and stability of many biologically important peptides and proteins. Despite extensive research, the controlled formation of intramolecular disulfide bridges still remains one of the main challenges in the field of peptide chemistry.[144]

The disulfide bond formation in a peptide is normally carried out using two main approaches:

(i) while the peptide is still anchored on the resin;

(ii) after the cleavage of the linear peptide from the solid support.

Solution phase cyclization is commonly carried out using air oxidation and/or mild basic conditions.[10] Conventional methods in solution usually involve high dilution of peptides to avoid intermolecular disulfide bridge formation. On the other hand, cyclization of linear peptides on the solid support, where pseudodilution is at work, represents an important strategy for intramolecular disulfide bond formation[145].

Several methods for disulfide bond formation were evaluated. Among them a recently reported on-bead method was investigated and finally modified to improve the yields of cyclopeptoids synthesis[10].

6.2 Results and discussion

6.2.1 Synthesis

In order to explore the possibility to form disulfide bonds in cyclic peptoids, we had to preliminarly synthesized the linear peptoids **68, 71, 74** and **78** (Figure XX.X).

To this aim, we constructed the amine submonomer *N*-*t*-Boc-1,4-diaminobutane **134**[146]**,** and the amine submonomer *S*-tritylaminoethanethiol **137**[147], as reported in scheme **6.1.**

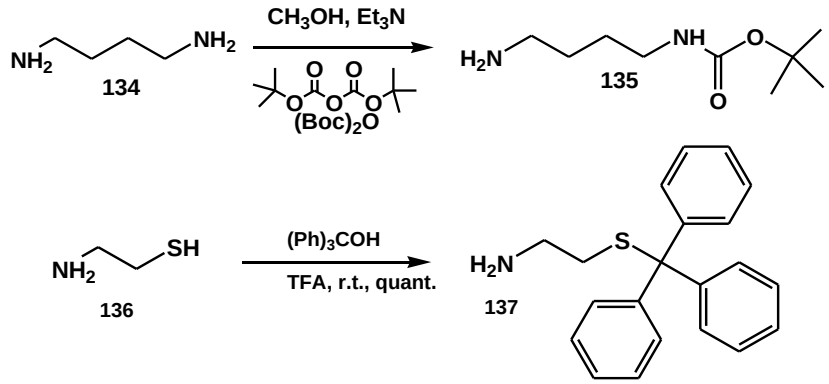

Scheme 6.1. *N*-Boc protection and S-trityl protection.

The synthesis of the liner peptoids was carried out on solid-phase (2-chlorotrityl resin), using the "sub-monomer" approach[148]. The identity of compounds **68, 71, 74** and **78** was established by mass spectrometry, with isolated crudes yield between 60 and 100% and purity greater than 90 % by

[144] Galanis A. S., Albericio F., Grøtli M. *Peptide Science*, **2008**, 92, 23-34.

[145] a) Albericio, F.; Hammer, R. P.; Garcìa-Echeverrìa, C.; Molins, M. A.; Chang, J. L.; Munson, M. C.; Pons, M.; Giralt, E.; Barany, G. *Int J Pept Protein Res* **1991**, *37*, 402–413. b). Annis, I.; Chen, L.; Barany, G. *J Am Chem Soc* **1998,** *120*, 7226–7238.

[146] Krapcho, A. P.; Kuell, C. S. *Synth. Commun* **1990**, *20***,** 2559–2564.

[147] Kocienski, P. J. *Protecting Group*, 3rd ed.; Georg Thieme Verlag: Stuttgart, **2005**.

[148] Zuckermann, R. N.; Kerr, J. M. ;. Kent, B. H ; Moos, W. H. *J. Am. Chem. Soc.*, **1992**, 114, 10646.

HPLC/MS analysis.[149]

Head-to-tail macrocyclization of the linear *N*-substituted glycines was performed in the presence of HATU in DMF and afforded protected cyclopeptoids **138, 139, 140** and **141** (figure **6.3**).

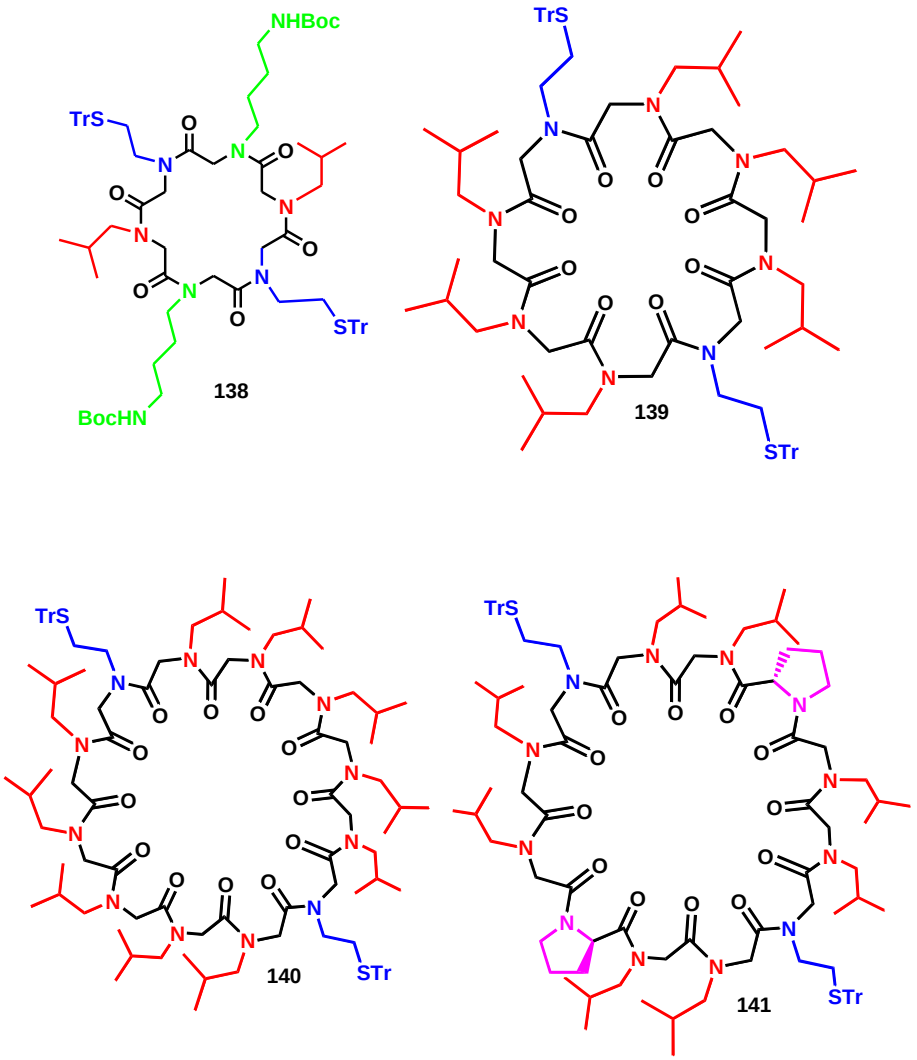

Figure 6.3. Protected cyclopeptoids **138, 139, 140** and **141.**

The subsequent step was the detritylation/oxidation reactions. Triphenylmethyl (trityl) is a common *S*-protecting group.[150] Typical ways for detritylation usually employ acidic conditions, either with protic acid[151] (e.g. trifluoroacetic acid) or Lewis acid[152] (e.g., $AlBr_3$). Oxidative protocols have been recently

[149] Analytical HPLC analyses were performed on a Jasco PU-2089 quaternary gradient pump equipped with an MD-2010 plus adsorbance detector using C_{18} (Waters, Bondapak, 10 µm, 125Å, 3.9 × 300 mm), reversed phase columns.

[150] For comprehensive reviews on protecting groups, see: (a) Greene, T. W.; Wuts, P. G. M. *Protective Groups in Organic Synthesis*, 2nd ed.; Wiley: New York, **1991**; (b) Kocienski, P. J. *Protecting Group*, 3rd ed.; Georg Thieme Verlag: Stuttgart, **2005**.

[151] (a) Zervas, L.; Photaki, I. *J. Am. Chem. Soc.* **1962**, *84*, 3887; (b) Photaki, I.; Taylor-Papadimitriou, J.; Sakarellos, C.; Mazarakis, P.; Zervas, L. *J. Chem. Soc. C* **1970**, 2683; (c) Hiskey, R. G.; Mizoguchi, T.; Igeta, H. *J. Org. Chem.* **1966**, *31*, 1188.

[152] Tarbell, D. S.; Harnish, D. P. *J. Am. Chem. Soc.* **1952**, *74*, 1862.

developed for the deprotection of trityl thioethers[153]. Among them, iodinolysis[154] in a protic solvent, such as methanol, is also used[16]. Cyclopeptoids **138, 139, 140** and **141** and linear peptoids **74** and **78** were thus exposed to various deprotection/oxidation protocols. All reactions tested are reported in Table 6.1.

Table 6.1. Survey of the detritylation/oxidation reactions.

Compound	Entries	Reactives	Solvent	Results
138	1	CuCl (40%), H_2O[20]	CH_2Cl_2	-
	2	TFA, H_2O, Et_3SiH	TFA	-
	3	(92.5/5/2.5)[17]		
	4	I_2 (5 eq.)[16]	AcOH/H_2O (4/	-
		DMSO (5%), DIPEA	CH_3CN	-
139	5	TFA, H_2O, Et_3SiH	TFA	-
	6	(92.5/5/2.5)[17]		
	7	DMSO (5%), DIPEA	CH_3CN	-
	8	DMSO (5%), DBU[19]	CH_3CN	-
	9	K_2CO_3 (0.2 M)	THF	-
		I_2 (5 eq.)[154]	CH_3OH	-
140	9	I_2 (5 eq.)[154]	CH_3OH	>70%
141	9	I_2 (5 eq.)[154]	CH_3OH	>70%
74	9	I_2 (5 eq.)[154]	CH_3OH	>70%
78	9	I_2 (5 eq.)[154]	CH_3OH	>70%

One of the detritylation methods used (with subsequent disulfide bond formation, entry 1), was proposed by Wang *et al.*[155] (figure **6.4**). This method provides the use of a catalyst, such as CuCl into an aquose solvent and it gives cleavage and oxidation of S-triphenylmethyl thioether.

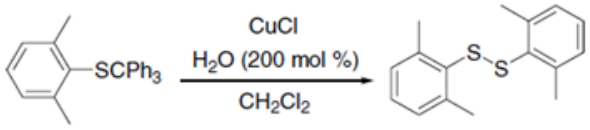

142 **143**

Figure 6.4. CuCl-catalyzed cleavage and oxidation of S-triphenylmethyl thioether.

[153] Gregg, D. C.; Hazelton, K.; McKeon, T. F., Jr. *J. Org. Chem.* **1953**, *18*, 36. b) Gregg, D. C.; Blood, C. A., Jr. *J. Org. Chem.* **1951**, *16*, 1255. c) Schreiber, K. C.; Fernandez, V. P. *J. Org. Chem.* **1961**, *26*, 2478. d) Kamber, B.; Rittel, W. *Helv. Chim. Acta* **1968,** *51*, 2061.e) Li, K. W.; Wu, J.; Xing, W. N.; Simon, J. A. *J. Am. Chem. Soc.* **1996**, *118*, 7237.

[154] K. W. Li, J. Wu, W. Xing, J. A. Simon *J. Am. Chem. Soc.* **1996**, 118, 7236-7238.

[155] Ma M., Zhang X., Peng L. and Wang J. *Tetrahedron Letters* **2007**, *48*, 1095–1097.

For compound **138**, Wang's method was applied, but it was not able to induce the sulfide bond formation. Probably, the reaction was condizioned by acquose solvent and by a constrain conformation of cyclohexapeptoid **138**. In fact, the same result was obtained using 1% TFA in the presence of 5% triethylsilane (TIS[17], entry 2**,** table **6.1**), in the case of iodinolysis in acetic acid/water, and in the presence of DMSO (entries 3 and 4).

One of the reasons hampering the closure of the disulfide bond, in compound **138**, could have been the distance between the two-disulfide terminals. For this reason, a larger cyclooctapeptoid **139** has been synthesized, and similar reactions were performed on the cyclic octamer. Unfortunately, reactions carried out on cyclo **139**, were inefficient, perhaps for the same reasons seen for the cyclo hexameric **138.** To overcome this disvantage, cyclo dodecamers **140** and **141** were synthesized. Compound **141** containing two prolines units, in order to induce folding[156] of the macrocycle and bring the thiol groups closer.

Therefore, dodecameric linears **74** and **78**, and cyclics **140** and **141** were subjectd to an iodinolysis reaction, reported by Simon[154] *et al*. This reaction provided the use of methanol such as a protic solvent and iodine for cleavage and oxidation. By HPLC and high-resolution MS analysis, compound **76**, **77**, **80** and **81** were observed with good yelds (>70%).

6.3 Conclusions

Differents cyclopeptoids with thiol groups were synthesized, with standard protocol of synthesis on solid phase and macrocyclization. Many proof of oxdidation were performed, but only iodinolysis reaction, were efficient to obtain desidered compound.

6.4 Experimental section

6.4.1 Synthesis

✓ *Compound **135***

Di-*tert*-butyl dicarbonate (0.4 eq., 10 g, 0.046 mmol) was added to 1,4-diaminobutane (10 g, 0.114 mmol) in CH_3OH/Et_3N (9/1) and the reaction was stirred overnight. The solvent was evaporated and the residue was dissolved in DCM (20 mL) and extracted using a saturated solution of $NaHCO_3$ (20 mL). Then water phase was washed with DCM (3 · 20 ml). The combined organic phase was dried over Mg_2SO_4 and concentrated in vacuo to give a pale yellow oil. The compound was purified by flash chromatography ($CH_2Cl_2/CH_3OH/NH_3$ 2.0M solution in ethyl alcohol, from: 100/0/0.1 to 70/30/0.1) to give **135** (0.51 g, 30%) as a yellow light oil; R_f (98/2/0.1, $CH_2Cl_2/CH_3OH/NH_3$ 2.0M solution in ethyl alcohol) 0.63; δ_H (300 MHz, $CDCl_3$) 4.68 (brs, 1H, N*H*-Boc), 3.12 (bq, 2H, CH_2-NH-Boc, J = 7.5 MHz), 2.71 (t, 2H, CH_2NH_2, J =7.0 MHz), 1.8 (brs, 2H, NH_2), 1.35 (s, 9H, (CH_3)$_3$); *m/z* (ES) 189 (MH^+); (HRES) MH^+, found 189.1600. $C_9H_{21}N_2O_2^+$ requires 189,1598.

[156] MacArthur M. W., Thornton J. M. *J. Mol. Biol.*, **1991**, *218*, 397.

✓ *Compound **137***

Aminoethanethiol hydrocloride (5 g, 0.044 mol) was dissolved in 12.5 mL of TFA. Triphenylcarbinol (11.5 g, 0.044 mol) was added to the solution portionwise under stirring at room temperature, until the solution became clear. The reaction mixture, a dense deeply red liquid, was left aside for 1 h and the poured in 200 mL of water under vigorous stirring. The suspension of the white solid was alkalinized with triethylamine and filtered and the solid washed with water alkaline for TEA. After drying, 18 g of the crude solid of **137**, slightly impure for TrOH, was obtained. The compound was used in the next step without purification, yeld:100%. R_f (98/2/0.1, $CH_2Cl_2/CH_3OH/NH_3$ 2.0M solution in ethyl alcohol) 0.63; δ_H (250 MHz, $CDCl_3$) 2.34 (t, 2H, C*H*$_2$-STr, *J*=7.5 Hz), 3.41 (t, 2H, C*H*$_2$NH$_2$, *J* =7.0 MHz), 7.19-7.41 (m, 15H, Ar); *m/z* (ES) 320 (MH^+); (HRES) MH^+, found 320.1470. $C_{21}H_{22}NS^+$ requires 320,1467. δ_C (100 MHz, $CDCl_3$) 31.9 (*C*H$_2$-STr), 40.1 (*C*H$_2$NH$_2$), 68.0 (*C*(Ph)$_3$), 127.8-128.5-128.9 (*C*H trityl), 145.7 (*C*q trityl).

6.4.2 General procedures for linear oligomers 68, 71, 74 and 78.

Linear peptoid oligomers **68, 71, 74** and **78** were synthesized using a sub-monomer solid-phase approach[11]. In a typical synthesis 2-chlorotrityl chloride resin (2,α-dichlorobenzhydryl-polystyrene crosslinked with 1% DVB; 100–200 mesh; 1.33 mmol/g, 400 mg, 0.532 mmol) was swelled in dry DMF (4 mL) for 45 min and washed twice with dry DCM (4 mL).

The first sub-monomer was attached onto the resin by adding 120 mg (1.2 eq, 0.63 mmol) of bromoacetic acid in dry DCM (4 mL) and 370 μL of DIPEA (2.10 mmol) on a shaker platform for 40 min at room temperature, followed by washing with dry DCM (4 mL) and then with DMF (4 x 4 mL). To the bromoacetylated resin was added a DMF solution (1 M, 5.3 mL) of the desired amine (isobutylamine -10 eq- or **135** -10 eq- or **137** -10 eq) the mixture was left on a shaker platform for 30 min at room temperature, then the resin was washed with DMF (4 x 4 mL). Subsequent bromoacetylation reactions were accomplished by reacting the aminated oligomer with a solution of bromoacetic acid in DMF (1.2 M, 5.3 mL) and 823 μL of DIC for 40 min at room temperature. The filtered resin was washed with DMF (4 x 4 mL) and treated again with the amine in the same conditions reported above. This cycle of reactions was iterated until the target oligomer was obtained (**68**, **71, 74** and **78** peptoids). The cleavage was performed by treating twice the resin, previously washed with DCM (6 x 6 mL), with 4 mL of 20% HFIP in DCM (v/v) on a shaker platform at room temperature for 30 min and 5 min, respectively. The resin was then filtered away and the combined filtrates were concentrated in vacuo. The final products were dissolved in 50% acetonitrile in HPLC grade water and analysed by RP-HPLC (purity >95% for all the oligomers, conditions: 5% to 100% B in 30 min [A: 0.1% TFA in water, B: 0.1% TFA in acetonitrile], flow: 1.0 mL/min, 220 nm. C18 reversed-phase analytical column [Waters, μBondapak, 10 μm, 125 Å, 3.9 mm x 300 mm]) and ESI mass spectrometry. The linear oligomers **68**, **71, 74** and **78** were subjected to the cyclization reaction without further purification.

✓ *Compound **68:*** t_R: 22.1 min; *m/z* (ES) 1419 (MH^+); (HRES) MH^+, found 1419,7497 $C_{80}H_{107}N_8O_{11}S_2^+$ requires 1419,7495. 100%

✓ *Compound **71:*** t_R: 23.0 min; *m/z* (ES) 1415 (MH^+); (HRES) MH^+, found 1415,7912 $C_{82}H_{111}N_8O_9S_2^+$ requires 1415,7910. 100%

✓ *Compound **74:*** t_R: 25.2 min; *m/z* (ES) 1868 (MH^+); (HRES) MH^+, found 1868,1278 $C_{106}H_{155}N_{12}O_{13}S_2^+$ requires 1868,1273. 100%

✓ *Compound **78:*** t_R: 24.0 min; *m/z* (ES) 1836 (MH^+); (HRES) MH^+, found 1836,0650 $C_{104}H_{147}N_{12}O_{13}S_2^+$ requires 1836,0647. 100%.

6.4.3 General cyclization reaction (synthesis of 138, 139, 140 and 141).

A solution of the linear peptoid (**68**, **71, 74** and **78**), previously co-evaporated three times with toluene, was prepared under nitrogen in dry DMF (20 mL).

✓ Linear **68** (1.0 eq., 200 mg, 0.141 mmol) was dissolved in DMF dry (10 mL) and the mixture was added drop-wise by syringe pump in 2 h to a stirred solution of HATU (4.0 eq., 214 mg, 0.564 mmol) and DIPEA (6.2 eq., 152 µl, 0.874 mmol) in dry DMF (37 mL) at room temperature in anhydrous atmosphere.

✓ Linear **71** (1.0 eq., 140.0 mg, 0.099 mmol) was dissolved in DMF dry (10 mL) and the mixture was added drop-wise by syringe pump in 2 h to a stirred solution of HATU (4.0 eq., 150 mg, 0.396 mmol) and DIPEA (6.2 eq, 168 µl, 0.614 mmol) in dry DMF (23 mL) at room temperature in anhydrous atmosphere.

✓ Linear **74** (1.0 eq., 100.0 mg, 0.054 mmol) was dissolved in DMF dry (8 mL) and the mixture was added drop-wise by syringe pump in 2 h to a stirred solution of HATU (4.0 eq, 81.0 mg, 0.214 mmol) and DIPEA (6.2 eq, 58 µl, 0.33 mmol) in dry DMF (10 mL) at room temperature in anhydrous atmosphere.

✓ Linear **78** (1.0 eq., 100.0 mg, 0.055 mmol) was dissolved in DMF dry (8 mL) and the mixture was added drop-wise by syringe pump in 2 h to a stirred solution of HATU (4 eq, 83.0 mg, 0.218 mmol) and DIPEA (6.2 eq, 59 µl, 0.34 mmol) in dry DMF (10 mL) at room temperature in anhydrous atmosphere.

After 12 h the resulting mixtures were concentrated in vacuo, diluted with CH_2Cl_2 (20 mL) and a solution of HCl (0.1 N, 20 mL). The single mixture was extracted with CH_2Cl_2 (2 x 20 mL) and the combined organic phases were washed with water (12 mL), dried over anhydrous Na_2SO_4, filtered and concentrated in vacuo.

All protected cyclic **138**, **139, 140** and **141** were dissolved in 50% acetonitrile in HPLC grade water and analysed by RP-HPLC (purity >85% for all the cyclic oligomers, conditions: 5%-100% B in 30 min [A: 0.1% TFA in water, B: 0.1% TFA in acetonitrile], flow: 1.0 mL/min, 220 nm. C18 reversed-phase analytical column [Waters, µBondapak, 10 µm, 125 Å, 3.9 mm x 300 mm]) and ESI mass spectrometry (zoom scan technique).

The crude residues were purified by HPLC on a C18 reversed-phase preparative column, conditions: 20%-100% B in 40 min [A: 0.1% TFA in water, B: 0.1% TFA in acetonitrile], flow: 2.0 mL/min, 220 nm. The samples were dried in a falcon tube under low pressure.

✓ *Compound **138:*** δ_H (400 MHz, CD_3CN:$CDCl_3$ (9:1), mixture of conformers) 7.39-7.21 (m, 30H, *H*-Ar), 4.21-2.48 (m, 34H, $NCH_2CH_2CH_2CH_2NHCO(CH_3)_3$, -$COCH_2N$-, $NCH_2CH(CH_3)_2$, CH_2CH_2STr, overlapped), 1.43 (m, 26 H, $NCH_2CH_2CH_2CH_2NHCO(CH_3)_3$); 0.72-0.90 (m, 12 H, $NCH_2CH(CH_3)_2$); m/z (ES) 1401 (MH^+); (HRES) MH^+, found 1401,7395. $C_{80}H_{105}N_8O_{10}S_2^+$ requires 1401,7390. **HPLC**: t_R: 25.0 min.

✓ *Compound **139:*** δ_H (400 MHz, CD_3OD, mixture of conformers) 7.60-7.20 (m, 30H, *H*-Ar), 4.90-2.34 (m, 38H, $NCH_2CH(CH_3)_2$, CH_2CH_2STr, -$COCH_2N$- overlapped), 1.45-0.70 (m, 36H, $NCH_2CH(CH_3)_2$). m/z (ES) 1397 (MH^+); (HRES) MH^+, found 1397,7810. $C_{82}H_{109}N_8O_8S_2^+$ requires 1397,7804. **HPLC**: t_R: 27.1 min.

✓ *Compound **140:*** δ_H (400 MHz, CD_3OD, mixture of conformers) 7.60-7.20 (m, 30H, *H*-Ar), 4.90-2.23 (m, 62H, $NCH_2CH(CH_3)_2$, CH_2CH_2STr, -$COCH_2N$- overlapped), 1.45-0.70 (m, 60H, $NCH_2CH(CH_3)_2$). m/z (ES) 1850 (MH^+); (HRES) MH^+, found 1850,1170. $C_{106}H_{153}N_{12}O_{12}S_2^+$ requires 1850,1167. **HPLC**: t_R: 33.0 min.

✓ *Compound **141:*** δ_H (400 MHz, CD_3OD, mixture of conformers) 7.60-7.20 (m, 30H, *H*-Ar), 4.90-2.23 (m, 70H, $NCH_2CH(CH_3)_2$, CH_2CH_2STr, -$COCH_2N$-, $CHCH_2CH_2CH_2NCO$ overlapped), 1.45-0.70 (m, 48H, $NCH_2CH(CH_3)_2$). m/z (ES) 1804 (MH^+); (HRES) MH^+, found 1804,0390. $C_{103}H_{143}N_{12}O_{12}S_2^+$ requires 1804,0384. **HPLC**: t_R: 29.1 min.

6.4.4 General Deprotection/Oxidation reactions reported in table 6.1 (synthesis of 69-70, 72-73, 75-76-77 and 79-80-81).

✓ *General procedure for Entry **1.***

Compound **68** (30 mg, 0.021 mmol) was dissolved in CH_2Cl_2 (1.0 mL), and to this solution was successively added CuCl (0.9 mg, 0.009 mmol) and H_2O (0.8 mg, 0.042 mmol), then the reaction bottle was sealed with a rubber plug. The reaction was conducted under ultrasonic irradiation for 3–7 h until detritylation was complete as judged by HPLC/MS.

✓ *General procedures for Entry **2** and **5.***

Compound **68** (27 mg, 0.019 mmol) and Compound **139** (20 mg, 0.014 mmol) was dissolved in a mixture of TFA/H_2O/Et_3SiH (92.5/5/2.5) and the reaction was stirred for 1h and 30min. After, products were precipitated in cold Ethyl Ether (20 mL) and centrifuged. Products recuperated was analyzed by HPLC/MS.

✓ *General procedure of Entry **3***

Compound **68** (5 mg, 0.007 mmol) was dissolved in 17.5 mL solution mixture of AcOH-H_2O (4/1) containing 9 mg of I_2 (0.035 mmol, 5 equivalents). The reaction mixture was stirred for 3 h, then mixture was concentrated in vacuo and analyzed by HPLC/MS.

✓ *General procedure for Entry **4** and **6***

Compound **68** (10 mg, 0.014 mmol) and compound **139** (10 mg, 0.011 mmol) were dissolved in about 11-13 mL of CH_3CN and 5% of DMSO and then DIPEA (24 µL, 0.14 mmol for **68**, and 19 µL, 0.11 mmol for **139**) were added. The mixtures were stirred for overnight. Mixtures were concentrated in vacuo and analyzed by HPLC/MS.

✓ *General procedure for Entry **7***

Compound **139** (1.5 mg, 0.0016 mmol) was dissolved in about 1.6 mL of CH_3CN and 5% of DMSO and then DBU (2.4 μL, 0.016 mmol) were added. The mixture was stirred for overnight. Mixture was concentrated in vacuo and analyzed by HPLC/MS.

✓ *General procedure for Entry **8***

Compound **139** (1.5 mg, 0.0016 mmol) was dissolved in about 1.28 mL of THF and K_2CO_3 (aq) (0.32 mL, 0.2 M) was added. The mixture was stirred for overnight. Mixture was concentrated *in vacuo* and analyzed by HPLC/MS.

✓ *General procedure for Entry **9***

A solution of iodine (7 mg, 0.027 mmol, 5 eq.) in CH_3OH (4 mL, ~10^{-3}M) was stirred vigorously and compound **139** (5.0 mg, 0.005 mmol), compound **140** (8 mg, 0.004 mml), compound **141** (10 mg, 0.005 mmol), compound **74** (10 mg, 0.005 mmol), compound **78** (10 mg, 0.005 mmol) in about 1 mL of CH_3OH were respectively added. The reactions were stirred for overnight and then were quenched by the addition of aqueous ascorbate (0.2 M) in pH 4.0 citrate (0.2 M) buffer (4 mL). The colorless mixtures extracted were poured into 1/1 saturated aqueous NaCl and CH_2Cl_2. The aqueous layer were extracted with CH_2Cl_2 (3 x 10 mL). The organic phases recombined were concentrated *in vacuo* and the crudes were purified by HPLC/MS.